# *Synechococcus* sp. PCC 7002 CpcB lyase null mutations alter phycocyanin chromophore function and, consequently, affect the redistribution of excitation energy via the light state transition.

by

Allen Kimbell Derks, B.Sc.

A Thesis

submitted to the Department of Biological Sciences

in partial fulfillment of the requirements

for the degree of

Master of Science

August, 2007

Brock University

St. Catharines, Ontario

## ABSTRACT

Phycobilisomes are the major light harvesting complexes for cyanobacteria and phycocyanin is the primary phycobiliprotein of the phycobilisome rod. The phycocyanobilin lyases responsible for chromophorylating the phycocyanin β subunit (CpcB) have been recently identified in the cyanobacterium *Synechococcus* sp. PCC 7002. Surprisingly, mutants missing the CpcB lyases were nevertheless capable of producing pigmented phycocyanin. 10K absorbance measurements revealed that the energy states of the β phycocyanin chromophores were only subtly shifted; however, 77K steady state fluorescence emission spectroscopy showed excitation energy transfer involving the targeted chromophores to be highly disrupted. Such evidence suggests that phycobilin orientation within the binding domain is specifically modified. We hypothesized that alternate, less specific lyases are able to act on the β binding sites. A phycocyanin linker-polypeptide deficient mutant was similarly characterized. The light state transition, a short term adaptation of the photosynthetic light harvesting apparatus resulting in the redistribution of excitation energy among the photosystems, was shown to be dominated by the reallocation of phycocyanin-absorbed excitation energy. Treatment with a high M phosphate buffer effectively prevented the redistribution of both chlorophyll *a*- and phycobilisome- absorbed excitation energy, suggesting that the two effects are not strictly independent. The mutant strains required a larger redistribution of excitation energy between light states, perhaps to compensate for their loss in phycobilisome antenna function.

# TABLE OF CONTENTS



## Thesis Body

## Acknowledgements

I would like to thank: Serguei Vasiliev, for his technical help with the equipment; Matt Scott, for introducing me to lab 'protocol'; John Veerman, for the insightful discussions (on all sorts of things); and every one else who has been brave enough to step into the Bruce lab. I also have to thank Doug Bruce for his consultation and especially for giving me this opportunity at Brock.

And a special Thank You to my family for putting up with me after long nights in lab collecting data and long days on the computer writing.

## List of Figures

## List of Tables

## Description of Abbreviations

1. APC, allophycocyanin, the major phycobiliprotein of PBS core
2. Chl*a*, chlorophyll a
3. CpcA, the α subunit of PC monomer
4. CpcB, the β subunit of PC monomer
5. D, dark treatment to drive cells to state 2
6. DD, cells locked in D with high phosphate followed by D treatment
7. DL, cells locked in D with high phosphate followed by L treatment
8. E, excitation energy
9. F, fluorescence intensity
10. FRAP, fluorescence recovery after photobleaching
11. FNR, ferredoxin $NAD(P)^+$ oxidoreductase
12. IEC, intersystem electron carriers
13. L, blue light treatment to drive cells to state 1
14. LD, cells locked in L with high phosphate followed by D treatment
15. LHCII, intrinsic thylakoid membrane Chl *a*/*b*-containing light-harvesting complex polypeptides of green algae and higher plants
16. LL, cells locked in L with high phosphate followed by L treatment
17. OCP, orange carotenoid protein
18. PBP, phycobiliprotein, composed of protein and associated chromophores
19. PBS, phycobilisome
20. PC, phycocyanin/ C-phycocyanin, the major phycobiliprotein of PBS rods
21. PCB, phycocyanobilin, the phycobilin (bilin/pigment/chromophore) of PC and APC
22. PE, phycoerythrin
23. PEC, phycoerythrocyanin
24. PQ, plastoquinone
25. PSI, photosystem I
26. PSII, photosystem II
27. TE, terminal emitters of PBS core
28. WT, wild-type

# INTRODUCTION

## I. Phycocyanin of the Cyanobacterial Phycobilisome

### Overview of the Phycobilisome

Phycobilisomes (PBS) are large water-soluble chromoprotein (biliprotein) complexes found in cyanobacteria, red algae, and cryptophytes. PBS serve to increase the antenna size of the photosynthetic apparatus and funnel this energy towards Chl*a* in the thylakoid membrane in a manner analogous to the family of intrinsic thylakoid membrane Chl *a*/*b*-containing light-harvesting complex polypeptides (LHCII) in higher plants (Glazer 1984; Glazer, 1989; Zilinska & Greenwald, 1986; Mullineaux *et al.*, 1990). PBS are primarily associated energetically with photosystem II (PSII) (Glazer, 1984), and are physically coupled with the stromal/cytoplasmic face of PSII dimers (Bald *et al.*, 1996). The chromophores of biliproteins are open chain tetrapyrroles that are covalently attached to the apoprotein by thioether bonds to cysteine residues. The biliproteins absorb radiation in regions of the visible spectrum where Chl*a* has low absorbance. The large biliprotein content in cyanobacteria gives these organisms their typical bluish colour. Though there are different structural types of PBS (MacColl, 1998), the typical cyanobacterial PBS is hemidiscoidal with 6 rods radiating out from a tricylindrical core. The core is composed of allophycocyanin (APC) trimers, arranged into cylinders. Stacks of hexameric phycoerythrin (PE) and/or phycocyanin (PC) disks form the rods (Figure 1; Glazer, 1989). Biliprotein organization within the PBS facilitates energy migration from rod to core; PE is the highest energy pigment, PC is of intermediate energy level, and APC is the lowest-energy pigment. Rod structure, number

of disks per rod, and PE:PC ratio can vary according to environmental light quantity and quality (Grossman *et al.*, 2001). The non-pigmented linker polypeptides serve in assembling rods (by connecting disks together) and cores (by binding APC trimers together), and also link the rods to the core. The $L_{CM}$ anchor polypeptide (ApcE) interconnects the core cylinders and is critical for PBS core assembly (Shen *et al.*, 1993).

Linkers modify the spectroscopic properties of biliprotein chromophores. Long wavelength emitting linkers help bridge the absorption/ fluorescence gap between dissimilar chromophores thereby insuring proper energy flow from PE to PC disk, PC rod to APC core, and APC core to the photosystems (MacColl, 1998; MacColl, 2004). The basal core cylinders also contain two copies each of the modified APC long wavelength chromophores ApcD (allophycocyanin-B or $\alpha^{B}$) and ApcF ($B^{18}$), and the N-terminal phycobilin protein domain of ApcE (Ashby & Mullineaux, 1999). These so-called "terminal emitters" (TE) are thought to be the source of intact PBS emission and are the prime candidates for donating excitation energy to Chl*a* of the photosystems (Glazer, 1987; Mullineaux, 1992; Stamatakis & Papageorgiou, 2001).

PBS were traditionally thought to be exclusively associated with PSII because the physical association between PBS and PSII is quite strong, allowing for the isolation of PBS-PSII complexes (Clement-Metral *et al.*, 1985), and PBS-absorbed excitation energy is predominantly transferred to PSII. However, PBS may also associate with photosystem I (PSI) for direct PBS to PSI energy transfer has been observed (Mullineaux, 1992; Mullineaux, 1994). The strong amino acid sequence homology between the rod terminal linker, CpcD, and the N-terminus of ferredoxin $NAD(P)^{+}$ oxidoreductase (FNR) has suggested that FNR binds to the distal regions of membrane proximal PC rods

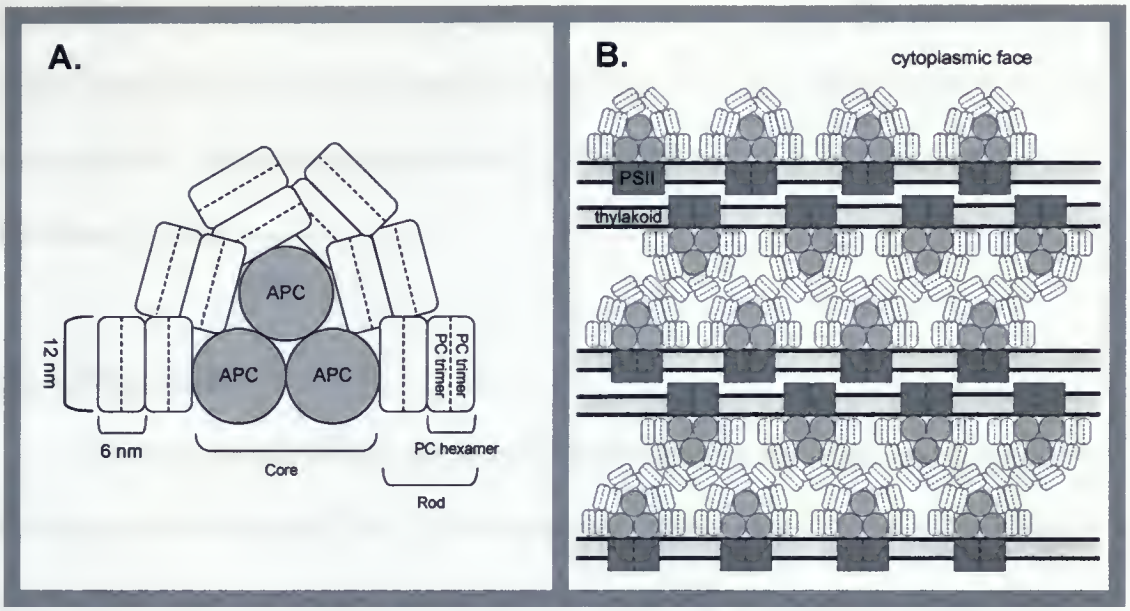


**Figure 1.** A cyanobacterial hemidiscoidal phycobilisome. **A**, Face view of a typical hemidiscoidal phycobilisome composed of (i) an APC containing tricylindrical core with (ii) PC containing rods radiating outwards. Some models propose that the four membrane-proximal PC rods run parallel to the thylakoid surface and to themselves and that the remaining two rods run parallel to themselves and perpendicular to the membrane (reviewed by Adir, 2005). The phycobilisome shown has rod lengths of two PC hexamers (also known as discs). See text for details. **B**, Schematic illustrating the interdigitating organization of phycobilisomes seen within many cyanobacterial thylakoid membrane systems (Lichtlé & Thomas, 1976; Olive *et al.*, 1986 & 1997). Phycobilisomes are shown associated with the cytoplasmic face of the thylakoid membrane positioned directly above PSII dimers in an arrangement characteristic of light state 1 conditions (Olive *et al.*, 1986 & 1997).

(Schluchter & Bryant, 1992; Gómez-Lojero *et al.*, 2003). This arrangement would facilitate $NADP^+$ reduction when PBS-PSI complexes form. It has also been proposed that direct excitation energy transfer occurs between rod PC and PSI Chl*a* (Bald *et al.*, 1996). In support, coreless PBS mutants were capable of transferring PC-absorbed excitation energy directly to PSI (Su *et al.*, 1992). Using studies with mutant cyanobacteria having defective PBS core terminal emitters, energy transfer pathways from PBS to PSII and to PSI have been presented for several cyanobacteria (Ashby & Mullineaux, 1999; Zhao *et al.*, 1992). The hydrophobic loop domain of ApcE is proposed to be involved in PBS coupling to the thylakoid membrane and/or PSII (Bald *et al.*, 1996; Barber *et al.*, 2003) yet mutants missing the loop domain have been shown to

have PBS functionally coupled to PSII (Ajlani & Vernotte, 1998). The detailed geometry of PBS-photosystem coupling is lacking, although there is information on the rates for energy transfer (Mullineaux & Holzwarth, 1991; Bittersmann & Vermaas, 1991; Mullineaux, 1994).

**Phycobiliproteins**

Phycobiliproteins (PBP) are found in cyanobacteria, red algae, and cryptophytes. PBP may account for up to 50% of soluble protein in cyanobacteria and red algae (Ke, 2001). Such a large metabolic commitment towards PBP synthesis illustrates the importance of PBP in light harvesting; PBS are the only auxiliary antenna system for PSII (and for PSI in cyanobacteria) in these organisms. PBP are water soluble, slightly acidic (PI ≈5), and stable from pH 5-9. All PBP are functionally and phylogenetically related, originating from a common ancestral protein (Apt *et al.*, 1995). PE rich PBS are often hemiellipsoidal; in contrast, PC rich PBS are usually hemidiscoidal in shape. There are four spectroscopic classes of PBP based on absorbance maxima: PE (500-565 nm), PEC (575 nm), PC (595-640 nm), and APC (650-655 nm). All cyanobacteria and red algae produce APC and PC; however, many cyanobacteria don't synthesize PEC or PE (Mimuro *et al.*, 1999). PBP are structurally related to the globin protein family (Apt *et al.*, 1995).

**PC Monomers, Trimers, and Hexamers**

Phycocyanobilin (PCB) is the phycobilin (chromophore) of PC and APC. Non-protein bound PCB assumes a cyclic conformation and shows an absorbance peak at 375

nm with a less intense peak at 690 nm. As PCB becomes more linear, as when bound in protein, UV absorption decreases while orange-red absorption increases (Scheer, 2003 and references therein). In native biliproteins the photophysical properties of the chromophores are changed dramatically over that of free phycobilin; absorptivities are increased by more than five fold ($\varepsilon \approx 10^5$), and the fluorescent lifetimes increase by four orders of magnitude increasing the yield of fluorescence to nearly 100% (Scheer, 2003). Upon association with linker polypeptides, absorptivities are further increased. The extinction coefficient of C-$PC_3$-$L_R$ complexes ("C-PC" denotes PC of cyanobacterial origin) show a 1100% increase and APC-$L_{CM}$ complexes show a 2600% increase over free un-protonated cyclic PCB, respectively (Klotz & Glazer, 1985).

The PC monomer is composed of one α (17 kDa) and one β (18 kDa) subunit, also known as CpcA and CpcB, respectively; the subunits show much sequence and structural homology (MacColl & Guard-Friar, 1987). A single PCB covalently binds to a cysteinyl residue at position 84 in the α subunit; two PCB covalently bind to cysteinyl residues at positions 83 and 153 in the β subunit (see Figure 2; residue numbering varies slightly among species). Protein-bound PCB are held in an extended conformation stabilized by H-bonding to neighboring amino acid residues, thereby promoting red shift in energy level and an increase in oscillator strength in the red region. Such reduction in chromophore flexibility reduces the de-excitation pathways of internal conversion, which in turn increases fluorescence yield (Ke, 2001). Specifically, the chromophore electronic states are influenced by the surrounding protein moieties via interactions with protein electric field, ionic interaction, and by H-bonds (Gantt *et al.*, 2003; Mimuro *et al.*, 1999).

PC trimers (and hexamers) aggregate spontaneously. PC trimer, $(\alpha\beta)_3$, is the smallest cytological occurring PC unit; monomers are only transiently formed during the PC assembly pathway. PC monomers link head to tail to form a trimer. The phycobilins are arranged in a circle, with α84 in the "paddles" of the wheel, β153 near the periphery, and β83 surrounding the central cavity (Figure 2). Trimers are 12 nm in diameter, 3 nm high, with a central cavity of 3.5 nm. In trimers the absorption maximum of the complex and of the individual chromophores are slightly red shifted and increased over that of monomers. Room temperature absorption maxima have been assigned to the chromophores β153 (598-602 nm), α84 (618-624 nm), and β83 (632-634 nm) (Mimuro *et al.*, 1986 a; MacColl & Guard Friar, 1987; MacColl, 1998). The close proximity (21 Å) of α84 to β83 in adjacent monomers may allow intermediate interaction with excitonic splitting giving a new absorbance band at 626 nm (Pizarro & Sauer, 2001). At 77K, *Synechococcus* sp. PCC 7002 $(\alpha\beta)_3$ PC shows three distinguishable absorbance peaks at 604, 626, and 636 nm (Pizarro and Sauer, 2001). However with *Spirulina platensis* at 5K, the absorption spectrum was divided into two sharp bands at 595 and 627.5 nm (Friedrich *et al.*, 1981). These temperature dependent changes may indicate that the β153 chromophore is being shifted to a less linear configuration at low temperature. The α84 and β153 chromophores are assigned as sensitizing while the β83 chromophore is assigned as fluorescing (Glazer, 1989).

Face-to-face aggregation of two trimers forms a hexamer with amalgamation mediated by the α subunits. The β subunits in the upper trimer are on top of the α subunits of the lower trimer. Figure 2 shows the x-ray structures of C-phycocyanin monomer, trimer, and hexamer.

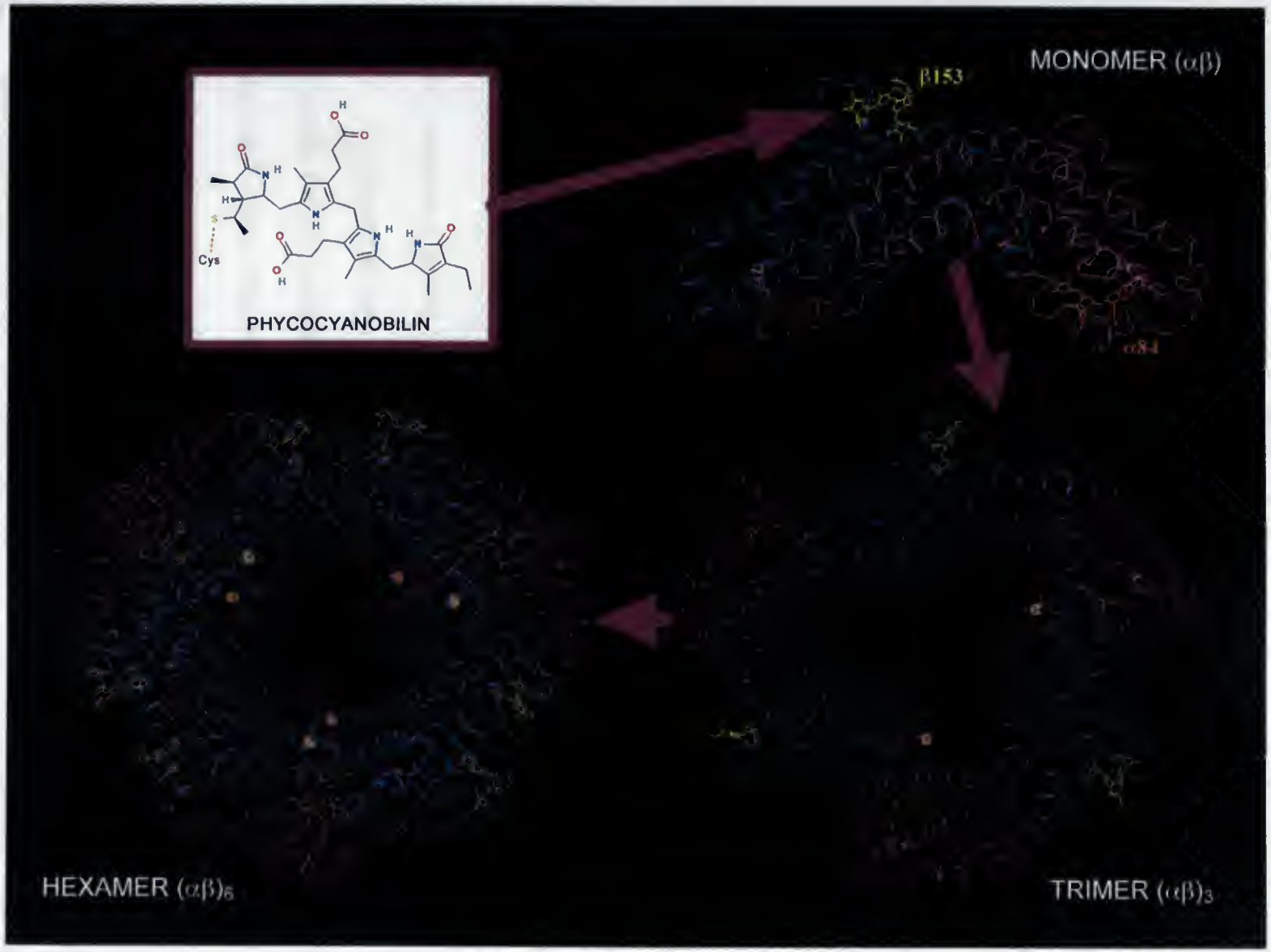


**Figure 2.** C-phycocyanin (PC) structure and oligomerization. PC monomer is composed of one α (shown as pink) and one β subunit (shown as blue). Phycocyanobilin is attached to PC apoprotein via a single thioether bond at positions β153 (chromophore shown as yellow), β83 (chromophore shown as red), and α84 (chromophore shown as orange). Three PC monomers link head to tail to form a trimer. The face to face aggregation of two trimers produces a hexamer. Linker polypeptides occupy the central cavity and serve to connect hexamers together to form PC rods. See text for further details. Monomer structure from *Synechococcus elongates*, Nield *et al.* (2003) PDB deposition # 1JBO. Trimer/hexamer structure from *Gracilaria chilensis*, Contreras-Martel *et al.* (2007) PDB deposition # 2BV8.

**PC Linkers**

Linkers are required for PBP assemblage above the hexamer level. Linkers are colorless polypeptides with molecular weights generally greater than any of the individual phycobiliprotein subunits (MacColl & Guard-Friar, 1987; Mimuro & Kikuchi, 2003). A linker of nomenclature $L_X^Y$ is associated with PBS domain X (i.e. R (rod) or C (core)) with a molecular weight of Y kDa. The molecular mass of linkers is estimated to be 10-20% of total PBS (Ke, 2001). The PC associated linkers of *Synechococcus* sp. PCC 7002 are: CpcD/ $L_R^{8.9}$, located at the distal end of the distal hexamer (terminates rod); CpcC/ $L_R^{32.3}$, located between PC hexamer stacks; and CpcG/ $L_{RC}^{28.5}$, positioned at the rod-core junction (de Lorimier *et al.*, 1990; Pizarro & Sauer, 2001). The exact location of linkers within hexamers is not known because no crystal structure that contains linkers has been obtained. A logical place for linkers to attach to PC hexamers would be to the central cavity as most linkers are basic and all are highly hydrophobic (Ke, 2001). Most of the linker polypeptide surface would be buried inside the hexamer with a short segment, the linker domain, projecting outward for attachment to adjacent PC hexamers or, as with $L_{RC}$, for attachment to APC core.

Major functions of linkers are to (i) stabilize hexamers, (ii) link hexamers together, and (iii) modulate energy levels of associated chromophores. As one works down a PC rod moving towards the core, the absorbance and fluorescence maxima of each hexamer become progressively more-red shifted. The most likely chromophore candidate for interaction with linkers would be the β83 chromophore because of its location in the central cavity. In addition to lowering energy levels, linkers also increase fluorescence lifetimes thus increasing the probability of energy transfer away from β83.

$L_{RC}$ may perturb the coupling interaction of the α84-β83 chromophore pair (Pizarro & Sauer, 2001) by further stretching the PCB tetrapyrole, thereby red shifting β83 spectroscopic properties. Without linker modification of the fluorescing chromophores' energy levels, inter-hexamer energy transfer would not be unidirectional - increasing the likelihood of back energy transfer up the rod and not down the rod towards the core.

A CpcC$^-$ strain of *Synechococcus* sp. PCC 7002, lacking in addition to the targeted $L_R^{32.3}$, $L_R^{8.9}$, showed reduced rod length (de Lorimier *et al.*, 1990). Whereas rods are typically two hexamers long in wild type PBS, CpcC$^-$ showed rods of only one hexamer in length. The N-terminal, CpcD-like domain of FNR is thought to substitute for $L_R^{8.9}$ allowing for attachment of FNR to the end of PC rods (Gómez-Lojero *et al.*, 2003). There are usually 1-2 FNR per PBS located at the distal ends of the thylakoid proximal rods (Gómez-Lojero *et al.*, 2003). In CpcC$^-$ and other mutants missing the terminal rod linker (de Lorimier *et al.*, 1990; Gómez-Lojero *et al.*, 2003), FNR could be found bound at the distal end of any rod with some PBS having FNR associated with all rods.

**Energy Flow in the PBS Antenna System**

With PC excitation, whole cyanobacteria cells show successive rise and fall in fluorescence from PC to APC to PSII/PSI (Mimuro, 1989; Mimuro *et al.*, 1989; Mimuro, 1990). Energy transfer efficiency from PBS to photosystem reaction centers is ~80-90%; by comparison the Chl*a*/*b* antenna system shows energy transfer efficiencies of ≥95% (Mimuro *et al.*, 1999). PBS have a large number of chromophores, so a small energy loss in individual steps will lead to a significant overall loss in transferred energy; for

example, a 1% loss in individual steps will result in 60% overall efficiency after a 50-step transfer (Mimuro *et al.*, 1999). So despite the high fluorescence yield in PBP, energy transfer in PBS is very efficient at individual transfer steps.

As shown in Figure 3, the main energy flow in the rod occurs via the β153 and α84 chromophores in dual pathways along the rod axis bridging adjacent trimers, with the β83 chromophores functioning as an energy pool in rapid equilibrium with the α84 chromophores (Mimuro *et al.*, 1986 a; Mimuro *et al.*, 1986 b; Mimuro *et al.*, 1989; Padyana & Ramakumar, 2006; Stec *et al.*, 1999). Linker-associated β83 serves as an energy sink for individual hexamers and transfers this energy down the rod to the next PC hexamer or, for core proximal hexamer, to APC of the core. Exclusive β153 energy transfer between adjoining hexamers may also occur. A "knob-into-holes" arrangement of PC discs, as mediated by van der Waals contacts and electrostatic interactions, creates a helical path of β153 chromophores around the periphery of the rod leading towards the PBS core; this pathway is favorable to excitation energy transfer (Stec *et al.*, 1999). Observable steady state fluorescence would arise most from chromophores with the largest fluorescence yield (i.e. lifetime * intensity). Because the hexamer is the primary energetic unit in PC rods, disc-to-disc and/or disc-to-core energy transfer are the limiting steps in energy flow thru rods (Glazer *et al.*, 1985; van Grondelle *et al.*, 1994; Mimuro *et al.*, 1999; Figure 3).

Fluorescence spectra of PC trimers show maxima between 640-653 nm, depending on linker association, with a much lesser peak/shoulder at 620-625 nm (Pizarro & Sauer, 2001; Shen *et al.*, 2006). The former fluorescence peak has been assigned to the β83 chromophore and the later peak has been assigned to β153. The β153

and α84 chromophores mainly act as sensitizing chromophores, whereas β83 functions as the fluorescing chromophore. α84 shows low fluorescence yield due to excitonic

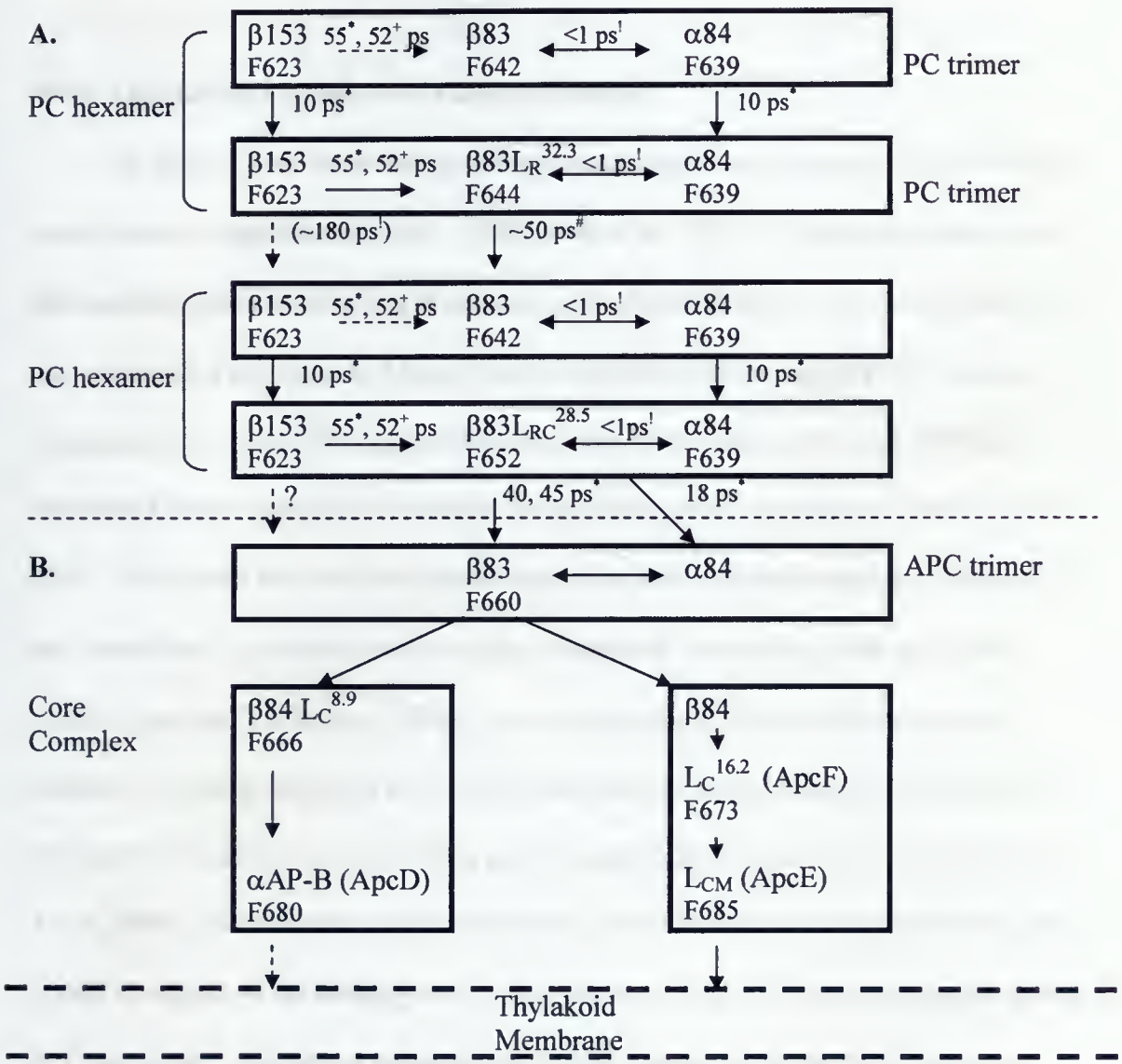


**Figure 3.** Energy flow among individual chromophores in a phycobilisome. **A,** Energy flow thru a 2 disc PC rod. **B,** Energy flow thru APC core to thylakoid membrane. Arrows represent viable excitation energy transfer pathways (those with transfer lifetimes less than 110 ps, excluding the β153 inter-disc pathway). Excitation energy transfer lifetimes between individual chromophores are shown above the arrows in A. Double arrows indicate excitonic splitting between α84-β83. Dashed arrows represent minor energy transfer pathways. Corresponding fluorescence emission maxima (F) appear below each chromophore. Pathways derived from: Mimuro (1989); Mimuro *et al.* (1989); Mimuro *et al.* (1986) a & b, within Ke (2001); Stec *et al.* (1999). Lifetimes from: *, Zhang *et al.* (1997); +, Debreczeny *et al.* (1995); #, Xie *et al.* (2002); !, Stec *et al.* (1999).

coupling with β83. Room and low temperature emission spectra of PBS show a major PC emission peak at ~650 nm which is characteristic of linker-associated β83 (Mimuro *et al.*, 1989; Pizarro & Sauer, 2001).

**Bilin Attachment and the PC Assembly Pathway**

A model for the early events in the assembly pathway of cyanobacterial PBS has been proposed (Anderson & Toole, 1998; Toole *et al.*, 1998). According to this model, chromophorylation of PC α and β subunits, as mediated by lyases, is a limiting step in the formation of monomer and higher order assemblies. Even though PBP subunits expressed in *E. coli* do form monomer complexes in the absence of attached bilins, attraction between subunits is strengthened by chromophore attachment (Arciero *et al.*, 1988). This could be caused by the chromophores inducing conformational changes in the apoproteins. Assembly mutations that disrupt α-β interactions, such as PC bilin deletion mutants (Toole *et al.*, 1998), would enlarge the population of transient free subunits as binding equilibria are pushed more towards dissociation, increasing subunit exposure to chaperones and providing greater opportunity for proteolysis (Anderson & Toole, 1998). The balance between degradation and biosynthesis for a phycobiliprotein is thus leveraged by the binding relationship between α and β in the monomer (Anderson & Toole, 1998). Significant populations of unassembled PC are not likely present in cells, for even PC assembly mutants show low levels of unassembled PC in the sucrose density gradients used in PBS isolation (Toole *et al.*, 1998; Swanson *et al.*, 1992) and stranded PBP subunits are rapidly degraded *in vivo* (Plank *et al.*, 1995).

The effect of a chromophore on αβ (monomer) formation can be attributed to the location of the chromophore within both the subunit individually and its location in reference to its binding partner (i.e. subunit interface). Using site directed mutagenesis of PBP genes in *Synechocystis* sp. 6701 in which bilin-binding cysteine residues were changed to alanines, Toole *et al.* (1998) showed the effect individual phycobilins have on α-β association. The β153 bilin spans the α-β subunit interface (Figure 2); the absence of β153 may distort CpcB protein conformation or disrupt β binding affinity to α, thereby shifting assembly equilibria towards dissociation and enhancing subunit degradation. Peripheral bilin deletion at β153 did cause a negative effect on PC stability in mutants of *Synechocystis* sp. 6701 and a mutant of *Synechococcus* sp. PCC 7002, which contained PC at ~20% of WT level (Toole *et al.*, 1998; Debreczeny *et al.*, 1993).

In the globin protein family, insertion of the haem group in a cleft analogous to that which the central bilin occupies in biliproteins, is a stabilizing factor for subunit folding (Lecomte *et al.*, 1996). Toole *et al.* (1998) proposed that the E and F helices of CpcA and CpcB may be disordered without the central bilin, introducing a structural flexibility at the interface that would antagonize subunit binding. Their β83 knock out mutants showed ~10% PC as wild-type (WT). Toole *et al.* (1998) further postulated that the interaction of an "unfinished" subunit with a bilin-replete assembly partner may stabilize the E–F domain at the subunit interface, forcing the final protein conformation without benefit of a central bilin. Their sedimentation equilibrium data indicate that such monomers are intrinsically weaker complexes that are subject to dissociation; however, subsequent assembly events (i.e. trimer formation and interaction with linkers) could stabilize PC complexes for incorporation into PBS (Toole *et al.*, 1998).

Absence of the central bilin (β83) and the resulting inability to complete the last step of the subunit folding pathway appears to have a greater impact on PC monomer formation than loss of the peripheral bilin (β153) and the ensuing disruption of α-β interactions (90% reduction in assembled PC compared to 80% reduction, respectively) (Toole *et al.*, 1998; Debreczeny *et al.*, 1993). Simultaneous deletion of both CpcB bilins blocked PC incorporation into PBS and reduced PC to levels where they could only be detected by immunodetection (Toole *et al.*, 1998). These results prove stability effects to be independent and additive for each CpcB bilin, and show that a CpcB subunit lacking both bilins makes a very poor binding partner for bilin-replete CpcA, thereby enhancing the exposure of both subunits to degradation pathways. CpcA lyase mutants of *Synechococcus* sp. PCC 7002 (Swanson *et al.*, 1992; Zhou *et al.*, 1992) incorporated PC αβ complexes into PBS at less than 10% of the WT level.

After PC αβ (monomer) complexes have formed, trimers assemble spontaneously. There is a proposed assembly pathway for PC rods (Mörschel & Rhiel, 1987; Yu & Glazer, 1982; Glazer, 1982). In brief, after trimer formation, trimers associate with a linker before an additional trimer is added to form a hexamer. Hexamers with $L_R$ can then join to form multiple-hexamer rods. All rods must terminate with hexamers associated with $L_{RC}$.

1) trimer + $L_R^{32.3}$ → trimer-$L_R^{32.3}$

2) trimer-$L_R^{32.3}$ + trimer → hexamer-$L_R^{32.3}$

3) hexamer-$L_R^{32.3}$ + hexamer-$L_{RC}^{28.5}$ → rod capable of binding to APC core

The $L_{RC}$ binding domain shows preferential binding to APC core and does not bind to other PC hexamers. The core-distal rod ends are capped with $L_R^{8.9}$ (CpcD) or, as

a substitute, the CpcD-like domain of FNR (de Lorimier *et al.*, 1990; Gómez-Lojero *et al.*, 2003). The central cavities of PC hexamers thus are required to be filled with linker polypeptide. This may aid in maintaining proper hexamer structural stability. PC hexamers without 2 associated linkers may become weakened and are more prone to disassociating into trimers (Bhalerao *et al.*, 1995).

The genes required for PC biosynthesis in *Synechococcus* sp. PCC 7002 are located within one major operon: $\overrightarrow{cpcBACDEF\_G}$ (Grossman *et al.*, 1993). This operon respectively contains the β subunit, α subunit, $L_R^{32.3}$, $L_R^{8.9}$, the α84 lyase (CpcE/F), and further downstream, $L_{RC}^{28.5}$. Thus translation order may reflect the assembly pathway. All structural genes required for rod synthesis are present and one PC lyase is also present, but two more lyase genes are required for complete PC synthesis.

**PC Lyases**

The attachment of phycobilins to apoprotein is mediated by lyases (Arcerio *et al.*, 1988; Swanson *et al.*, 1992; Zhao *et al.*, 2006 a & b; Shen *et al.*, 2006). It appears that specific enzymes facilitate bilin attachment at specific cysteine residue positions. However, spontaneous bilin addition to PC has been shown to occur in genetically engineered *E. coli* (Arcerio *et al.*, 1988). Different reactivities were described for each of the three bilin attachment sites in PC. No addition occurred at the β153 site; the product at the α84 site was primarily mesobiliverdin (a more oxidized bilin which contains an extra double bond between C2 and C3, characterized by ~$30^+$ nm red shift in the red-region absorbance maximum), and the product at the β83 site was a mixture of PCB and mesobiliverdin (Arcerio *et al.*, 1988; Shen *et al.*, 2006). This suggests different

accessibilities for PCB to binding site cysteine residues. Other studies have shown mesobiliverdin adducts capable of attaching to all three sites under high PCB concentrations (Zhao *et al.*, 2006 a; Shen *et al.*, 2006). The stereochemistry of PCB-attachment sites at β83 and α84 is *R*, whereas the stereochemistry at β153 is *S* (Duerring *et al.*, 1991; Ritter *et al.*; 1999), suggesting that at least two different enzymes would be required.

The enzyme mediating CpcA-84 bilin attachment has been identified in several cyanobacteria (Schluchter & Glazer, 1999; Swanson *et al.*, 1992). It is composed of two subunits, CpcE and CpcF, which are often coded on the PC operon (Bhalerao & Gustafsson, 1994; Bhalerao *et al.*, 1994; Zhou *et al.*, 1992). Similar genes have been found for phycoerythrobilin attachment to the α84 site in phycoerythrocyanin (PEC) (Fairchild *et al.*, 1992; Fairchild and Glazer, 1994). CpcS (CpeS) has been identified as a lyase for PCB attachment to β83 in PC and PEC (Shen *et al.*, 2004; Zhao *et al.*, 2006 a & b). Homologues for this gene have been identified in several cyanobacteria (Zhao *et al.*, 2006 a). Recently a new class of bilin lyase, CpcT, has been identified as being able to specifically attach PCB to the CpcB-153 site (Shen at al, 2006). *cpcT*- and *cpeT*-like genes are present in the genomes of all sequenced cyanobacteria that contain β153 equivalent chromophore positions - suggesting that this class of lyase is responsible for β153 chromophorylation (Shen *et al.*, 2006).

**_Synechococcus_ sp. PCC 7002 CpcB Lyase Null Mutants**

Mutations of the *cpcTSUV* genes in *Synechococcus* sp. PCC 7002 have yielded strains deficient in CpcB bilin attachment (Personal communication, Gaozhong Shen,

Penn State University). This gene family was first identified in *Fremyella diplosiphon* as *cpeS* and *cpeT* and is not part of the *cpcBACD* operon or related to the *cpcE* and *cpcF* genes that encode the CpcA lyase (Cobley *et al.*, 2002). There are three *cpeS*-like genes (*cpcSUV*) and one *cpeT*-like gene (*cpcT*) within the genome of *Synechococcus* sp. PCC 7002. *cpcT* and *cpcV* code for a putative PC lyase(s) for PCB attachment at β153; *cpcS* and *cpcU* code for a putative PC lyase(s) for PCB attachment at β83 and, possibly as well, PCB attachment to α82 and β82 cysteines of APC (Shen *et al.*, 2004; Shen *et al.*, 2006).

PBP lyases may not be as site specific as first considered. In *Synechococcus* sp. PCC 7002 the CpcB-83 lyase can apparently chromophorylate the CpcA-84 site (Swanson *et al.*, 1992; Shen *et al.*, 2004) and *cpcE/F* inactivation mutants of *Synechococcus* sp. PCC 7942 still showed chromophorylated PC (Bhalerao *et al.*, 1994). It has also been shown that CpeS can attach PCB to cysteine α84 of both PEC and PC (Zhao *et al.*, 2006 a). CpcA-84 lyase may in turn be able to chromophorylate the CpcB-83 site. Thus lyases responsible for cysteine 84 (83) bilin attachment are somewhat interchangeable, probably due to the fact that these sites are in the *R* conformation. Conversely, CpcT-like lyases may be able to bind bilin to the β153 cysteine residue (*S* conformation) of several different biliproteins.

In *Synechococcus* sp. PCC 7002, reversions of *cpcE/F* inactivation mutants showed PCB attachment at α129 due to a single amino acid substitution from Tyr to Cys located 5 Å from the α84 residue (Swanson *et al.*, 1992). This residue, which is conserved in all sequenced PC, forms part of the α84 binding domain. Perhaps the new α129 cysteine was more accessible to the β84 lyase. Absorption spectra of PC from this

revertant mutant and several descendent strains resembled that of wild type PC, though the extinction coefficient may have been decreased due to the presence of some bilin-deplete PC (missing PCB at α84) (Swanson *et al.*, 1992). Thus small changes in the position of the PCB chromophore may not cause strong enough alterations in tetrapyrole conformation and/or surrounding electrostatic field to induce changes in absorbance; however, such changes in chromophore orientation could affect energy transfer to neighboring pigments. The major form of energy transfer among phycobilins is by weak dipole-dipole interactions described in general by Förster (1948, 1959, 1965) and is directly proportional to the orientation and inversely proportional to the distance between donor and acceptor chromophores. Thomas *et al.* (1995) modified the protein environment of the β84 (β83) chromophore in *Synechococcus* sp. PCC 7002 by changing the β72 amino acid residue and indeed negatively affected intra- and inter-PC hexamer energy transfer.

## II. The Light State Transition of Cyanobacteria

### Overview

The light state transition (state transition) refers to a short term adaptation of the photosynthetic light harvesting apparatus in response to changing environmental and metabolic conditions resulting in a redistribution of excitation energy among PSII and PSI. The state transition mechanism in green plants involves a reversible association of LHCII with PSII and PSI triggered by the redox state of intersystem electron carriers

(IEC) and driven by the reversible phosphorylation of LHCII (for review see Allen, 1992; Wollman, 2001).

The state transitions of cyanobacteria are less characterized than those of plants even though a substantial amount of research has occurred in the field for over 40 years. State transitions in cyanobacteria are also triggered by changes in the redox state of IEC much in the same way as in plants (Mullineaux & Allen, 1990; Zhao *et al.*, 2001; Huang *et al.*, 2003; Li *et al.*, 2004). State 1 is achieved through oxidation of IEC (usually by "excess" excitation of PSI) and is characterized by an increase in PSII absorbance cross section and a rise in the amplitude of PSII fluorescence emission, occurring on a time scale of seconds to minutes (Fork & Satoh, 1983; McConnell *et al.*, 2002). State 2 is characterized by a decrease in the absorption cross section of PSII, a decrease in PSII variable fluorescence, and an increase in PSI absorbance cross section as compared with state 1 and is triggered by reduction of IEC either through "excess" PSII excitation or a net input of electrons from dark respiration (Mullineaux & Allen, 1986; Mullineaux, 1992; Huang *et al.*, 2003). Under state 1, PBS-absorbed excitation energy and Chl*a*-absorbed excitation energy have a higher probability of reaching PSII than PSI (van Thor *et al.*, 1998; McConnel *et al.*, 2002; Mullineaux & Emlyn-Jones, 2005). In cyanobacteria grown under "normal" conditions the PBS-dependent effect is quantitatively more significant and better characterized than that of Chl*a* (Emlyn-Jones *et al.*, 1999; McConnell *et al.*, 2002).

There are two principal schools of thought for explaining the mechanism behind state transitions in cyanobacteria, although no consensus can be drawn (van Thor *et al.*, 1998; Mullineaux, 1999; McConnel *et al.*, 2002; Mullineaux & Emlyn-Jones, 2005).

These are the "spillover" model in which there is a spillover of excitation energy from PSII Chl*a* to PSI Chl*a* in state 2 (Biggins & Bruce, 1989; Bruce *et al.*, 1989) and the "mobile PBS" model in which PBS can associate and disassociate from both PSII and PSI (Allen & Holmes, 1986; Mullineaux, 1992; Joshua & Mullineaux, 2004).

**Spillover Model**

In the spillover model, excess PSII Chl*a* excitation energy spills over to PSI Chl*a* in state 2 (Biggins & Bruce, 1989, Bruce *et al.*, 1989; Rouag & Dominy, 1994). This mechanism depends on a strong coupling between PBS and PSII Chl*a* and a variable coupling between PSII Chl*a* and PSI Chl*a*. Freeze fracture electron microscopy has shown the state transition to be accompanied by large-scale ultrastructural changes in PSII-containing EF particle organization in the thylakoid membrane (Olive *et al.*, 1986; Olive *et al.*, 1997). Linear dichroism studies have shown that state transitions in cyanobacteria are associated with changes in the orientation of APC and Chl*a* (Bruce & Biggins, 1985; Brimble & Bruce, 1989; Homer-Dixon *et al.*, 1994). Reversible changes in the association of isolated PSII and PSI induced by altering detergent concentration have been shown to be associated with state transition-like changes in low temperature emission spectra, providing further evidence for a role of varying PSII-PSI association in the state transition (Federman *et al.*, 2000). However, studies using fluorescence recovery after photobleaching (FRAP) have shown PSII to be immobile (Mullineaux *et al.*, 1997) and there has been no direct measure of PSI mobility (Mullineaux, 2004).

A gene specifically required for state transitions in cyanobacteria has been identified (Emlyn-Jones *et al.*, 1999). This gene, designated *rpaC*, codes for a previously

uncharacterized putative membrane protein unique to cyanobacteria (Emlyn-Jones *et al.*, 1999). *rpaC* deletion mutants grew more slowly than respective wild type cells under light limiting conditions and appeared to be permanently fixed in state 1, showing no state transition indicative fluorescence emission changes for excitation of PBS, but interestingly, retained some state transition-like changes with Chl*a* excitation (Emlyn-Jones *et al.*, 1999; McConnell *et al.*, 2002). Mutants of the *apcD* gene, which codes for the terminal emitter protein ApcD, have also been found to be state transition deficient with PBS excitation, yet still capable of state transition fluorescence emission changes with Chl*a* excitation (Zhao *et al.*, 1992; McConnell *et al.*, 2002). Such findings clearly indicate that the state transition mechanism is more complex than the simple spillover model. An updated model based on association changes between PBS-PSII complexes and PSI, consistent with independent pathways for the redistribution of PBS- and Chl*a*-absorbed excitation energy, has been presented (McConnell *et al.*, 2002).

**Mobile PBS Model**

The alternative model for the state transition mechanism involves the physical movement of PBS between the photosystems in a manner quite analogous to the redistribution of Chl*a*/*b* binding protein found in green plants (Allen & Forsberg, 2001). In this mobile PBS model, PBS are transiently bound to both photosystems with the majority of PBS associated with PSII under state 1 conditions (Mullineaux, 1992; Mullineaux *et al.*, 1997). Under state 2 conditions the affinity for PBS to PSII decreases and/or the affinity for PBS to PSI increases and a significant proportion of the PBS population would then spend the majority of its time functionally coupled to PSI

(Mullineaux, 1992; Mullineaux *et al.*, 1997; Aspinwall *et al.*, 2004; Joshua & Mullineaux, 2004; Sarcina & Mullineaux, 2004).

The application of FRAP to the cyanobacterial thylakoid has given much support towards mobile PBS. PBS seem to diffuse rapidly across the thylakoid membrane surface (Mullineaux *et al.*, 1997; Aspinwall *et al.*, 2004; Joshua & Mullineaux, 2004). PSI trimerisation and high osmotic strength buffers, which affect state transitions as determined from 77K emission spectra, also affect PBS diffusion (Aspinwall *et al.*, 2004; Joshua & Mullineaux, 2004). Although such evidence supports the involvement of mobile PBS in state transitions, this model can not stand alone and explain PBS-independent redistribution of Chl*a* excitation energy.

**Dual Nature (Combination) Models**

Both the "spillover" and "mobile PBS" models have substantial supporting evidence, however neither can completely explain all situations. Spillover requires PBS to be strongly coupled to PSII yet FRAP studies have shown PBS to be very mobile and PSII immobile (at least for large scale movement) (Mullineaux *et al.*, 1997). Mobile PBS cannot explain the apparent spillover of Chl*a* excitation energy between PSII and PSI, so the state transition is likely a representative of both models somehow intertwined. From the above-mentioned findings, it can be deduced that *rpcA* and ApcD are involved in PBS-mediated state transitions, with ApcD a likely candidate for excitation energy transfer from the PBS core to PSI and the *rpcA* gene product somehow involved in the signal transduction pathway (Mullineaux & Emlyn-Jones, 2005). Hence it seems that the classically observed state transition is really a combination of two separate components,

one being spillover of Chl*a* excitation energy and the other being variable PBS-absorbed excitation energy transfer to the photosystems.

Li *et al.* (2006) has shown spillover to be exclusive to "dark adaptation" in *Spirulina platensis* and dependent on PSI oligomerization with monomers predominant in dark adapted state 2, and trimers predominant in light adapted state 1. Yet many dark adapted state 2 emission spectra from other cyanobacteria do not show the corresponding blue shifts in PSI emission associated with trimer to monomer formation. In trimeric PSI of many cyanobacteria, far red Chl*a* are situated at the monomer-monomer interface and show a distinctive emission peak at ~760 nm (Shubin *et al.*, 1991; Shubin *et al.*, 1992; Kruip *et al.*, 1999; Karapetyan, 2004).

**Low- and High-Light State Transitions**

State transitions are enhanced in cyanobacterial cultures grown under low light conditions (Aspinwall *et al.*, 2004). The typical low-light state transition, as classically studied, functions to maximize the efficient use of absorbed light energy under conditions where light is limiting (Mullineaux & Emlyn-Jones, 2005). It has also been suggested that state transitions may play a role in protection against photoinhibition in high-light adapted cells (Fujimori *et al.*, 2005). Under high light conditions both photosystems are receiving more than adequate photon flux, so what is the reason for preferentially exciting one photosystem over the other? PSII is continually experiencing photodamage at all light levels but even more so in high light situations (Aro *et al.*, 1993). Reducing PSII antenna size would then help reduce the rate of PSII photodamage. Moreover, PSI mediated cyclic electron transport could provide a supply of ATP required for the PSII

repair cycle (Finazzi *et al.*, 2001). PSII photoprotection may also be mediated by PBS under high light conditions. Wilson *et al.* (2006) has recently described a mechanism for the quenching of PBS fluorescence involving the orange-carotenoid protein (OCP). OCP may act as the receptor and/or the quencher under high light conditions (Wilson *et al.*, 2006) and APC fluorescence seems to be specifically quenched (Scott *et al.*, 2006). Quenched PBS could then serve as a shield for PSII, protecting it from excess excitation. PBS excitation energy has also been shown to be quenched by IsiA protein complexes in iron stressed cyanobacteria (Joshua *et al.*, 2005).

It is unlikely, however, that low- and high-light state transitions involve the same mechanism. *rpaC* deletion mutants showed comparable doubling times to the wild type when grown under high light conditions (Emlyn-Jones *et al.*, 1999). The rate of PSII photodamage was not increased in the mutants and the PSII repair cycle was not inhibited (Mullineaux & Emlyn-Jones, 2005). This evidence leads to the conclusion that high-light state transitions are not governed by the same mechanism as low-light state transitions.

**Physiological Rationale behind the State Transition**

State transitions have been found to be physiologically important only at very low light levels (Emlyn-Jones *et al.*, 1999). In the wild, planktonic species can be exposed to both extremely intense light near the surface and to dim light at deeper depths during their continual vertical movement through the water column. Benthic species also experience varying light conditions due to floating matter blocking sunlight and ecological competition. A means to optimize use of absorbed photon energy would be

very beneficial to these organisms. Photosynthetic and respiratory electron flow both occur in cyanobacterial thylakoids, sometimes simultaneously, and they share numerous electron transport intermediates (Jones & Myers, 1963; Campbell *et al.*, 1998). Differing metabolic demands on ATP and NADPH supply would change the redox status of IEC and, consequently, induce a state transition. The state transition has enabled cyanobacteria to efficiently regulate their energy supply in response to the dynamic environmental and metabolic conditions that they encounter in nature.

**III. Purpose of Study**

The creation of the CpcB lyase null mutant strains (Shen *et al.*, 2004; Goazhong Shen, Penn State University, personal communication) has created an opportunity to examine the function of the individual β PC chromophores in light absorption and energy transfer in a manner analogous to the studies involving binding site Cys residue substitution mutations (Debreczeny *et al.* 1993, 1995). The CpcTV$^-$, CpcSU$^-$, and CpcSUT$^-$ strains are respectively missing the lyases attributed to β153, β83, and both β153 and β83 chromophorylation, and consequently, are expected to form PC rods lacking these specific chromophores. The purpose of this study is to use the CpcB lyase$^-$ mutants to identify the roles of the individual β PC chromophores in excitation energy transfer within the PC rod, and more generally, between PBS and photosystem Chl*a*. Any comprehensive examination of PBS to photosystem energy transfer must also include the light state transition. To preferentially study PBS to PSII energy transfer,

cells in light state 1 are favored; conversely, to study PBS to PSI energy transfer, state 2 cells are preferred.

The terminal rod linker-polypeptide mutant, CpcC$^-$, has been shown to be lacking the rod linker polypeptide $L_R^{33}$ and the rod terminal linker $L_R^{8.9}$ resulting in reduced PC rod length to only one hexamer and minor changes in room temperature spectroscopic properties (de Lorimier *et al.*, 1990). In order to see the effect the CpcB lyase$^-$ mutations have on PC disc and rod structure, CpcC$^-$ will be used in this study as a PC-structural-defect "standard" to compare to the CpcB lyase$^-$ strains.

The CpcB lyase$^-$ (and CpcC$^-$) mutants will be analyzed using room temperature and 10K absorbance and 77K steady state fluorescence emission spectroscopy. Altered chromophore-protein and chromophore-chromophore interactions are revealed as shifts in peak amplitude and position within the spectra. If the CpcB lyase$^-$ mutations are indeed preventing phycobilin attachment to the targeted binding sites then the absorption and emission bands associated with the targeted chromophore(s) will be missing, and other chromophores which interact with the targeted chromophore(s) will show shifted absorption bands only if they interact intimately (as with the excitonic splitting pair of $\alpha$84-$\beta$83); however, all chromophores involved directly or indirectly in energy transfer with the targeted chromophore(s) will show shifts in emission. What if the targeted chromophore's absorption and emission bands are not missing in the CpcB lyase$^-$ mutants (assuming the mutations are stable)? How then could phycobilin attachment transpire?

# MATERIALS AND METHODOLOGIES

**Strains and Growth Conditions**

*Synechococcus* sp. PCC 7002 wild type (WT) and the derived mutant strains CpcTV$^-$, CpcSU$^-$, CpcSUT$^-$, and CpcC$^-$ were a generous gift from Gaozhong Shen, Department of Biochemistry and Molecular Biology, Pennsylvania State University, University Park, PA. Cultures were grown in clear glass tubes of 3.5 cm diameter x 30 cm long, continuously bubbled with air, and continuously illuminated with light provided by spiral fluorescent bulbs at an intensity of 60 $\mu molm^{-2}\ s^{-1}$. A water bath was used to maintain cultures at a constant 38°C. Liquid cultures were grown in medium $A^+$ (McConnell *et al.*, 2002). All mutant cultures were supplemented with kanamycin at a final concentration of 100 mg/ml; gentamycin at a final concentration of 50 mg/ml was additionally added to the CpcTV$^-$, CpcSU$^-$, and CpcSUT$^-$ cultures. Mid-late log phase cultures were used to inoculate new cultures. Before collection of culture samples for experimental analysis the cultures were maintained at mid-late log phase for at least one week (or three growth cycles) by continuously draining some culture from the growth tube and adding fresh growth media. Cultures were not allowed to reach cell densities over $OD_{730} \approx 0.5$ to minimize self shading. Fresh antibiotics were added to the mutant strain cultures when starting a new culture, whenever new $A^+$ was added, or after 4 days of exposure of the antibiotic to 38°C (the point at which degradation of the antibiotics may begin). All cells were collected at mid-late log phase for experimental analysis.

**Room Temperature Absorbance Spectroscopy and Pigment Content Analysis**

Room temperature absorption spectra were taken on a DW-2 spectrophotometer equipped with computer driven Olis data acquisition (Aminco, Silver Springs, MD) using 1 cm path length quartz cuvette. A frosted glass plate was located directly behind the sample holder to compensate for light scattering of the sample. Slit width was set to 0.5 nm. Cell solutions were diluted with $A^+$ to a concentration at which $OD_{440}$= 0.7-0.8. Samples from six separate cultures were averaged. Chl*a* and PCB content were calculated using the method of Myers *et al.* (1980); however, PCB concentrations instead of PC concentrations were reported, as was also done by Ashby & Mullineaux (1999) and Emlyn-Jones *et al.* (1999). Chl*a* and PCB concentrations were normalized to $OD_{730}$ as an indicator of cell density (Zhao *et al.*, 2001). PC and APC content were calculated according to MacColl & Guard-Friar (1987).

**Low Temperature Absorbance Spectroscopy**

Cell samples for low temperature analysis had room temperature absorption spectra within the error of the above mentioned averaged spectra. Samples were prepared by spinning down 25 ml of mid-late log phase cells at 5,000 x **g** for 10 min and resuspending the pellets in 200 µl $A^+$. 140 µl of this concentrated cell suspension was combined with 5 ml 2.5 M sucrose. A home built absorption spectrometer was used to collect the data. It consisted of a 150 W halogen lamp as a light source and a spectrograph composed of a Triax 320 monochromator equipped with a liquid nitrogen ($LN_2$) cooled Symphony CCD detector using SynerJY software for data acquisition (HORIBA Jobin Yvon Inc, Edison, NJ). A HC-2 compressed helium cryostat was used

to cool samples to 10K (APD Cryogenics Inc, Allentown, PA). Samples were held between 2 polycarbonate discs sandwiching a silicon-rubber gasket. The distal (from the light source) polycarbonate disk was etched to compensate for light scattering of the sample. Sample path length was 0.13 cm. A lens was located between the sample holder and the spectrograph entrance slit. Spectrograph entrance slit was 0.006 mm and grating was 300 grooves/mm. Absorption spectra were created using the equation "$A=\mathrm{Log}(I_o I^{-1})$" in which $I_o$ was collected using 2.5 M sucrose only and $I$ was collected using the cell/sucrose suspension. Real $A$ values were ~ 0.5 at absorbance maxima.

**77K Steady State Fluorescence Emission Spectroscopy**

Preparation of Sample Tubes

"Dark adapted stock cell suspensions" refer to cell pellet/$A^+$ suspensions of $OD_{730}$=1.0 that had been dark adapted for 15 min. $OD_{730}$ measurements were taken with a Spectronic 20 spectrophotometer (Bausch and Lomb, Rochester, NY). 1M phosphate solutions were made from $KH_2PO_4$, pH 7.8. Sample tubes were made from 5 mm outer diameter x 3.5 mm inner diameter borosilicate glass. Aliquots of 0.2 ml were transferred to the sample tubes under dark conditions.

D and L tubes: 10 ml $A^+$ was added to 0.5 ml dark adapted stock cell suspension and then dark adapted for 5 min before for being distributed to sample tubes. "D" tubes were dark adapted for a further 5 min before being quickly submerged in $LN_2$ in the dark. "L" tubes were exposed to blue light (as defined by a Hoya glass B440 bandpass filter, HOYA Corporation USA, San Jose, CA) at an intensity of 50 $\mu molm^{-2}s^{-1}$ for 5 min before being quickly submerged in $LN_2$ in the presence of blue light.

LD and LL tubes: 0.5 ml dark adapted stock cell suspension was exposed to blue light for 5 min before adding 10 ml 1M phosphate. The suspension was then continuously stirred under the blue light for 5 more min before being distributed to sample tubes. "LD" tubes were dark adapted for 5 min before being frozen. "LL" tubes were exposed to blue light for a further 5 min before being frozen in $LN_2$.

DD and DL tubes: 10 ml 1M phosphate was added to 0.5 ml of dark adapted stock cell suspension. The suspension was then continuously stirred in the dark for 5 more min before being distributed to sample tubes. "DD" tubes were further dark adapted for 5 min before being frozen. "DL" tubes were exposed to blue light for 5 min before being frozen in $LN_2$.

A home built spectrofluorometer was used. The light source was a 75 W Xe arc lamp. The excitation monochromator was a Sciencetech Model 9055 controlled by a computer. Lamp housing and monochromator were from Sciencetech Inc. (London, ON). The sample holder was a custom dewar filled with $LN_2$. The emission side spectrograph was the same as described under "Low Temperature Absorbance Spectroscopy". Excitation bandwidth was 2 nm. Spectrograph entrance slit width was 0.100 mm and grating was 300 grooves/mm. The sample was protected with excitation appropriate short pass filters located at the exit slit of the excitation side monochromator. Samples were illuminated with light of intensity 3.5 $\mu molm^{-2}s^{-1}$ at all excitation wavelengths. The detector was protected with a Hoya glass R-60 longpass sharp cut filter; for the collection of excitation spectra the detector was further protected with a Hoya R-66 longpass sharp cut filter. To compensate for the random scattering and

heterogeneity associated with frozen samples, the sample tubes were continuously spun during data collection using a compressed air powered rotor. Errors in fluorescence yield from the same sample in different tubes were within 3% using this method. Baselines obtained from "blank" tubes containing only buffer (either $A^+$ or 1M phosphate) were subtracted from the collected spectra. At the sample concentrations used, further dilution did not produce noticeable changes in emission spectral shape. The same cell captures used for the 10K absorbance measurements were used for the 77K emission measurements.

**Spectral Fourth Derivative Analysis**

Fourth derivatives were taken of absorption and emission spectra using Synergy software (HORIBA Jobin Yvon Inc, Edison, NJ). For absorption spectra, differentiation intervals were varied according to chromophore type of interest; phycobilin absorbance peaks are characterized as having larger full width at half maximum (FWHM) than Chl*a* absorbance peaks.

# RESULTS AND DISCUSSION

## I. The effect of the Cpc$^-$ mutations on PC Chromophore Function

Phycobiliprotein (in this case PC) lyases have traditionally been identified by over expressing apo-PC and the lyase gene of interest in *E. coli* in the presence of extraneous PCB or by *in vitro* reconstitution experiments with the resultant PC spectroscopically characterized *in vitro* as trimers or even monomers (Arcerio *et al.*, 1988; Swanson *et al.*, 1992; Zhao *et al.*, 2006 a & b; Shen *et al.*, 2006). Likewise, detailed spectroscopic analysis of genetically engineered PC is usually done on isolated phycobiliproteins. Such *in vitro* studies would not adequately capture the phycobiliprotein's true native properties because defective PC is structurally weakened and tends to disassociate when isolated. There has never been a detailed *in vivo* spectroscopic examination of the *Synechococcus* sp. PCC 7002 CpcB lyase null mutant strains CpcTV$^-$, CpcSU$^-$, and CpcSUT$^-$. How will the loss of specific CpcB chromophores affect PC light absorption and energy transfer within the rod, PBS antennae function, and even the light state transition?

To answer these critical questions a strictly *in vivo* approach was taken. In this work, room and low temperature absorption and low temperature steady state fluorescence emission spectra were collected from whole cells: room temperature absorbance is used for pigment assays, 10K absorption spectra can reveal shifts in the energy states of individual PC chromophores, while 77K emission spectra are used to characterize energy transfer among the PC chromophores and thylakoid Chl*a*. 77K emission spectra were collected with preferential Chl*a* and PC excitation and with an excitation range spanning that of the yellow/orange phycobiliprotein absorbance region

(i.e. excitation spectra). To study the state transition, emission spectra were obtained from cells in both light state 1 and 2, and to further investigate the role of PBS mobility cells were "locked" into their pre-adapted light state with high M phosphate treatment.

**Cell growth**

The CpcB lyase null mutations, CpcTV$^-$, CpcSU$^-$, and CpcSUT$^-$ and the PC linker mutation, CpcC$^-$, were disrupting to cell growth. The mutants grew ~2.5x slower than WT under low light conditions (60 μmolm$^{-2}$ s$^{-1}$), yet they grew very poorly under high light conditions where WT grows optimally (150 μmolm$^{-2}$ s$^{-1}$). To increase the PC "signal" when collecting whole cell absorption and emission spectra, low light

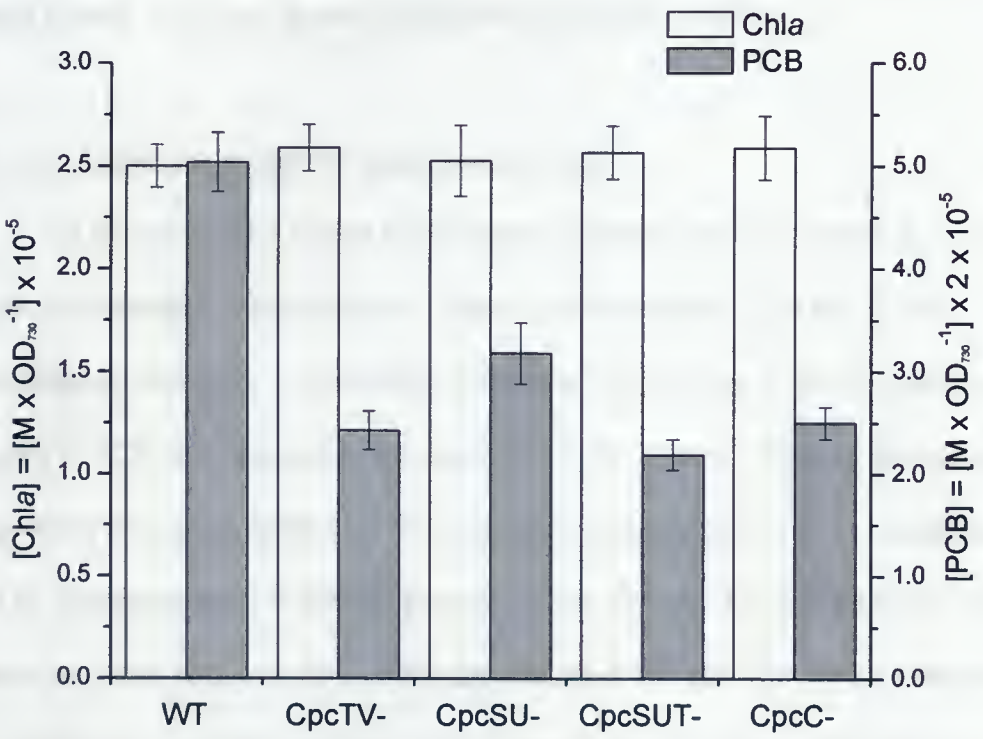


**Figure 4.** Cellular pigment content of *Synechococcus* sp. PCC 7002 strains. Chl*a* and phycocyanobilin (PCB) concentrations were calculated from whole cell room temperature absorbance according to the method of Myers *et al.* (1980) and normalized to $OD_{730}$ as an indicator of cell density. Error bars represent standard error among 6 separate cultures.

growth conditions (60 $\mu molm^{-2} s^{-1}$) were employed throughout the current study. Low light conditions increase cellular PC content by increasing PBS rod length (de Lorimier *et al.*, 1992). Even though the strains grew slowly they exhibited Fv/Fm values identical to WT (data not shown), indicating PSII function was not directly targeted by the mutations. A modulated light preferentially exciting Chl*a* (at 407 nm) was used to collect the room temperature fluorescence traces used in calculating Fv/Fm to negate any distorting phycobilin contributions to Fo.

The Cpc$^-$ mutations appeared stable as witnessed from monitoring liquid cell cultures systematically onward from the time of initial inoculation from agar plates. Absorption spectra and 77K emission spectra (435 nm and 575 nm excitation, data not shown) from cultures of the same growth phase did not change notably over a period of several growth cycles and growth cycle times did not vary either.

**The Cpc$^-$ mutations target PC absorbance *in vivo***

All strains showed similar Chl*a* content; however, the Cpc$^-$ strains showed significant decreases in PCB content. Figure 4 shows cellular Chl*a* and PCB concentrations and Table 1 shows the reduction of PBP content in the Cpc$^-$ strains. The majority of PCB decrease is linked to decreases in PC content. Figure 5 shows room temperature absorption spectra for WT and Cpc$^-$ cultures. Spectra were normalized to the Chl*a* $Q_y$ absorption band at 680 nm because strains showed little difference in Chl*a* content and other pigments show weak absorbance at 680 nm. It is easily seen that the Cpc$^-$ strains show a drastic decrease in PBP absorbance at ~630 nm and this peak may also be slightly red shifted. It is also evident that the mutant strains show a

**Table 1.** Changes in phycobiliprotein content induced by Cpc$^-$ mutations. Values are based on % of WT level and were calculated from the cell captures used for low temperature spectroscopy measurements.

| Strain | Decrease in PC | Decrease in APC |
|---|---|---|
| CpcTV$^-$ | 49.3 | 1.74 |
| CpcSU$^-$ | 24.1 | 6.79 |
| CpcSUT$^-$ | 48.5 | 3.74 |
| CpcC$^-$ | 46.8 | 0.00 |

noteworthy increase in carotenoid content as observed by the increase in absorbance from 425-530 nm.

To identify the chromophores responsible for the altered PBP absorbance observed within the Cpc$^-$ strains, 10K absorbance measurements were taken. At low temperature, absorption bands are narrowed due to decreases in temperature dependent random oscillation of the pigments' electrostatic field allowing room temperature absorption bands to be often split into their constituents (LeClerc *et al.*, 1979). As seen in Figure 6A, 10K absorption spectra show much more structure than that observed at room temperature (Figure 5). Absorbance from 660 nm outwards is dominated by Chl*a* containing protein complexes (i.e. photosystems); absorbance from 550-655 nm is dominated by PBP absorption (i.e. PBS). The strong shoulder at ~651 nm largely belongs to APC of PBS core and the major peaks around ~630 nm belong to PC. It is clear that the Cpc$^-$ strains showed less PC absorbance. To identify peak shifts among individual PBP absorption bands fourth derivatives were taken of the spectra. Fourth derivative analysis is very sensitive to changes in spectral shape associated with changes

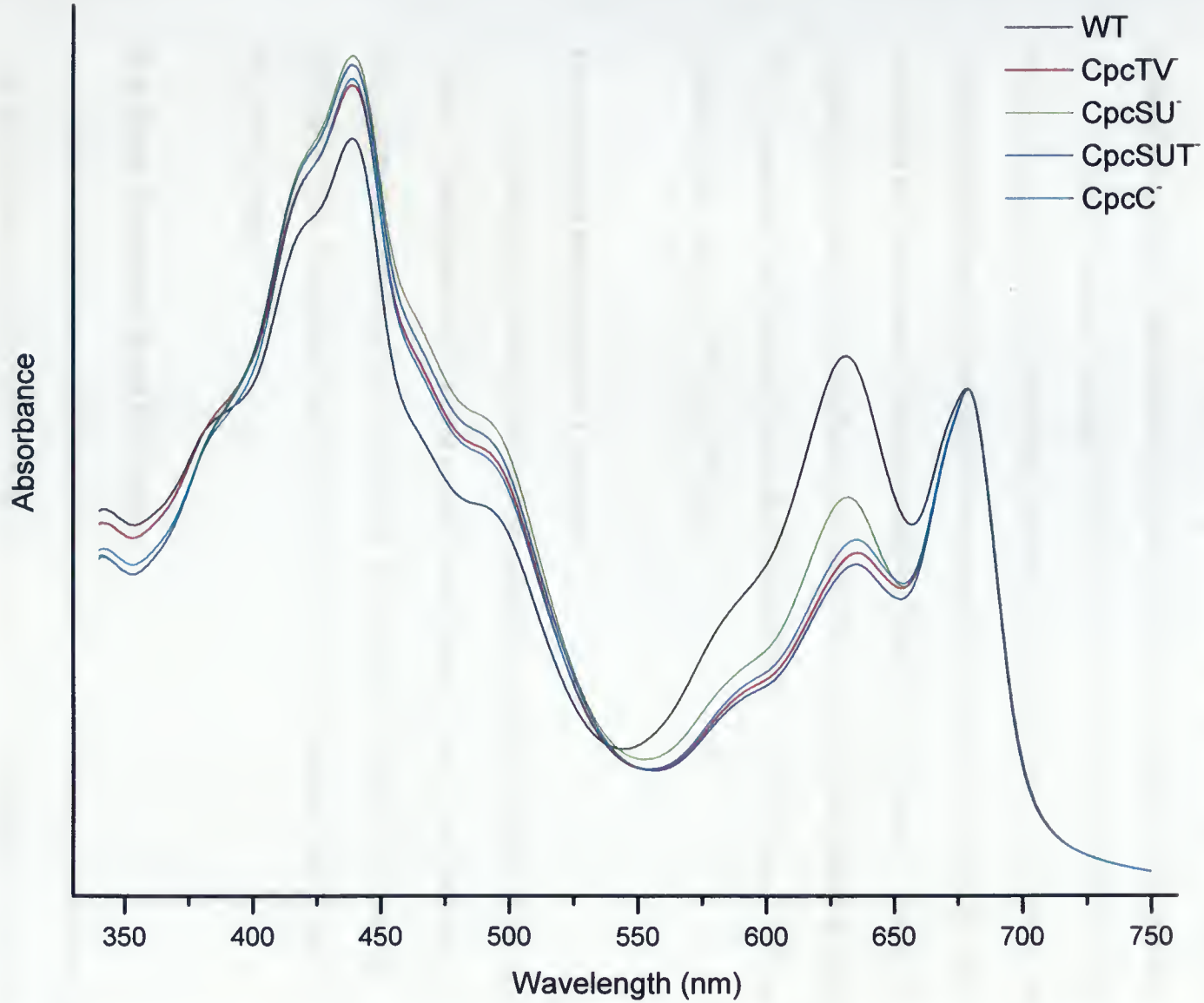


**Figure 5.** Whole cell room temperature absorption spectra for *Synechococcus* sp. PCC 7002 strains. Shown are the average spectra from six separate cultures. Standard error was within ±1.5% at absorption peaks for all strains. Spectra are normalized to the Chl*a* $Q_y$ absorption band at 680 nm.

in peak location (LeClerc *et al.*, 1979). The Cpc$^-$ strains show slight to significant peak location shifts within the PBP absorption region, particularly the 628 and ~609 nm bands (Figure 6B). Absorbance peak assignments are found in Table 2. Figure 6C shows fourth derivative analysis of the Chl*a* absorption region. No observable peak shifts are evident; hence the Cpc$^-$ mutations do not seem to affect photosystem Chl*a* absorbance.

To better characterize changes in PC absorbance induced by the Cpc$^-$ mutations, difference spectra were calculated from the 10K absorption spectra. Prior to subtracting Cpc$^-$ absorbance from WT, the spectra were normalized to 650 nm to correct for APC absorbance and, consequently, PBS core number (Figure 7A). The insert in Figure 7A emphasizes the shifts in PC absorbance maxima; difference spectra are shown in Figure 7B. It is apparent that the major loss in absorbance is from PC trimers ($\lambda_{max}$ of 631 nm with secondary peaks at ~591 and ~577 nm).

**The peripheral bilin is vital to PC assembly**

The mutations involving *cpcT* induce a substantial (~50%) decrease in PC content (Table 1). Recall that the β153 bilin bridges the αβ-subunit interface and may play a key role in monomer formation (see *Introduction: Bilin Attachment and the PC Assembly Pathway*). With disruption of this bilin, PC monomers and subsequent assemblages were less likely to form.

**Rod length is decreased in the Cpc$^-$ strains**

The ~50% decrease in PC found in the CpcTV$^-$/SUT$^-$/C$^-$ strains is accompanied by only small changes in APC content (Table 1). Thus PC:APC stoichiometry is cut in half, which is consistent with a reduction in rod length by half. Under low light levels WT

*Synechococcus* sp. PCC 7002 cells show PBS with rod length of two discs (de Lorimier *et al.*, 1990). PBS with half the PC as WT would contain rods of only one disc. For further evidence, PC absorbance at 625 nm is preferentially decreased relative to absorbance at 637 nm (Figure 7A insert). 625 nm is the absorption maximum of PC

**Table 2.** Peak assignments for fourth derivative analysis of *Synechococcus* sp. PCC 7002 whole cell 10K absorption spectra.

**A. Phycobiliprotein PCB (520-655 nm)**

| Peak position (nm) | Assigned absorbance band | Primary responsible phycobiliprotein | Reference |
|---|---|---|---|
| 578 | common shoulder | PC | 1 |
| 591 & ~609* | β153 | PC | 2 |
| 618 | α84 | PC | 3 |
| 626/628 | α84-β83 band splitting | PC | 1 |
| 638 | $L_{RC}$ associated β83 $\lambda_{max}$ | PC | 1 |
| 651.5 | APC core $\lambda_{max}$ (650#, 653! nm); PC $L_{RC}$ associated β84 shoulder (648 nm) | APC (& PC) | 4, 5, (1) |

**B. Photosystem Chl*a* (655-750 nm)**

| Peak position (nm) | Assigned absorbance band | Primary responsible photosystem | Reference |
|---|---|---|---|
| 660.5 | Chl*a* $Q_y$ | PSI and PSII | 6 |
| 670.5 | 669 nm shoulder | PSI | 7 |
| 679 | $\lambda_{max}$ | PSI | 7 |
| 685 | CP43 absorbance peak | PSII | 8 |
| 691 | CP47 absorbance peak | PSII | 9 |
| 698 | P700 $\lambda_{max}$ | PSI | 7 |

*Deconvoluted room temperature absorption spectra show broad peak at ~593 nm and a shoulder at 608 nm (ref 2). #650 nm, $\lambda_{max}$ of APC trimers (ref 4); !653 nm, $\lambda_{max}$ APC core with associated linkers and terminal emitters (ref 5). References are followed by temperature at which absorption spectra were recorded: 1, Pizarro & Sauer (2001), 77K; 2, Demidov & Mimuro (1995), room temp; 3, Mimuro *et al.* (1989), 77K; 4, MacColl & Guard-Friar (1987), room temp; 5, Gindt *et al.* (1994), room temp; 6, Scheer (2003), room temp; 7, Andrizhiyevskaya *et al.* (2002), 5K; 8, Groot *et al.* (1999), 4K; 9, Groot *et al.* (1995), 4K.

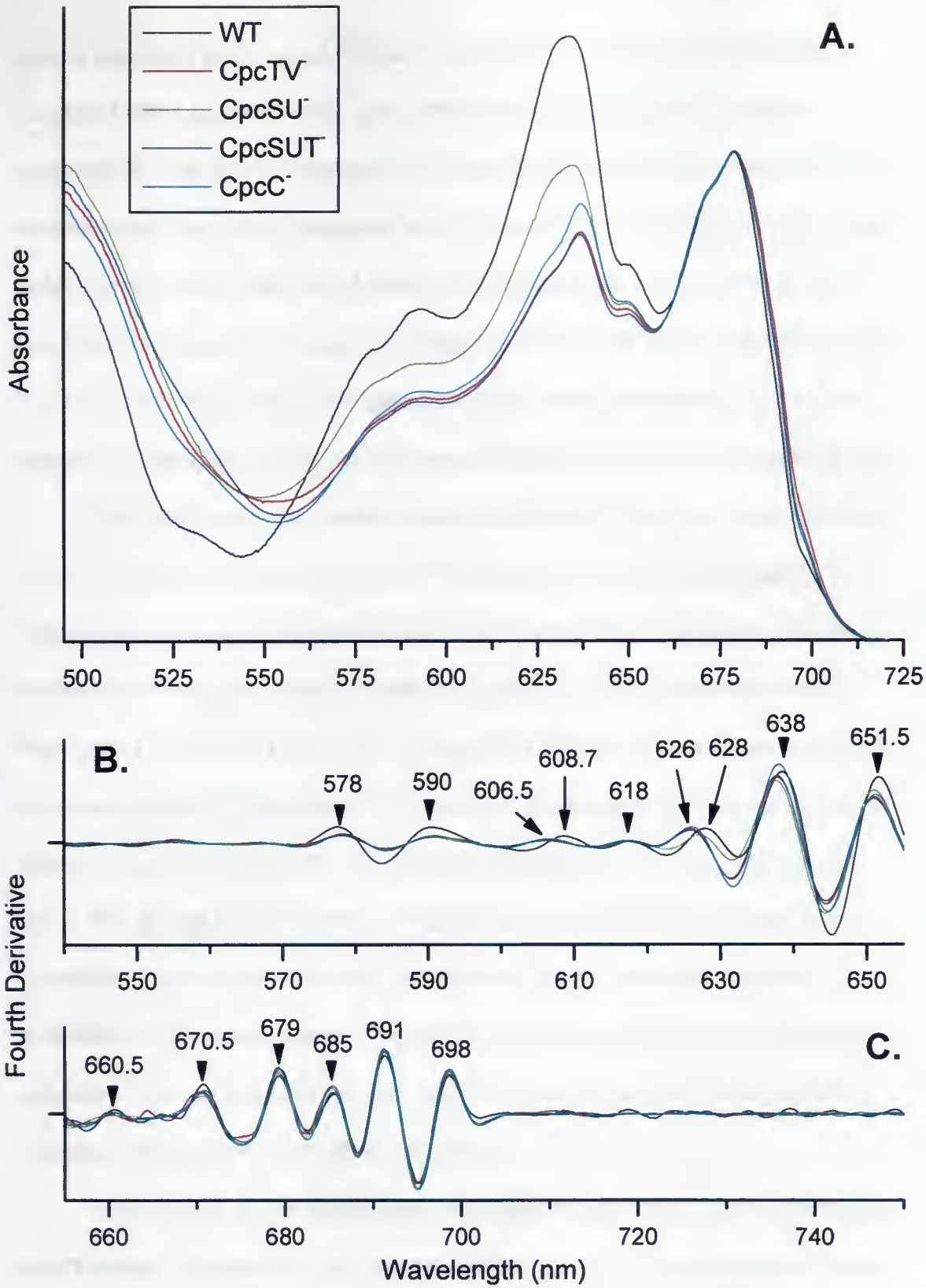


**Figure 6.** Absorbance at 10K for *Synechococcus* sp. PCC 7002 strains. Whole cells were suspended in 2.5 M sucrose. **A**, absorption spectra normalized to the Chl*a* $Q_y$ absorption band at 679 nm. **B**, Fourth derivative of spectra from 520-655 nm, which is dominated by phycobilin absorbance. Differentiation interval was 10 nm. **C**, Fourth derivative of spectra from 655-750 nm, which is dominated by Chl*a* absorbance. Differentiation interval was 5 nm.

trimers associated with $L_R$, and 637 nm is the absorption maximum of PC trimers associated with $L_{RC}$ (de Lorimier *et al.*, 1990; Pizarro & Sauer, 2001). It seems reasonable that the loss of absorbance at 625 nm in the CpcTV$^-$/SUT$^-$/C$^-$ strains is from a decrease in rod length from two discs, as in WT, to one disc. The PBS in CpcSU$^-$ would mostly contain rods of two discs, however to take in account the loss in PC (Table 1), they would be missing an average of ~2 discs per PBS (assuming each PBS has six rods), as is also visible from looking at Figure 7A (insert), where absorbance at 625 nm as compared to absorbance at 637 nm is decreased slightly in CpcSU$^-$ as compared to WT.

The CpcC$^-$ strain may contain a small population of trimer-only rods. Because CpcC$^-$ is missing core distal linkers, its PC hexamers are less stable and could disassociate into trimers, thereby forming rods of a single trimer associated with the $L_{RC}$. Evidence for trimer-only rods can be seen in Figure 7A; CpcC$^-$ shows very similar absorbance to that of the CpcTV$^-$/SUT$^-$ strains from 575–625 nm but shows an increase in absorbance at the 637 nm peak. The 637 nm peak is characteristic of $L_{RC}$ associated PC trimers (Pizarro & Sauer, 2001). This enhanced absorbance at 637 nm over the other strains that showed similar decreases in rod length (i.e. CpcTV$^-$/SUT$^-$) is thus from a population of rods composed of only one trimer in length. In support, electron microscopy of *Synechococcus* sp. 7942 mutants lacking either the 30 or 33 kDa rod-associated linker polypeptides (i.e. core distal linkers) showed an increased number of rods that terminated with a PC trimer (Bhalerao *et al.*, 1995).

Interestingly, the lyase mutations, in particular CpcSU$^-$/SUT$^-$, induced a decrease in APC content, whereas the CpcC$^-$ mutation did not (Table 1). In congruence, Shen *et al.* (2004) postulated that CpcS/U may act as an APC lyase.

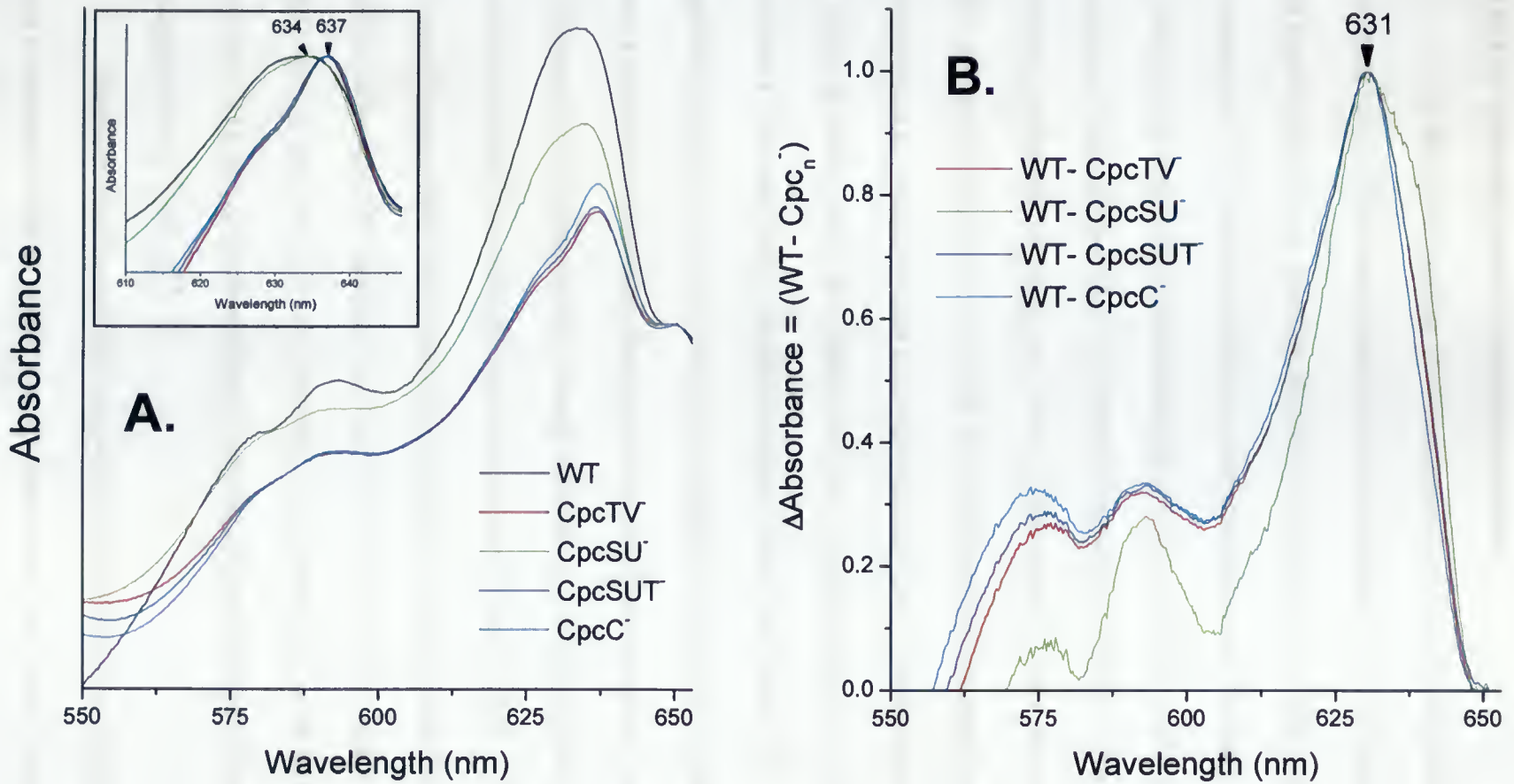


**Figure 7.** Differential PC absorbance among *Synechococcus* sp. PCC 7002 strains. **A**, the major phycobiliprotein absorbance region of the 10K absorption spectra normalized to the APC absorption peak (650 nm) where PC shows little absorbance. Normalized spectra can therefore be considered as approximately adjusted to APC concentration. Insert, PC absorption peaks normalized to maxima for ease of comparison. **B**, 10K absorption difference spectra. Spectra were calculated from the spectra in panel A (absorbance of Cpc⁻ strains was subtracted from that of WT); the resulting spectra were normalized to difference maxima for ease of comparison and are representative of missing PC absorbance.

**The Cpc⁻ mutations shift PC absorbance bands**

Not only is the quantity of PC decreased in the mutant strains but the energy levels of certain PC chromophores themselves are modified. When looking at the α84-β83 band splitting peak in Figure 6B (at 626/28 nm), the Cpc⁻ strains are blue shifted as compared to WT. Excitonic splitting is very sensitive to chromophore distance/ orientation; if bilin position or surrounding protein environment are altered (as when missing a linker polypeptide) this interaction would be modified. CpcC⁻ is known to be missing a linker (de Lorimier *et al.*, 1990), which may interact with the central bilin at β83, and in fact did show a 2 nm blue shift in the α84-β83 splitting band. If β83-linker associations are weakened then linker induced red shifting would also be reduced (Pizarro & Sauer, 2001). In support, the CpcC⁻ strain (and the rest of the mutant strains) showed a 1 nm blue shift in the β83-$L_{RC}$ absorbance band (Figure 6B). In CpcSU⁻ the α84-β83 band may be slightly blue shifted (Figure 6B); the loss of absorbance at ~645 nm (Figure 7B) may indicate alterations in $L_{RC}$-β83 interactions as $L_{RC}$-PC trimer complexes have a characteristic absorption shoulder at 648 nm (Pizarro & Sauer, 2001). The blue shifting of the α84-β83 band is strongest in CpcTV⁻/SUT⁻/C⁻ (Figure 6B), suggesting augmented disruption of the chromophore-chromophore interaction within these strains. Even though the CpcC⁻ mutation does not directly target PC chromophores, the effect on absorbance is very much the same as with the CpcTV⁻/SUT⁻ mutations – thus the β153 chromophore must play a similar structural/stabilizing role as the linker polypeptides $L_R^{33}$ and $L_R^{8.9}$.

Demidov & Mimuro (1995) showed a broad absorbance maximum at ~593 nm and a shoulder at 608 nm in their deconvoluted room temperature spectra of β153. In

congruence, I assigned two absorbance bands from the fourth derivative analysis to the β153 chromophore (at 591 and 609 nm, Table 2). Even though excitonic band splitting with other chromophores is infeasible for β153 (because there are no close neighboring chromophores) two distinct absorbance bands seem to be consistently assigned to β153. Perhaps the ~608 nm band represents an electronic state from a population of chromophores with a slightly different conformation and/or surrounding protein environment. The β153 chromophore is partially exposed to solvent molecules (Figure 2), making it more susceptible to conformational changes induced by solvent action, in particular during the freezing process. Low temperature absorption spectra of PC trimers, rod-core complexes, isolated PBS, and whole cells show β153 assigned absorption peaks ranging anywhere from 590-605 nm (Gray & Gantt, 1975; Friedrich *et al.*, 1981; Pizarro & Sauer, 2001) depending on buffer and species, which is the largest range among PC/APC chromophores. This variability in energy level probably arises from the relative flexibility of the PCB tetrapyrole within the β153 binding domain since, according to the PC hexamer crystal structure (Contreras-Martel *et al.*, 2007), it is not completely encapsulated in protein.

The mutant strains all show a blue shift in the ~608 nm absorbance band associated with the β153 chromophore in its most extended state (Figure 6B). It seems likely then that the $Cpc^-$ mutations are causing the PCB chromophore to be placed within the β153 binding site in a less stretched conformation and/or the influence of the surrounding protein environment has been altered.

The 651.5 nm absorbance band, attributed to APC, is blue shifted 0.5 nm in the mutant strains (Figure 6B). If these mutations specifically target PC chromophores, why

then is APC absorbance altered? The 651.5 nm peak from the fourth derivative analysis, in actuality, contains several populations of PBP absorbance bands: linker- and TE-associated APC of the basal core cylinders have a collective $\lambda_{max}$ of 653 nm (Gindt *et al.*, 1994), while APC of the upper core cylinder has a $\lambda_{max}$ of 650 nm (MacColl & Guard-Friar, 1987); furthermore, $L_{RC}$ associated β83 of PC has strong absorbance at 648 nm (Pizarro & Sauer, 2001). Recall that the mutant strains have a larger population of $L_{RC}$ associated β83 relative to non-$L_{RC}$ associated β83 than WT (because of reduced rod length) and, hence, would show more of the 648 nm absorbance component relative to overall PC absorbance. So the slight blue shift in the ~650 nm absorbance band may merely be the result of increased co-resolution of the β83-$L_{RC}$ band with the APC bands.

**The CpcB lyase null mutations did not inhibit chromophorylation at the targeted binding sites: An alternate lyase hypothesis for β phycobilin attachment**

If the CpcB lyase null mutations inhibited chromophorylation at the targeted bilin binding sites, corresponding absorbance bands should be missing; however, all mutants still show the same bands as in WT, albeit with some shifted (Figure 6B). Furthermore 77K steady state emission spectra show emission bands characteristic of CpcB chromophores (discussed below under "Excitation energy transfer within whole cells"). Thus chromophorylation is still viable; in fact, no significant levels of bilin-deplete PC could be detected from absorbance assays on any of the mutant strains (data not shown). If this was spontaneous bilin addition, mesobiliverdin would be the most likely PCB adduct and PC absorbance (and fluorescence) bands would be considerably red shifted (by $30^{+}$ nm) (Shen *et al.*, 2006). Possible explanations for lyase mediated

chromophorylation would include (i) another lyase can act at the site as is or (ii) point replacement mutations have occurred creating a new cysteine binding site within the bilin binding domain (as observed by Swanson *et al.*, 1992) allowing another lyase access to the binding site. Scenario (i) will be emphasized because the mutant strains appeared very stable during culturing and bilin lyases have been experimentally shown to be somewhat interchangeable (Swanson *et al.*, 1992; Bhalerao *et al.*, 1994; Shen *et al.*, 2004; Zhao *et al.*, 2006 a).

If the phycobilins are indeed being attached by another less specific lyase, the orientation of the attached bilin may be shifted. Such alterations would not drastically change the absorbance properties of chromophores that do not interact intimately with other chromophores (for there would be no extensive change in the surrounding protein environment); however, chromophores which share excitonic splitting would be more sensitive to small changes in chromophore distance and/or alignment, as was seen with the blue shifting of the α84-β83 absorbance band in the mutants. Conversely, energy transfer to neighboring chromophores could be severely altered for chromophore orientation is a determining factor in Förster resonance energy transfer. Modification of the β83 protein environment in *Synechococcus* sp. PCC 7002, as was done by changing the β72 amino acid residue in Thomas *et al.* (1995), negatively affected energy transfer within and between PC hexamers. The amino acid substitution caused a decrease in the longest fluorescence lifetime of the β83 chromophore and molecular dynamics calculations showed changes in tetrapyrole geometry to be responsible for decreasing fluorescence yield (Thomas *et al.*, 1995). A similar effect may be occurring in the $Cpc^-$ strains.

**Excitation energy transfer within whole cells**

77K steady state fluorescence emission spectra were collected to study energy transfer among the thylakoid associated chromophores within whole cells. Spectra were taken with 435 nm excitation (preferentially exciting Chl*a*) and 575 nm excitation (preferentially exciting PC). 77K emission spectra of cyanobacteria vary according to the light state they are in at time of freezing. To study state transition associated changes in excitation energy (E) transfer, state 1 and state 2 adapted cells were used. Cells were also locked in their pre-adapted light state using 1M phosphate buffer; high molar phosphate buffers prevent PBS mobility across the thylakoid membrane and can prevent state transition associated changes in the distribution of phycobilin-absorbed E (Joshua & Mullineaux, 2004).

Because PSI contains more than double the Chl*a* content of PSII (Rögner *et al.*, 1990), illumination of cells with light mainly absorbed by Chl*a* (i.e. blue and/or far red light) will preferentially excite PSI and induce a transition to state 1. However, because PBS fluorescence quenching can occur (Wilson *et al.*, 2006; Scott *et al.*, 2006), one must be careful to not use overly strong blue light. Dark adaptation allows for dark respiration to reduce the IEC pool driving cells to state 2. In this study blue light was used to drive cells to state 1.

Figures 8-1 and 8-2 show 77K steady state emission spectra for blue light- and dark- adapted cells with 435 and 575 nm excitation, respectively. Three major emission peaks are visible with 435 nm excitation: the 715 nm peak (F715) originates from the long wavelength Chl*a* of PSI, the 695 nm peak (F695) originates from the long wavelength Chl*a* of the CP47 protein of PSII, and the 685 nm peak (F685) is largely

attributed to Chl*a* of the PSII core. Relative photosystem stoichiometry can be estimated from the 435 nm excitation emission spectra by comparing the fluorescence intensity at F695 to the fluorescence intensity at F715. None of the Cpc$^-$ strains show drastic increases in PSII over WT indicating that their PBS were competent at providing the majority of light harvesting for PSII under growth conditions. Yet there are subtle changes; CpcTV$^-$ and CpcSU$^-$ may show an increase in PSI, and CpcSUT$^-$ and CpcC$^-$ may show an increase in PSII. The low shoulder at 670 nm may reflect back energy transfer from photosystem Chl*a* to PBS core. State 2 cells are characterized as showing an increase in PSI emission and a decrease in PSII emission. Table 3A shows peak assignments for fourth derivative analysis of the 77K emission spectra obtained with 435 nm excitation. The major fluorescence peak positions show no dependence on light state (Figure 9-1).

As seen in Figure 8-2, upon PC excitation the phycobiliproteins are the major contributors to cell emission either by direct fluorescence or from energy transfer to the photosystems. PC fluorescence components are visible from 620-650 nm and non-TE APC fluorescence peaks at 665 nm. With bilin excitation, F685 (now actually F684) is dominated by the TE of the PBS core. PSII and PSI fluorescence are still visible at F695 and F715, respectively. The light states are also quite evident from the spectra; state 1 can generally be described as an increase in PBS-PSII energy transfer at the expense of PBS-PSI energy transfer over state 2. Table 3B assigns the 575 nm excitation fluorescence peaks as identified from fourth derivative analysis. As with 435 nm excitation, emission peak positions are independent of light state (Figure 9-2).

High M phosphate treatment effectively locked all strains into their pre-adapted light state as determined from excitation at both 435 nm (Figure 10-1) and 575 nm

**Table 3.** Peak assignments for fourth derivative analysis of *Synechococcus* sp. PCC 7002 whole cell 77K steady state emission spectra. ( ) indicate chromophore responsible for fluorescence emission.

**A. 435 nm excitation**

| Peak position (nm) | Primary contributing component | Reference |
|---|---|---|
| 665.5 | APC ($\beta$83-$L_C^{8.9}$) | 1 |
| 670 | PSII (Chl*a*) | 2 |
| 673 | TE (ApcF) | 1 |
| 685 | PSII (all core antenna Chl*a*) | 2 |
| 695 | PSII (antenna Chl*a* of CP47 protein) | 2 |
| 715 | PSI (long wavelength Chl*a*) | 3 |

**B. 575 nm excitation**

| Position (nm) | Primary contributing component | Reference |
|---|---|---|
| ~620 & ~632 | PC ($\beta$153)* | 1, 4 |
| 640 | PC ($\alpha$84 ) | 1 |
| 642 | PC ($\beta$83) | 5 |
| 644 | PC ($\beta$83-$L_R^{32.3}$) | 1, 6 |
| 652.3 | PC ($\beta$83-$L_{RC}^{28.5}$) | 1, 6 |
| 665.5 | APC ($\beta$83-$L_C^{8.9}$) | 1 |
| 673 | TE (ApcF) | 1 |
| 684/685 | $TE^+$ (ApcE/$L_{CM}$; 683 nm) & $PSII^+$ (core antenna Chl*a*; 685 nm) | 1, 2, 7 |
| 695 | PSII (long wavelength Chl*a* of CP47 protein) | 2 |
| 715 | PSI (long wavelength Chl*a*) | 3 |
| 755! | PSI (far-red antenna Chl*a* found at monomer-monomer interface of PSI trimers) | 8 |

*$\beta$153 shows broad emission peak at 625 nm (ref 1, 4); however, deconvoluted spectra show splitting into peaks at 619 and 631 nm (ref 4). +Bands are co-resolved with ApcE being the major contributor. !Band not readily resolved with fourth derivative; yet broad shoulder visible in emission spectra. 1, Mimuro *et al.* (1989); 2, van Amerongen & Dekker (2003); 3, Shen & Bryant (1995); 4, Demidov & Mimuro (1995); 5, Mimuro *et al.* (1986 a); 6, Pizarro & Sauer (2001); 7, Gindt *et al.* (1994); 8, Karapetyan (2004).

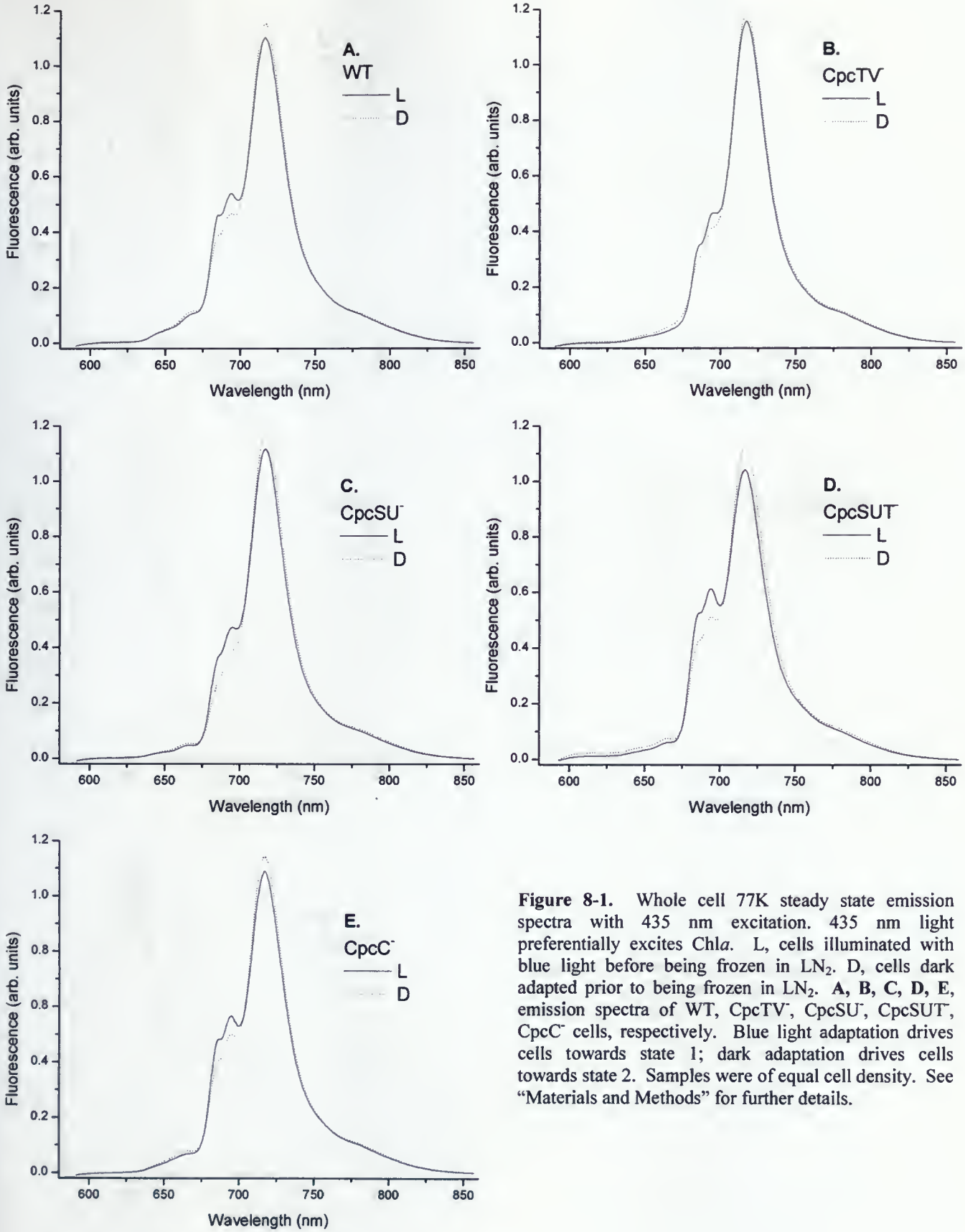


**Figure 8-1.** Whole cell 77K steady state emission spectra with 435 nm excitation. 435 nm light preferentially excites Chl*a*. L, cells illuminated with blue light before being frozen in $LN_2$. D, cells dark adapted prior to being frozen in $LN_2$. **A, B, C, D, E,** emission spectra of WT, CpcTV⁻, CpcSU⁻, CpcSUT⁻, CpcC⁻ cells, respectively. Blue light adaptation drives cells towards state 1; dark adaptation drives cells towards state 2. Samples were of equal cell density. See "Materials and Methods" for further details.

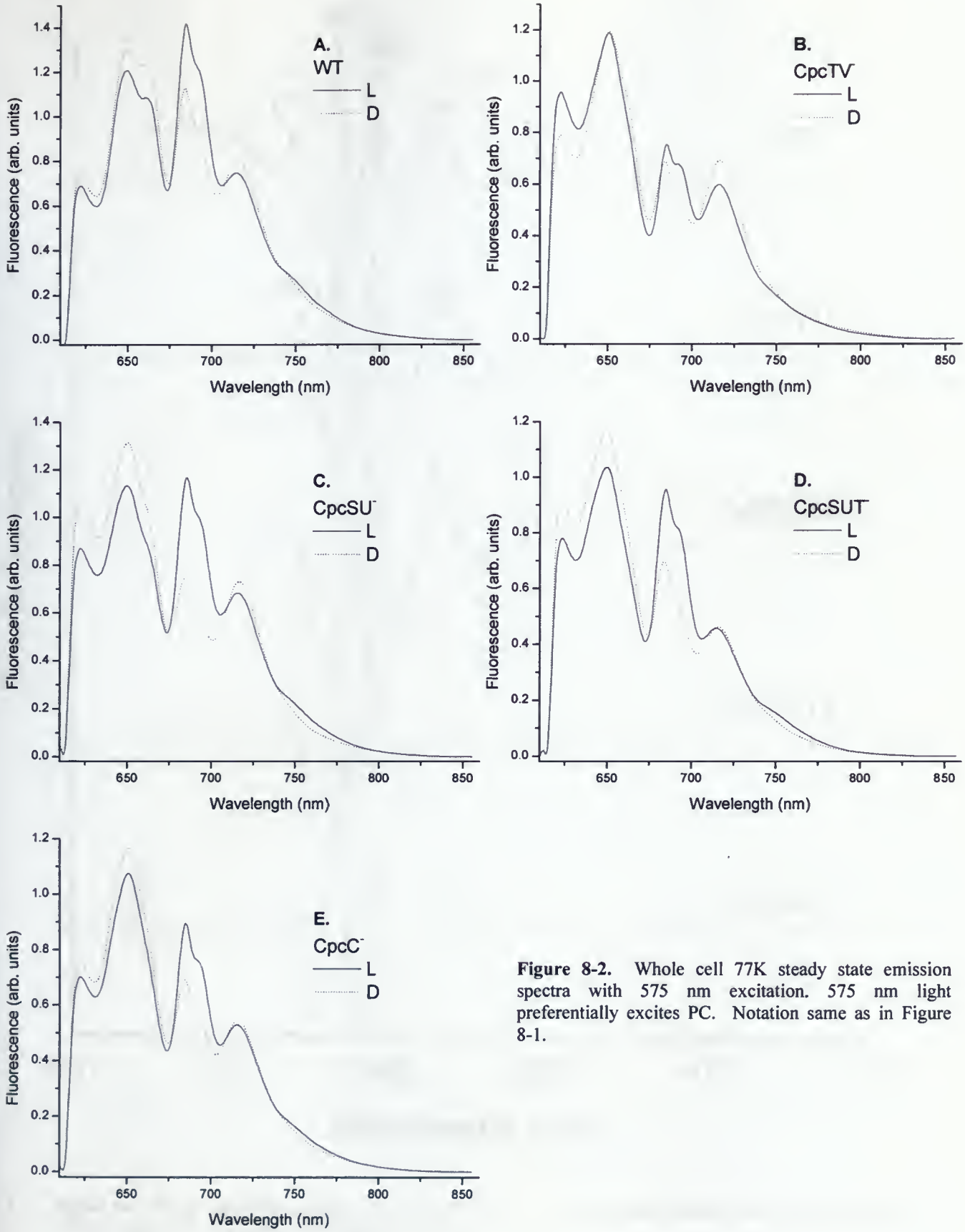


**Figure 8-2.** Whole cell 77K steady state emission spectra with 575 nm excitation. 575 nm light preferentially excites PC. Notation same as in Figure 8-1.

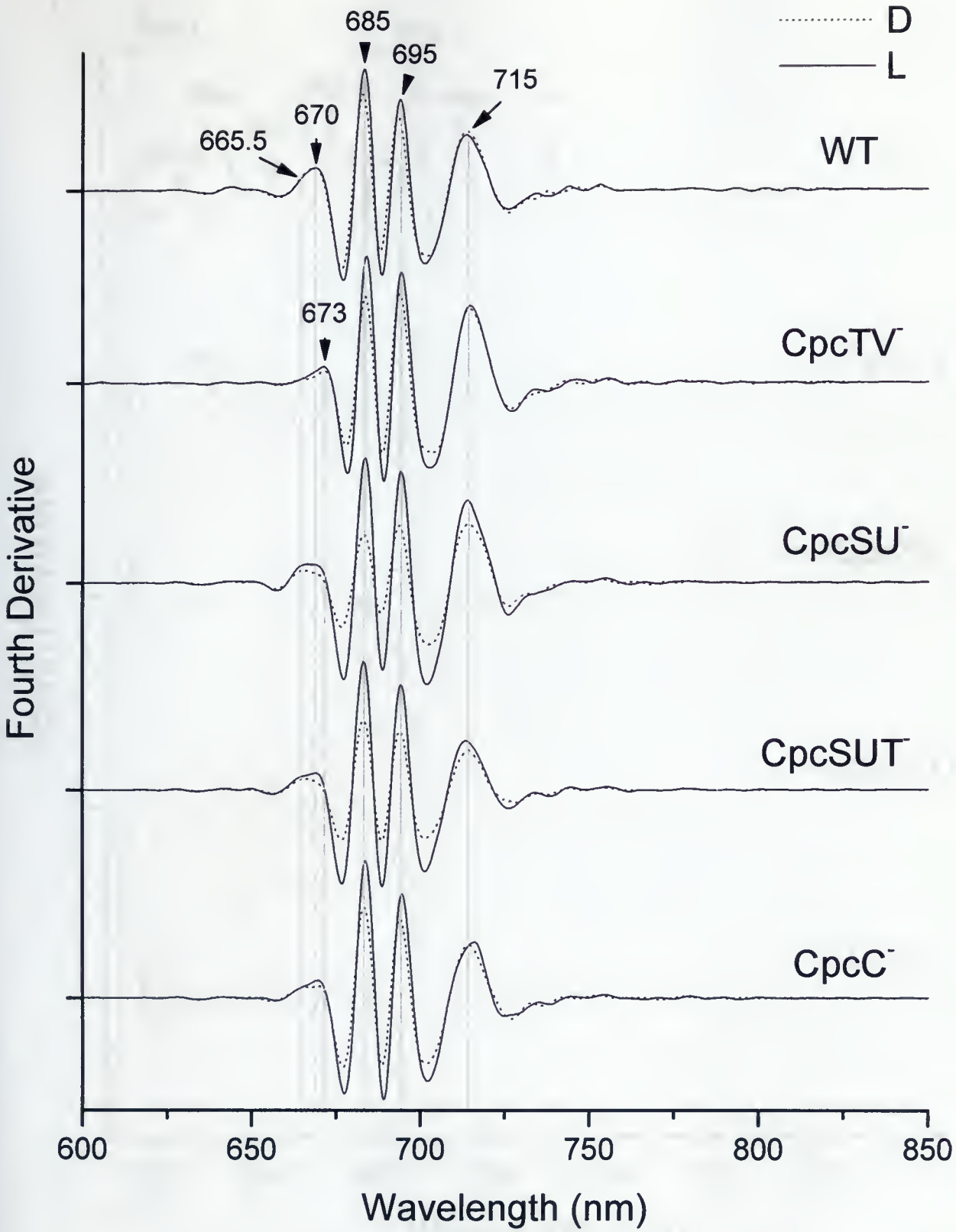


**Figure 9-1.** Fourth derivative analysis of whole cell 77K steady state emission spectra with 435 nm excitation. Notation same as in Figure 8-1. Differentiation interval of 7.5 nm.

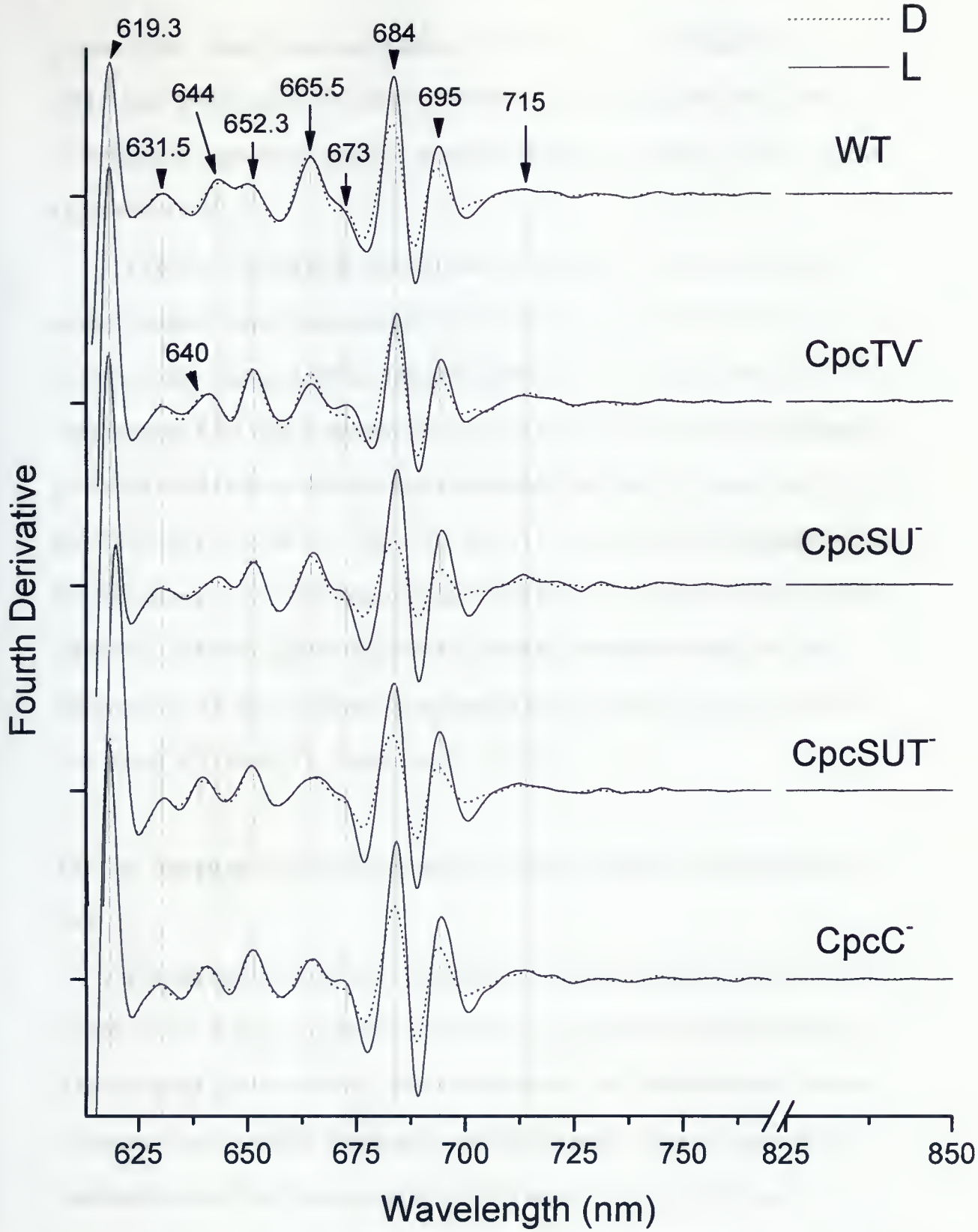


**Figure 9-2.** Fourth derivative analysis of whole cell 77K steady state emission spectra with 575 nm excitation. Notation same as in Figure 8-1. Differentiation interval of 7.5 nm.

(Figure 10-2). Minor discrepancies among "fixed" spectra are examined in Appendices XVI-XVIII. Fourth derivative analysis of emission spectra from phosphate treated cells gave the same peaks as in Figures 9-1 and 9-2 with both 435 nm and 575 nm excitation (Appendices I-IV).

To further investigate E transfer pathways involving PC-absorbed excitation energy, emission spectra were collected with excitation encompassing that of the PC/APC yellow/orange absorbance region (Figures 11-15). These excitation spectra were collected from cells in standard state 1 and state 2 conditions and from the high M phosphate treated cells to determine which pigments preferentially transfer their E to PSII and PSI in state 1 and state 2. F685, F695, and F715 were monitored to determine which terminal acceptors PC E was reaching (Figures 16 & 17). To detect at which excitation wavelengths absorbed light energy was not reaching the terminal energy acceptors, difference spectra were calculated by subtracting the excitation spectra of the mutants from that of WT (Figure 18, Appendices XI & XII).

**The Cpc$^-$ mutations alter excitation energy transfer among PC chromophores *in vivo***

Fluorescence intensity ratios can indicate E transfer pathways - observed as a loss of fluorescence at donor chromophore and rise of fluorescence at acceptor chromophore. If the E transfer pathway between them is disconnected, an increase in donor emission will occur at the expense of the acceptor. For cells exposed to non-photodamaging light conditions, phycobilin fluorescence (particularly that arising from PC) is rarely quenched *in vivo*. For steady state emission at 77K quenching of fluorescence through photochemistry is also negligible.

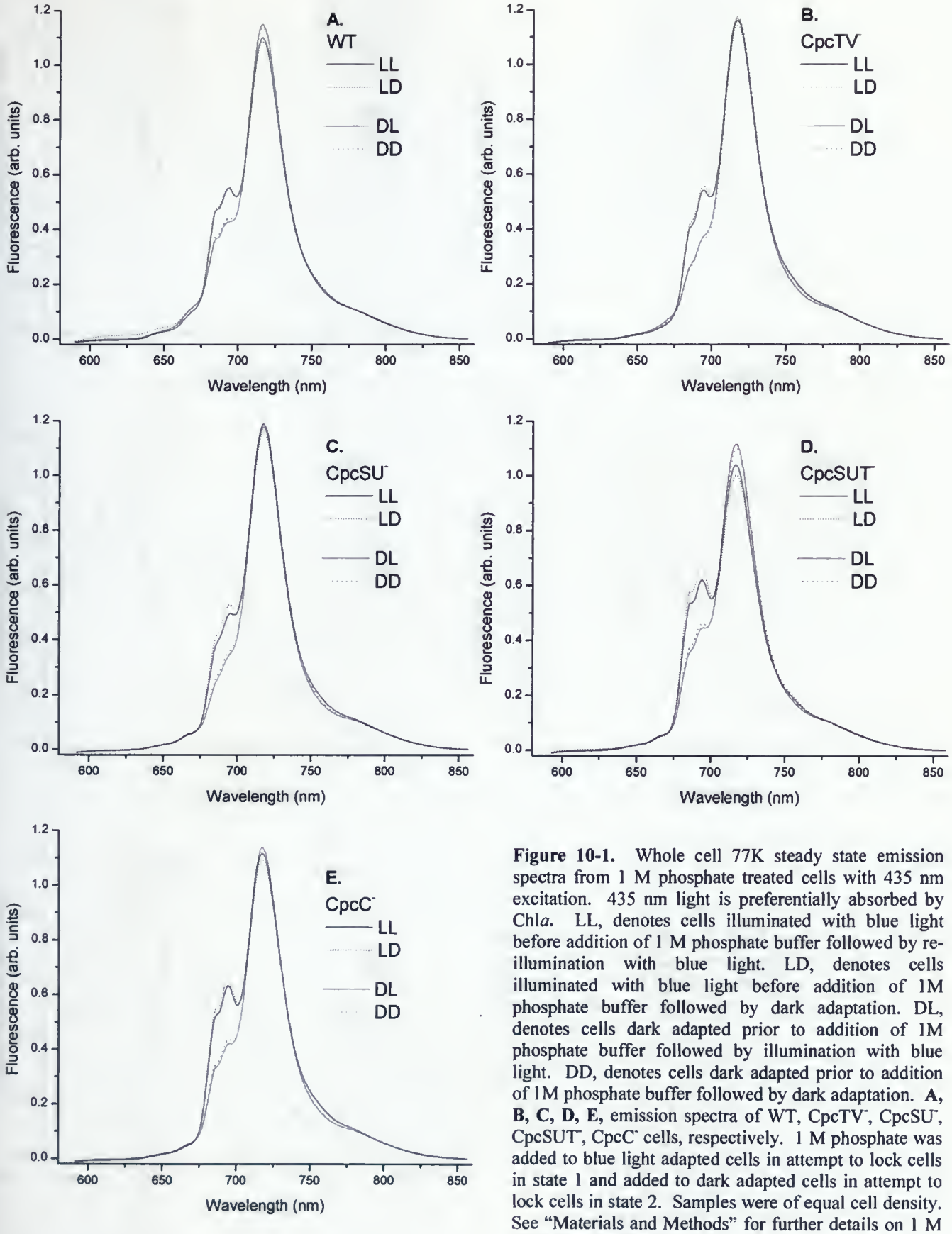


**Figure 10-1.** Whole cell 77K steady state emission spectra from 1 M phosphate treated cells with 435 nm excitation. 435 nm light is preferentially absorbed by Chl*a*. LL, denotes cells illuminated with blue light before addition of 1 M phosphate buffer followed by re-illumination with blue light. LD, denotes cells illuminated with blue light before addition of 1M phosphate buffer followed by dark adaptation. DL, denotes cells dark adapted prior to addition of 1M phosphate buffer followed by illumination with blue light. DD, denotes cells dark adapted prior to addition of 1M phosphate buffer followed by dark adaptation. **A, B, C, D, E,** emission spectra of WT, CpcTV⁻, CpcSU⁻, CpcSUT⁻, CpcC⁻ cells, respectively. 1 M phosphate was added to blue light adapted cells in attempt to lock cells in state 1 and added to dark adapted cells in attempt to lock cells in state 2. Samples were of equal cell density. See "Materials and Methods" for further details on 1 M phosphate treatments.

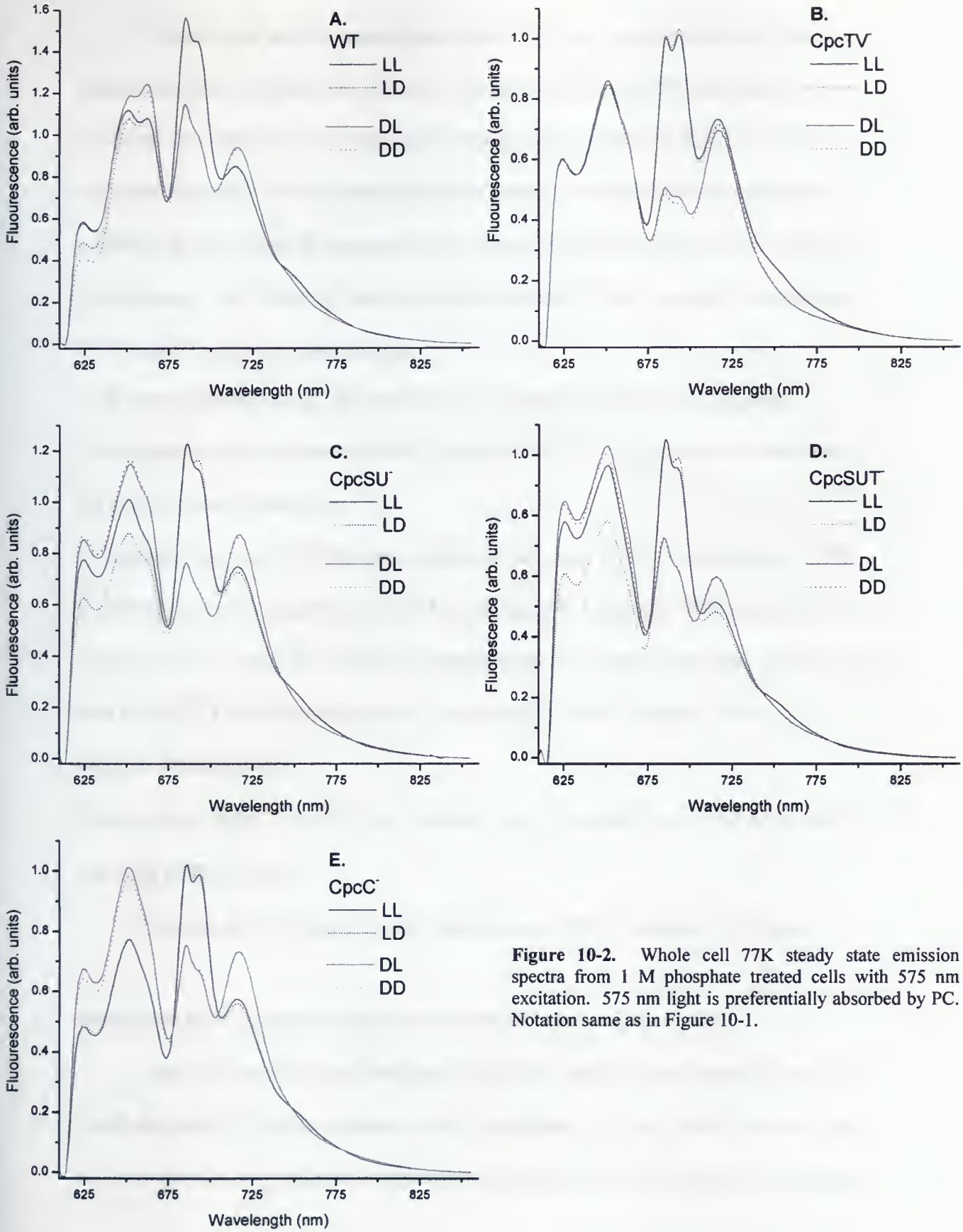


**Figure 10-2.** Whole cell 77K steady state emission spectra from 1 M phosphate treated cells with 575 nm excitation. 575 nm light is preferentially absorbed by PC. Notation same as in Figure 10-1.

The effect of the Cpc$^-$ mutations on the 77K emission spectra is quite visible; terminal acceptor pigment fluorescence is decreased while PC:APC fluorescence is increased. By examining emission peak ratios (Appendix VI) and spectral shapes, one can make the assumption that energy transfer from PC to acceptor chromophores is perturbed in such a way that causes an increase in dissipation of E from PC in the form of fluorescence. The following state transition-independent trends support perturbation of PC E transfer within the Cpc$^-$ strains:

1) A general increase in PC fluorescence as compared to all other chromophore fluorescence would indicate a loss of E transfer from PC to chromophores downstream in the energy transfer pathways.

2) A general increase in PC hexamer emission via $L_R/L_{RC}$ (F650) as compared to APC fluorescence (F663) indicates a loss of PC disc-to-APC E transfer. Keeping in mind that CpcTV$^-$/SUT$^-$/C$^-$ show PC:APC levels decreased by about half, an increase in FPC:FAPC over that of WT would be indicative of a substantial loss of E transfer from PC to acceptor chromophores.

3) An increase in F624 to F650 may indicate loss of E transfer from β153 down the PC rod, with β153 "isolated".

The loss of PC E transfer within the mutants' PBS is illustrated in Figure 19.

**Disruption of PC energy transfer at the α84-β83 chromophore pair**

With 575 nm excitation, the CpcTV$^-$/SUT$^-$/C$^-$ strains show a partially resolved fourth derivative PC emission band at ~640 nm whereas WT and CpcSU$^-$ show the band at 644 (Figure 9-2); F640 can be attributed to α84 and F644 to $L_R$ associated β83 (Table

3). As the ~640-44 nm peaks become more-blue shifted this represents enhanced contribution from α84 emission, as indicative of decrease in energy transfer between α84 and β83. The lack of the 640 nm shift in CpcSU$^-$ signifies no loss in α84 to β83 E transfer. Additionally, CpcSUT$^-$ shows a red shift in the F619 band which may represent a shift in the electronic state of β153; however, the other β153 band at 631.5 nm is not shifted (Figure 9-2).

In Figure 16 it is obvious that the mutant strains show a loss in PC excitation contribution to TE, PSII, and PSI fluorescence (under both light states). Figure 16 was normalized to fluorescence intensity at F685 with 650 nm excitation to correct for number of fluorescing PBS cores. Raw excitation spectra which show real differences in fluorescence yield are given in Appendices IX & X. The resulting difference excitation spectra (Figure 18) closely resemble that of PC absorption spectra with difference peaks of ~626/7 nm for CpcTV$^-$/SUT$^-$/C$^-$ and ~629 nm for CpcSU$^-$ (the red shift in CpcSU$^-$ is discussed below under "PC rod-to-PBS core energy transfer is specifically disrupted in CpcSU$^-$"). The losses in excitation contribution are non-discriminating on terminal acceptor indicating loss in E transfer is occurring within the PBS. Excitation at 626/7 nm corresponds to the α84-β83 excitonic splitting absorbance band (Table 2). This loss of PC excitation contribution is not merely due to the decrease in PC content and consequent loss in PC absorbance, for the absorption difference spectra (Figure 7B) show a peak at 631 nm, which is considerably red shifted over that of the excitation difference spectra.

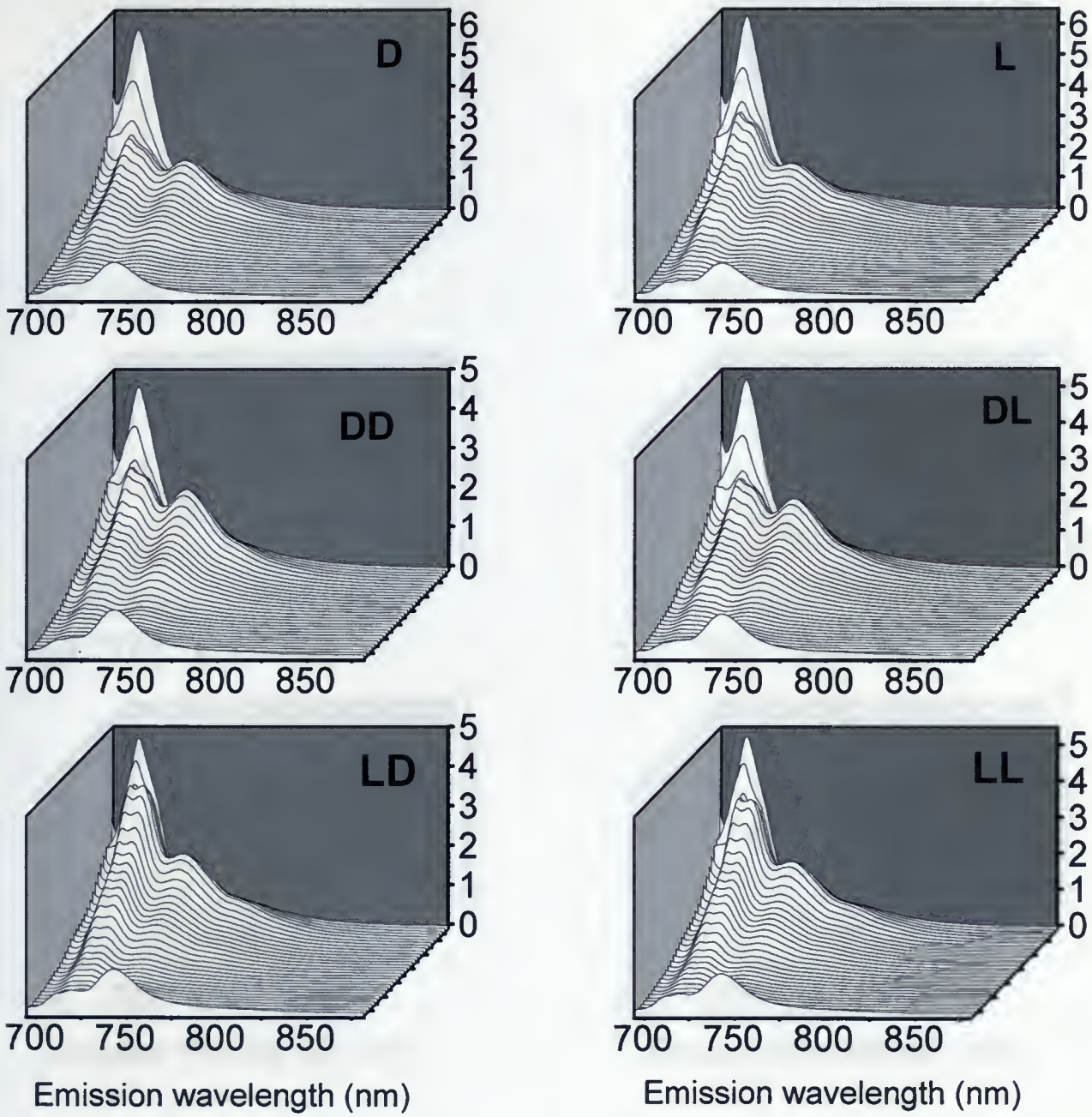


**Figure 11.** 77K excitation spectra for WT cells. The foremost emission spectra were collected with 435 nm excitation; the subsequent spectra were collected with excitation from 500-650 nm in 5 nm increments. D, L, DD, DL, LD, LL, as previously described. Spectra are corrected for differences in excitation intensity. Fluorescence intensity values are set to the same scale is in Figures 8 & 10 for ease of comparison.

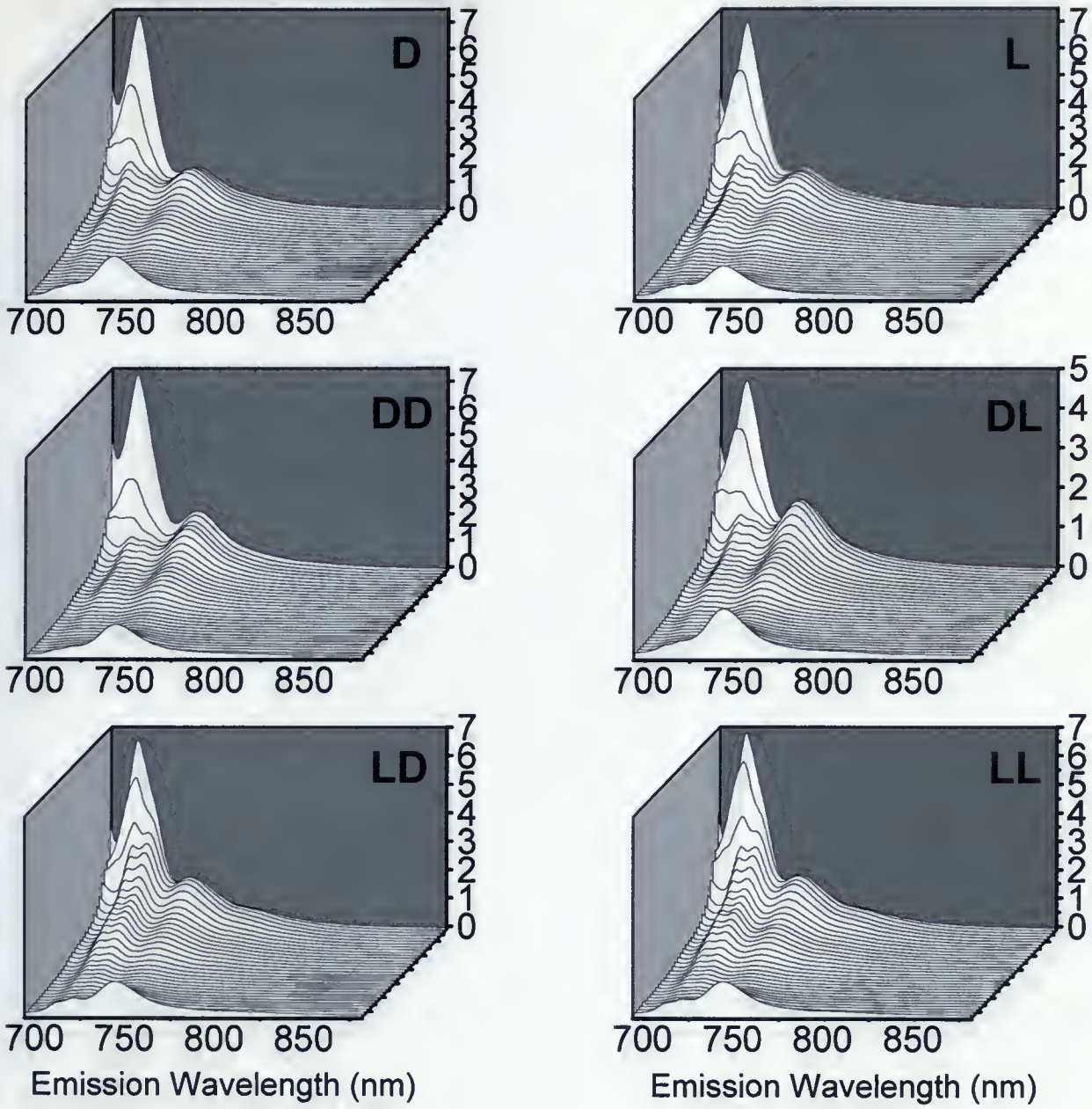


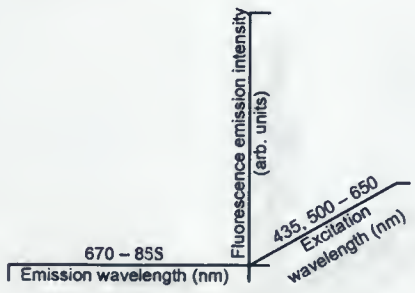


**Figure 12.** 77K excitation spectra for CpcTV⁻ cells. The foremost emission spectra were collected with 435 nm excitation; the subsequent spectra were collected with excitation from 500-650 nm in 5 nm increments. D, L, DD, DL, LD, LL, as previously described. Spectra are corrected for differences in excitation intensity. Fluorescence intensity values are set to the same scale is in Figures 8 & 10 for ease of comparison.

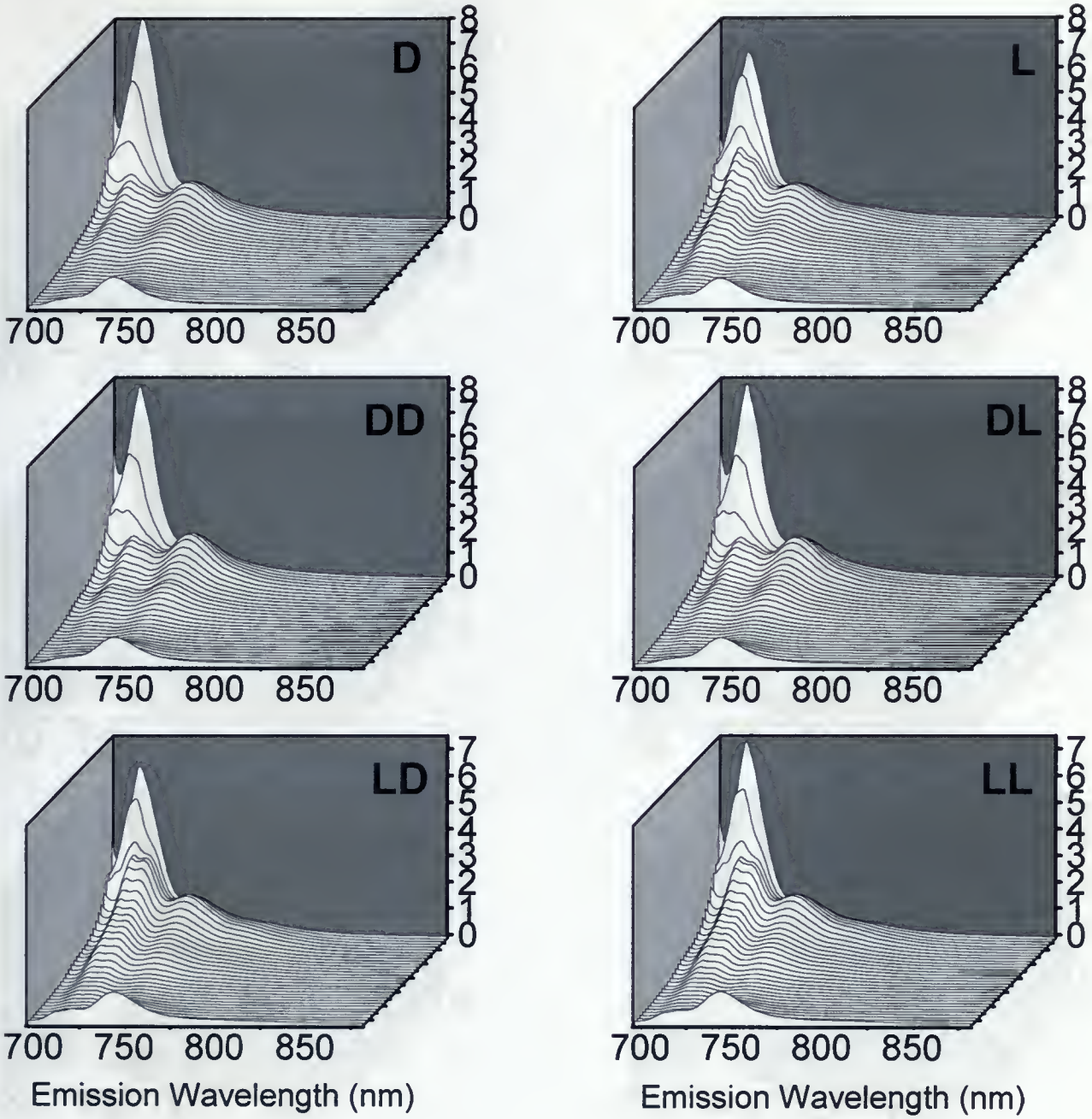


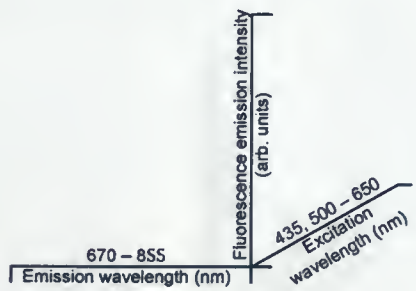


**Figure 13.** 77K excitation spectra for CpcSU⁻ cells. The foremost emission spectra were collected with 435 nm excitation; the subsequent spectra were collected with excitation from 500-650 nm in 5 nm increments. D, L, DD, DL, LD, LL, as previously described. Spectra are corrected for differences in excitation intensity. Fluorescence intensity values are set to the same scale is in Figures 8 & 10 for ease of comparison.

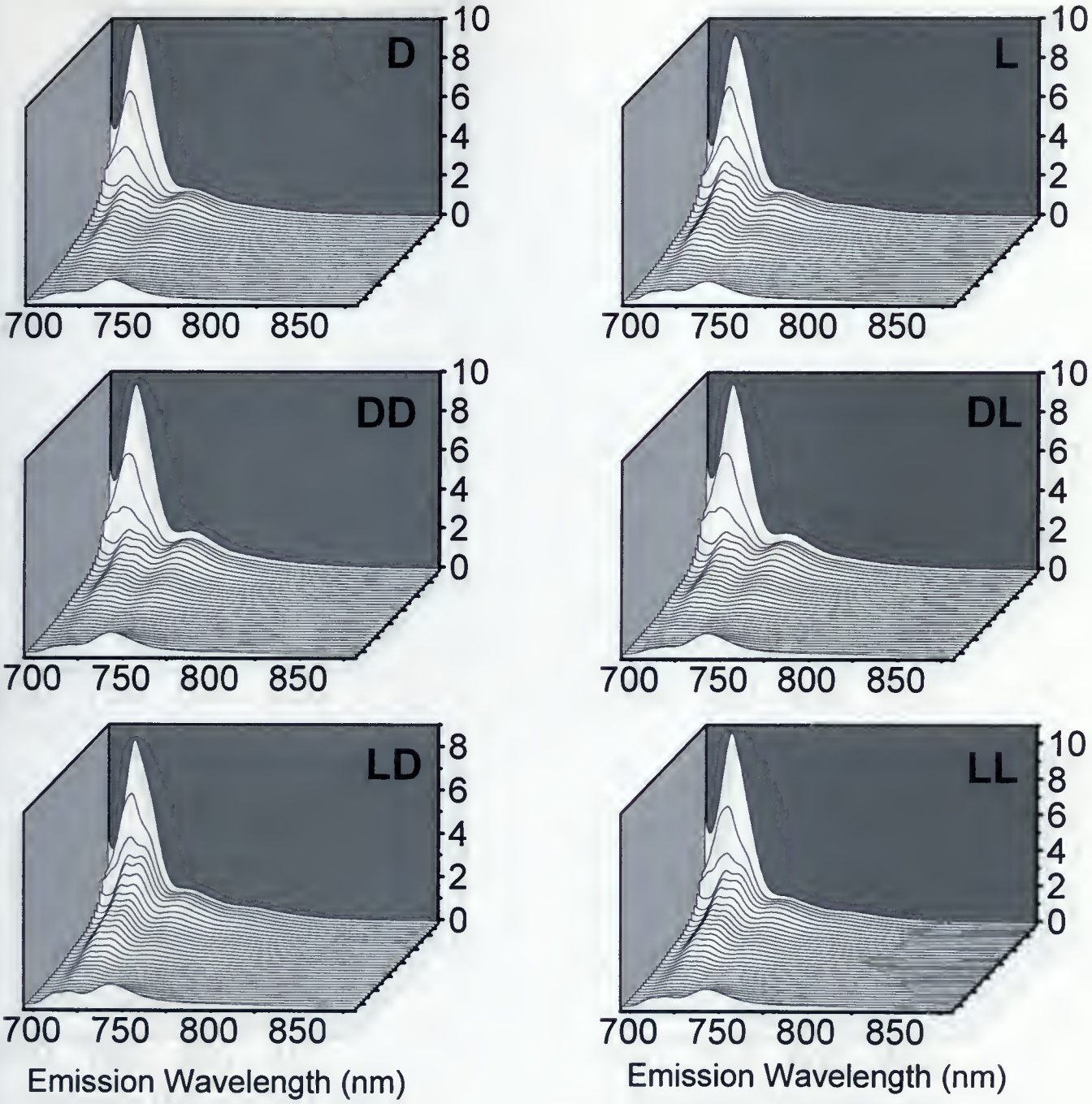


**Figure 14.** 77K excitation spectra for CpcSUT⁻ cells. The foremost emission spectra were collected with 435 nm excitation; the subsequent spectra were collected with excitation from 500-650 nm in 5 nm increments. D, L, DD, DL, LD, LL, as previously described. Spectra are corrected for differences in excitation intensity. Fluorescence intensity values are set to the same scale is in Figures 8 & 10 for ease of comparison.

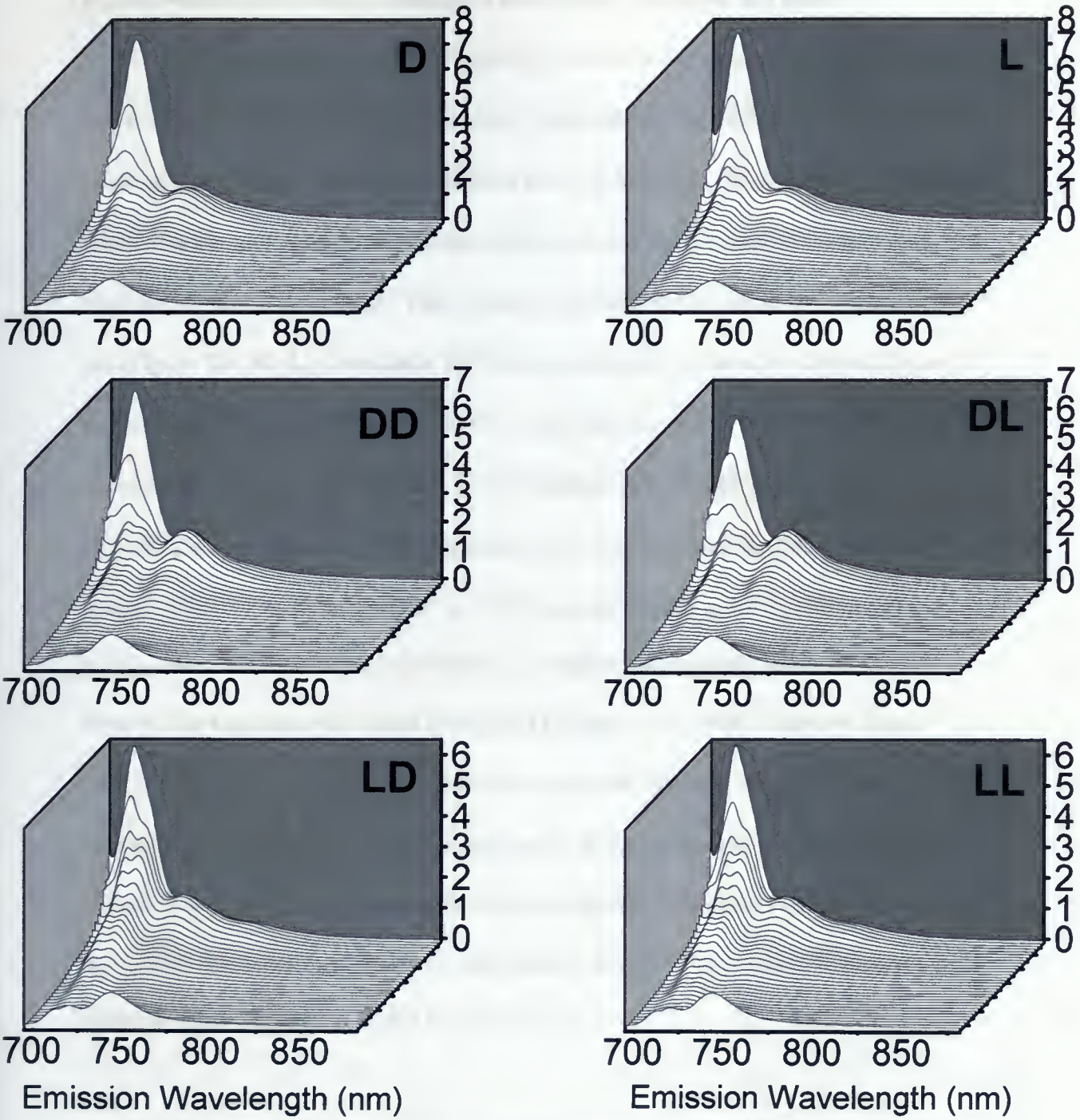


**Figure 15.** 77K excitation spectra for CpcC$^-$ cells. The foremost emission spectra were collected with 435 nm excitation; the subsequent spectra were collected with excitation from 500-650 nm in 5 nm increments. D, L, DD, DL, LD, LL, as previously described. Spectra are corrected for differences in excitation intensity. Fluorescence intensity values are set to the same scale is in Figures 8 & 10 for ease of comparison.

**PC rod-to-PBS core energy transfer is specifically disrupted in CpcSU$^-$**

The major disruption of PC E transfer within CpcSU$^-$ arises from a loss of β83-$L_{RC}$ to APC E transfer. The 2-3 nm red shift in the excitation difference peak over the other mutants (Figure 18) can be attributed to a loss in β83-$L_{RC}$ E transfer to APC, not so much of a loss in E transfer within the rod (seen as no enhancement of the α84 emission band as previously discussed). This is likely correlated to the loss in absorbance at 638 nm (Figure 7B), for $L_{RC}$ associated β83 shows an absorbance band at 638 nm (Pizarro & Sauer, 2001). Thus the CpcSU$^-$ mutation is affecting not only E transfer but also the energy level of $L_{RC}$ associated β83. If this blockage of E transfer out of the rods is caused by a disruption in the β83-$L_{RC}$ interaction, then why was the β83-$L_{RC}$ emission peak (at 653 nm) not blue shifted? $L_{RC}$ functions not strictly to lower chromophore energy level, but, even more importantly, to lengthen fluorescence lifetimes so as to improve the likelihood of Förster E transfer (Thomas *et al.*, 1995; Pizarro & Sauer, 2001). Though there was no peak shift associated with β83-$L_{RC}$ emission in the mutants, fluorescence lifetime may have been decreased. If the chromophore-linker interaction is altered in such a way as to shorten fluorescence lifetime then energy transfer from rod to core would be diminished. Further experimentation with time-resolved fluorescence measurements would be required for verification.

**The β83 binding site is more accessible to alternate lyase activity than the β153 site**

The mutant strains have shown highly perturbed PC E transfer yet showed only minor shifts in chromophore energy levels (no more than a ~2 nm blue shift in absorbance bands). Change in chromophore orientation is the most likely culprit. The

dipole orientations between donor and acceptor chromophores are a determining factor in Förster energy transfer (Förster, 1948, 1959, 1965). Relatively small changes in dipole orientation can severely disrupt E transfer. The experimental evidence advocates that less specific, alternate lyases can still attach PCB to the appropriate bilin binding sites, albeit less effectively; however, the resulting orientation of the chromophore within the binding domain is altered. Linear dichroism studies would provide further evidence in support of altered chromophore orientation.

Bilin attachment is a precursor to α/β subunit folding, monomer formation, and all other subsequent higher order assemblages within the PC assembly pathway (Anderson & Toole, 1998; Toole *et al.*, 1998). Substantially improper insertion of the chromophore into the subunit would result in loss of PC assembly, as was seen in the CpcB lyase$^-$ mutants. The β83 binding site must be relatively accessible to alternate lyase activity for the CpcSU$^-$ strain showed only a 24% decrease in cellular PC content, whereas the CpcTV$^-$/SUT$^-$ strains showed a ~50% decrease (Table 1). CpcE/F, the lyase for CpcA-84, is likely the substitute lyase responsible for β83 chromophorylation. α84 and β83 binding sites (as well as all APC binding sites) share the same stereochemistry, *R* (Duerring *et al.*, 1991; Ritter *et al.*, 1999). It is more difficult for the β153 site to receive PCB attachment because this binding site has *S* stereochemistry and no other known phycobiliprotein lyase within *Synechococcus* sp. PCC 7002 can act on this site (Duerring *et al.*, 1991; Ritter *et al.*, 1999; Shen *et al.*, 2006).

Not only is the substitute β83 lyase better at accessing its binding site, it is also more proficient at attaching the chromophore in the appropriate orientation. CpcSU$^-$ showed the least shifting in both absorbance and emission bands (Figures 6B & 9-2) and

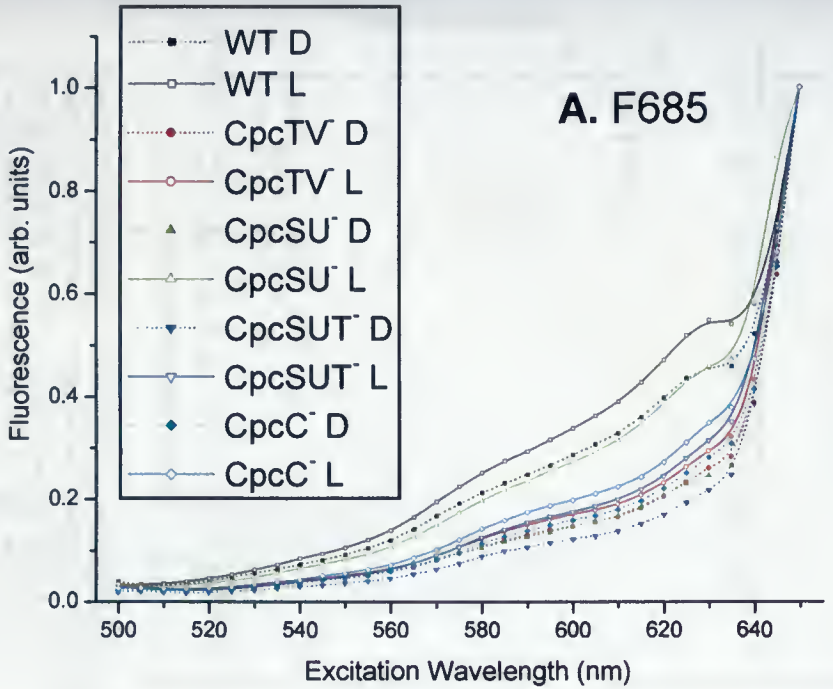


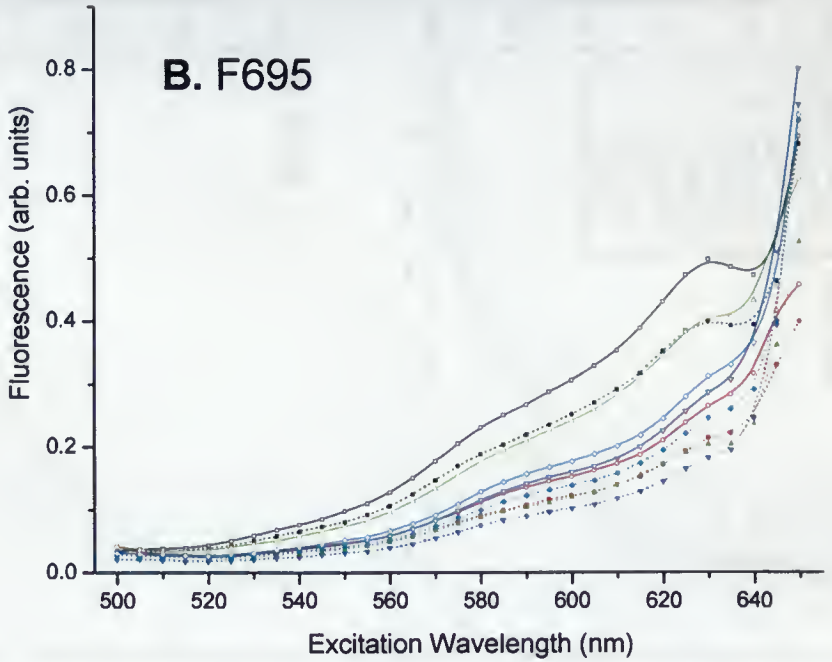


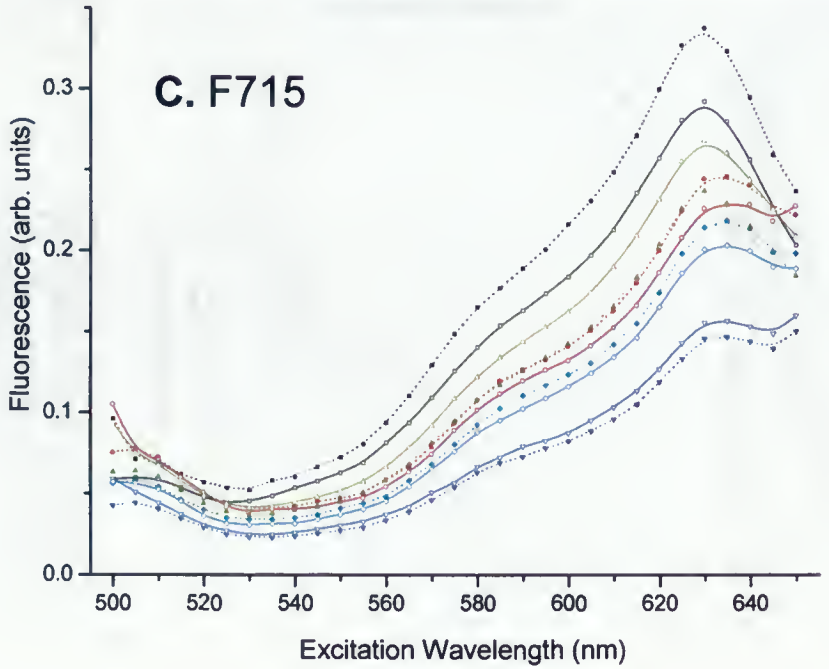


**Figure 16.** Phycobiliprotein excitation contribution to terminal acceptor emission at 77K. Plotted are excitation wavelength vs. fluorescence amplitude at the emission peaks of F685 (**A**), F695 (**B**), and F715 (**C**). Emission spectra collected as in Figures 11 – 15; spectra where then normalized to F685 with 650 nm excitation to correct for number of fluorescing PBS core terminal emitters. L, D, as previously described.

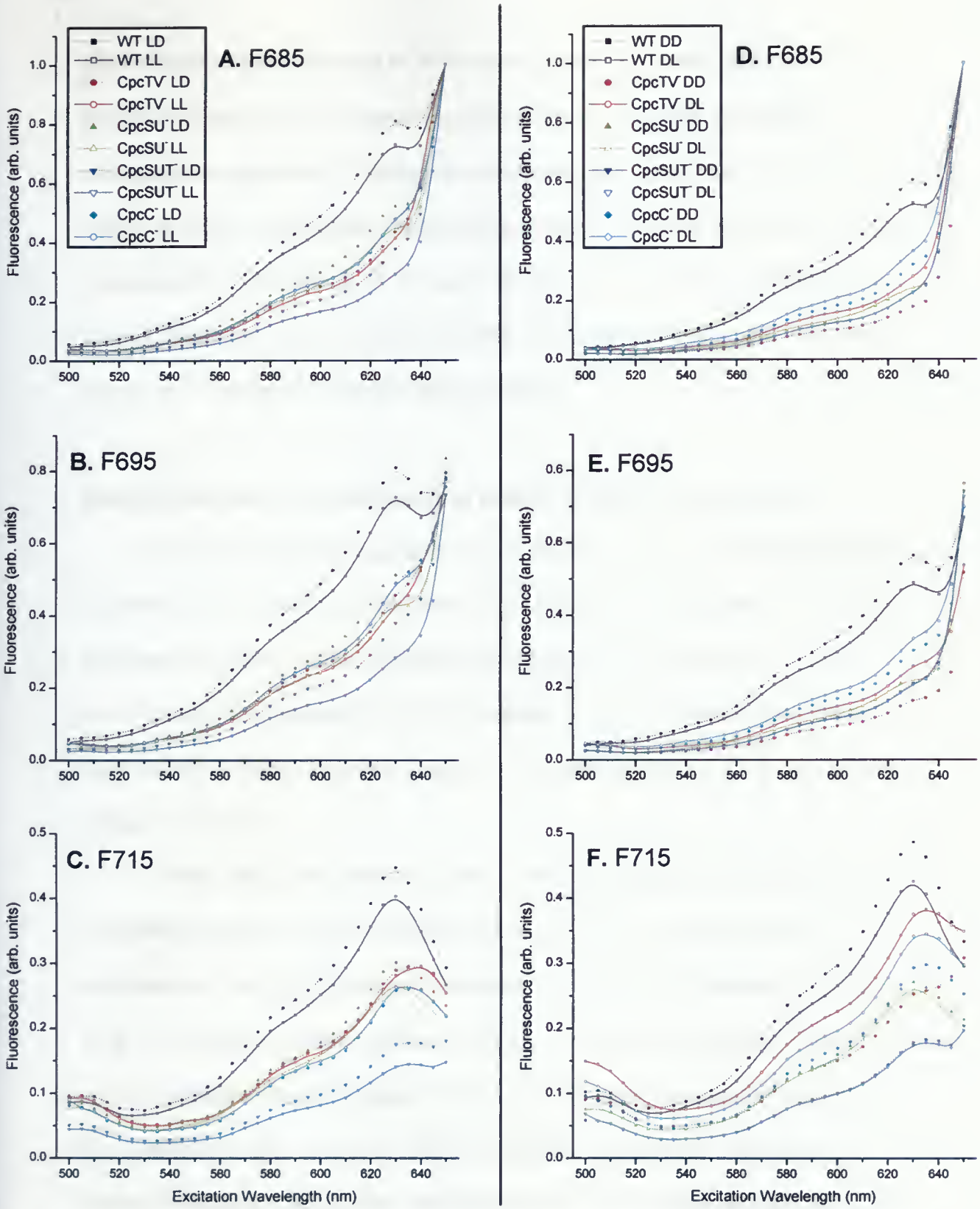


**Figure 17.** Phycobiliprotein excitation contribution to terminal acceptor emission at 77K among 1 M phosphate treated cells. Plotted are excitation wavelength vs. fluorescence amplitude for LL/LD samples (**A**, **B**, **C**) and DD/DL samples (**D**, **E**, **F**) at the emission peaks of F685 (**A**, **D**), F695 (**D**, **E**), and F715 (**C**, **F**). Emission spectra collected as in Figures 11 – 15; spectra where then normalized to F685 with 650 nm excitation to correct for number of fluorescing PBS core terminal emitters. LL, LD, DD, DL, as previously described.

showed the least perturbation in PC E transfer (Figure 8-2). Conversely, the substitute β153 lyase is not only poor at accessing its binding site but is also incompetent at attaching the chromophore in the correct orientation. The CpcTV$^-$/SUT$^-$ strains showed similar absorbance and emission band shifts as the CpcC$^-$ strain (Figures 6B & 9-2) and showed similar disruptions in PC E transfer (Figure 8-2); thus the *cpcT*$^-$ mutations are altering chromophore-protein and chromophore-chromophore interactions in the same manner as if missing a structural linker polypeptide.

**High M phosphate treatment improves excitation energy flow within cells**

High M phosphate treated cells showed an increase in PC to APC energy transfer (as shown by increased FPC:FAPC ratios; Figures 8-2 & 10-2, Appendix VI). Likewise, the increased resolution of F673 with 575 nm excitation (Appendices III & IV) may further illustrate augmented PC to APC E transfer. Phosphate treatment also greatly enhanced PC excitation contribution (relative to that of APC) to TE and PSII emission (Figures 16 & 17).

Energy flow within PBS was enhanced because the high M phosphate buffer stabilizes the protein complex during the freezing process preventing structural deformations. The high M phosphate treatment red shifted β153 emission (Appendices III & IV). Because this chromophore is peripheral in the PC disc, phosphate treatment would cause the solvent exposed chromophore and neighboring protein environment to lose associated water molecules, which may cause stretching of the PCB tetrapyrole thereby lowering its energy state. The electric charge of the phosphate ions could also lower the chromophore's energy level by: (i) directly interacting with the chromophore's

electric field, (ii) interfering with hydrogen bonding (between amino acid residues and/or between protein and chromophore), and (iii) altering the protonation state of surrounding amino acid residues. The phosphate treatment had a greater effect on E transfer in the mutant strains than in WT - the high M buffer may help stabilize the mutants' "weakened" PC rods allowing for enhanced E transfer.

The greater effect of phosphate treatment is to improve the coupling between PBS cores and photosystems. With PBS "glued" to the thylakoid membrane TE would be able to form more stable associations with PSII (and PSI) thereby increasing energy transfer. This can be easily seen as an increase in F695:F685 (compare Figure 10-2 to Figure 8-2, Appendix VI-M). PC-PSI association may similarly be enhanced.

**Excitonic breakage between PC rod and APC core?**

Surprisingly, in all the strains, including WT, the PC rods seemed to be somewhat excitationally isolated from the APC core. The excitation spectra in Figure 16 show far less PC-absorbed excitation energy reaching TE (F685) and PSII (F695) than was expected; the contribution from APC excitation was greater than that from PC excitation. PBS absorbance is dominated by PC because there are more PC chromophores than APC chromophores in a PBS. If E transfer through PBS is efficient, PC excitation should contribute more to TE emission than APC excitation. In fact, the excitation spectra for TE emission at F685 (Figure 16) should be close replicates of the PBS-absorption-region spectra in Figure 7A. The majority of PC emission at 77K arose from $L_{RC}$ associated β83 at the emission peak of F652; in such correlating with loss of E transfer from β83-$L_{RC}$ to APC. Excitons reaching β83-$L_{RC}$ would be strongly "pushed" towards the APC core and

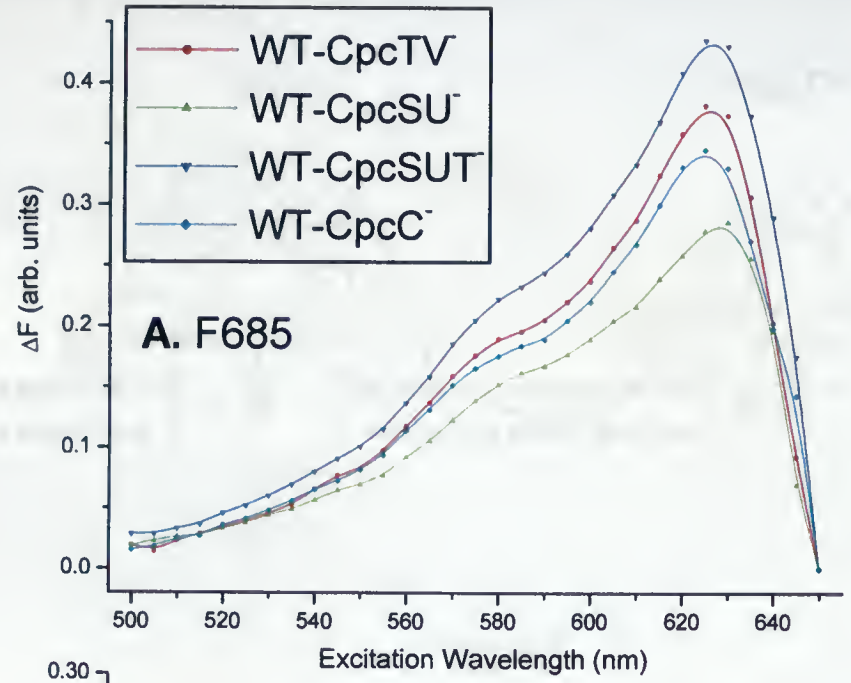


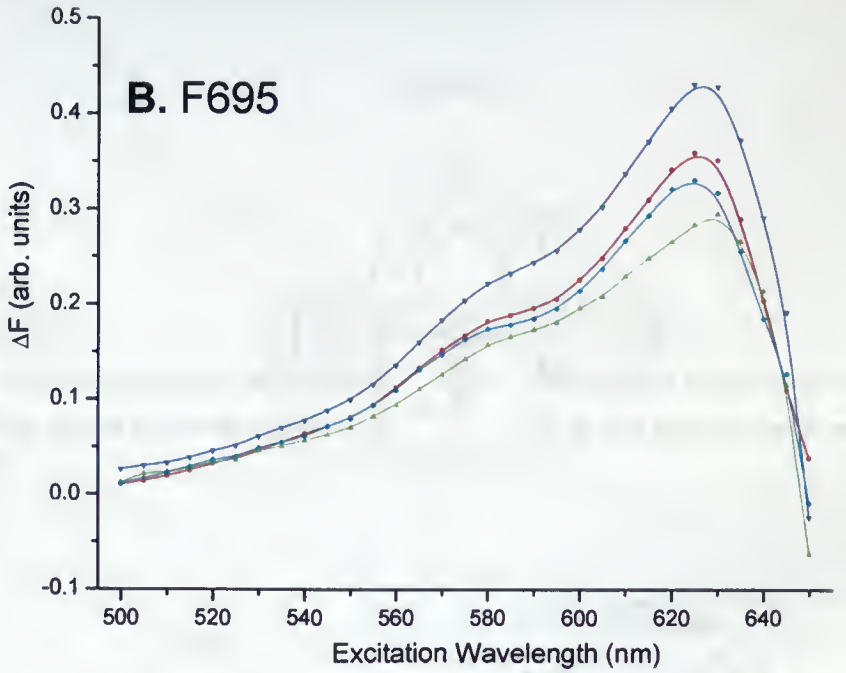


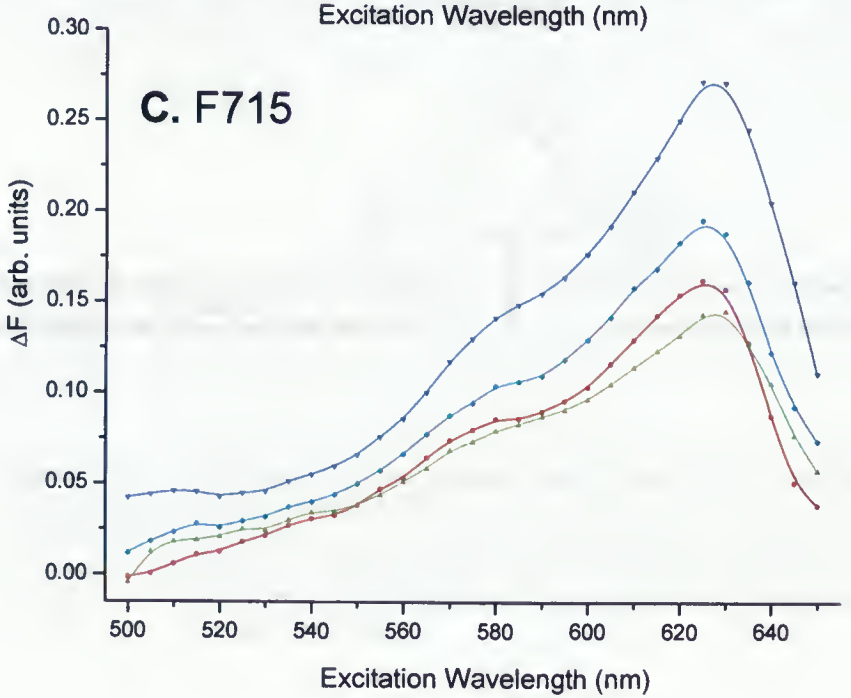


**Figure 18.** Differential loss in phycobiliprotein excitation contribution to terminal acceptor emission at 77K among the mutant strains. **A, B, C,** the subtractions (ΔF) of Cpc⁻ strain fluorescence intensity from that of WT at the emission peaks F685, F695, and F715, respectively. Excitation spectra were normalized to F685 with 650 nm excitation (as in Figure 16) prior to subtraction; spectra can therefore by considered as corrected to number of fluorescing PBS core terminal emitters. LD samples were used in creating the difference spectra; LD, as previously described.

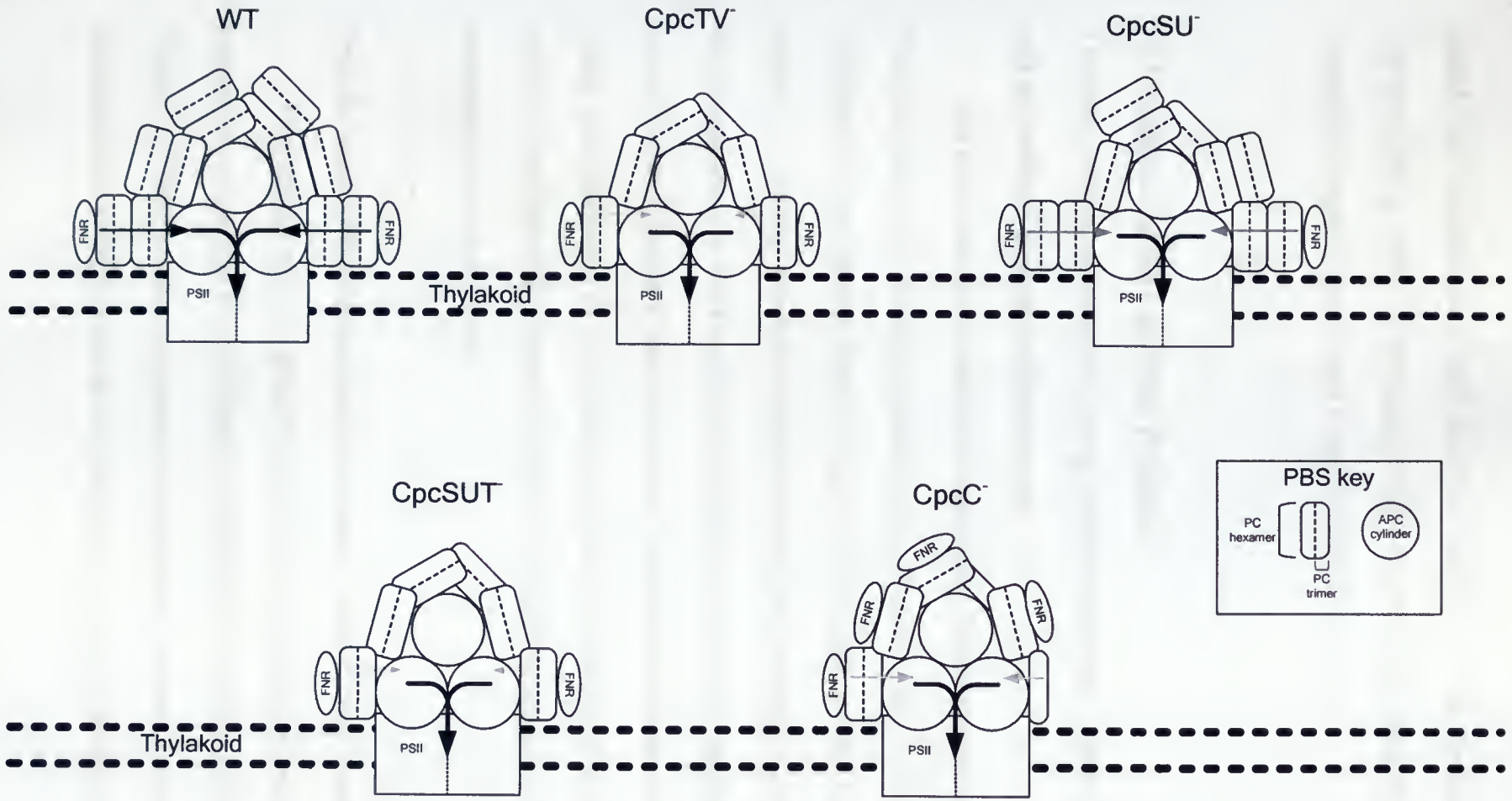


**Figure 19.** Models describing the principal phycobilisome (PBS) population observed in each strain. Rod structures are consistent with accumulated spectroscopic evidence. PBS are positioned on top of PSII dimers. Arrows indicate excitation energy (E) transfer within PBS. Only E transfer involving the two thylakoid proximal rods is shown; other rods in a PBS would be similar. The connectedness between PC arrows and APC arrows represents the relative connectivity of E transfer between rod and core. The darker the arrow, the more efficient the E transfer. The thicker the arrow, the larger the magnitude of E migration. FNR (ferredoxin NAD(P)$^+$ oxidoreductase) positioning is based on previous knowledge (de Lorimier *et al.*, 1990; Gómez-Lojero *et al.*, 2003) not on this work's spectroscopic evidence.

would either be transferred to APC or lost as fluorescence. This blockage of E transfer may simply be an artifact of freezing, for high M buffer treated samples showed substantially improved rod-to-core E transfer (Figures 16 &17).

**II. Investigation of the Light State Transition**

**The effect of state transitions on energy transfer pathways: redistribution of Chl*a*- and phycobilin- absorbed excitation energy**

All strains were state transition competent and showed redistributions of both Chl*a*- and phycobilin- absorbed excitation energy (Figures 8, 20, 21). Overall the reallocation of phycobilin excitation energy was more significant than that of Chl*a* (Figure 21). Through the study of state transition dependent changes in emission peak ratios (Appendices V-VIII) and by analyzing state 2-minus-state 1 excitation difference spectra (Figure 20) one can formulate models to explain the redistribution of excitation energy occurring during the state transition. Table 4 summarizes the redistributions of both Chl*a*- and phycobilin- absorbed excitation energy during the state 1-to-state 2 transition for each of the strains.

**Does the loss of PBS antenna function promote a "larger" state transition?**

Once treated with 1 M phosphate, all of the mutant strains showed a larger state 1-to-state 2 transition than WT as witnessed with both Chl*a* and phycobilin excitation (Figure 21). The true extent of potential energy transfer was more visible in the phosphate treated samples because the phosphate buffer helped stabilize the chromo-

protein complexes during the freezing process keeping E transfer conducive chromophore alignments intact. The phycobilisomes of the mutants had smaller absorbance cross sections (due to loss in rod length) and were less efficient at funneling absorbed photon energy towards the photosystems (because of perturbed PC E transfer). Do the mutant strains require a larger scale rearrangement/redistribution of antennae excitation energy during the state transition to compensate for the reduced PBS antenna size/function? Assume that dark adaptation drives cells to state 2 by fully reducing the PQ pool via input of $e^-$ from dark respiration and the transition to state 1 is induced by a net oxidation of the IEC. When *Synechococcus* sp. PCC 7002 cells are treated with 3-(3,4-dichlorophenyl)-1,1-dimethylurea (DCMU) to inhibit PSII reduction of the PQ pool and then exposed to blue/ far-red light, a stronger state transition is produced than with the light treatment alone (data not shown); in such suggesting that the state transition mechanism responds dynamically to IEC redox status and is not simply an "on-or-off" phenomenon.

The direct effect of the $Cpc^-$ mutations on the photosynthetic apparatus was a loss in PBS light harvesting capability. What antenna-dependent scenarios then would lead to "over" oxidation of the IEC to induce a stronger transition to state 1? (a) An increase in the absorbance cross section of PSI relative to PSII and (b) a decrease in the absorbance cross section of PSII relative to PSI would preferentially oxidize IEC. Any reduction in PBS antenna function induced by the $Cpc^-$ mutations will be less detrimental to PSI light harvesting than to PSII light harvesting, because PSI receives at least half of its excitation energy directly via Chl*a* whereas Chl*a*-originating excitation energy does not contribute significantly to PSII excitation (Appendices IX & X). So scenario (b) is most likely to bring on the enhanced oxidation of IEC and is promoting the "enlarged" state transition

observed within the mutants. Since the PBS of the mutant strains are less capable of collecting and transferring PC-absorbed excitons to PSII, more PBS would need to be energetically coupled with PSII in state 1 to provide optimal PSII excitation.

Time resolved room temperature analysis of the state 2-to-state 1 transition using pulse amplitude modulated (PAM) fluorescence traces revealed that the mutants generally took more time to reach full state 1 levels of PSII emission than did WT (data not shown). The state transition likely took longer in the mutant strains because they required a larger scale rearrangement of their antenna systems (namely PBS) to counter the redox state of IEC (as described above). If a regulatory promoter needs to activate PBS movement, as suggested by Mullineaux & Emlyn-Jones (2005), then the state transition may take more time in the mutants because more PBS have to be "primed" for movement. Depending on the rate of promoter regulation, some time may be required for the full state transition to develop.

Inducing state 1 with far-red light results in similar redistributions of antenna excitation energy as when using blue light, however the magnitude of the effect from far-red light is less (data not shown). Why? The blue light used in this study to drive cells to state 1 contains wavelengths that are weakly absorbed by the phycobilins (at ~400 nm). Upon exposure to this blue light, after dark adaptation, Chl*a* are primarily excited (which preferentially excites PSI) but phycobilins are also excited, and depending on the functional PBS antenna sizes for PSII and PSI, remembering in state 2 PBS are coupled with PSI, the degree of IEC oxidation may be intensified. If there is a greater demand for PSII reduction of PQ (as when exposed to blue instead of far-red light) then PSII will be "hyper-up-regulated" and the state transition mechanism will work "harder" to increase

the PSII absorbance cross section, resulting in a larger scale redistribution of excitation energy. So once again it seems that the state transition mechanism does allow for variability in the scale of antenna excitation energy redistribution. Directly measuring the response of the strains' photosynthetic machinery to the redox status of their IEC (as via time resolved room temperature fluorescence measurements of PSII in concordance with titrations of the IEC) would clarify the role of IEC redox status in controlling the magnitude of the state transition.

The Cpc$^-$ strains may have simply shown an enhanced state transition because their mutations promoted mobility of the antenna systems. The mutant strains have physically smaller PBS due to shortened rod length, thus it would be easier for their PBS to migrate across the thylakoid membrane because the cytoplasmic surface would be less crowded (if following the mobile PBS state transition mechanism). However, the CpcSU$^-$ strain contained PBS of mostly full rod length yet showed large (greater than WT) redistributions of both Chl*a* and PBS excitation energy (Figure 21). An explanation strictly dependent on the modified physical structure of the PBS is therefore not likely.

**1 M phosphate treatment inhibits state transition dependent redistributions of both Chl*a*- and phycobilin- absorbed excitation energy**

High M phosphate treatment has been shown to prevent state transition associated changes in the redistribution of PBS-absorbed excitation energy by preventing PBS mobility; however, the redistribution of Chl*a*-absorbed excitation energy was not completely inhibited (Joshua & Mullineaux, 2004). Yet 1 M phosphate treatment in the present study prevented all standard state transition dependent redistributions of both

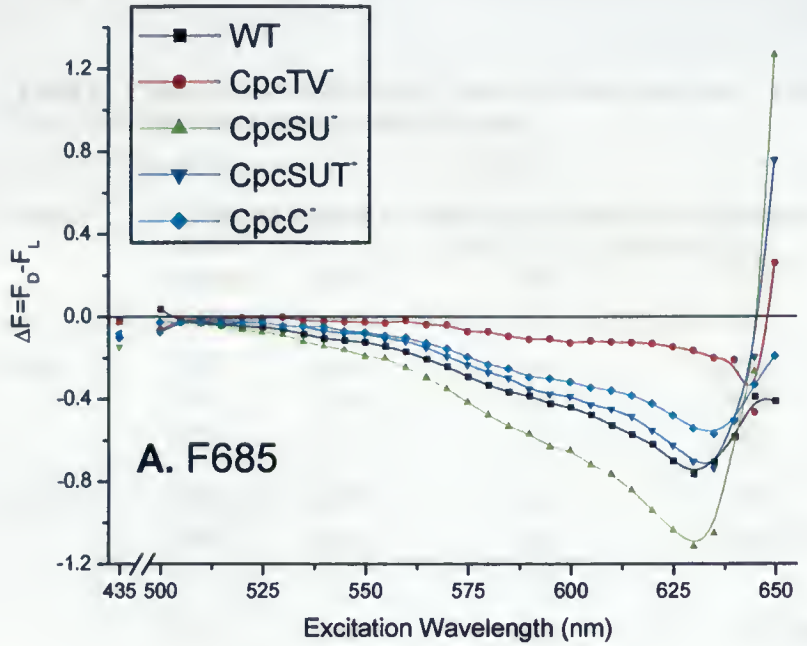


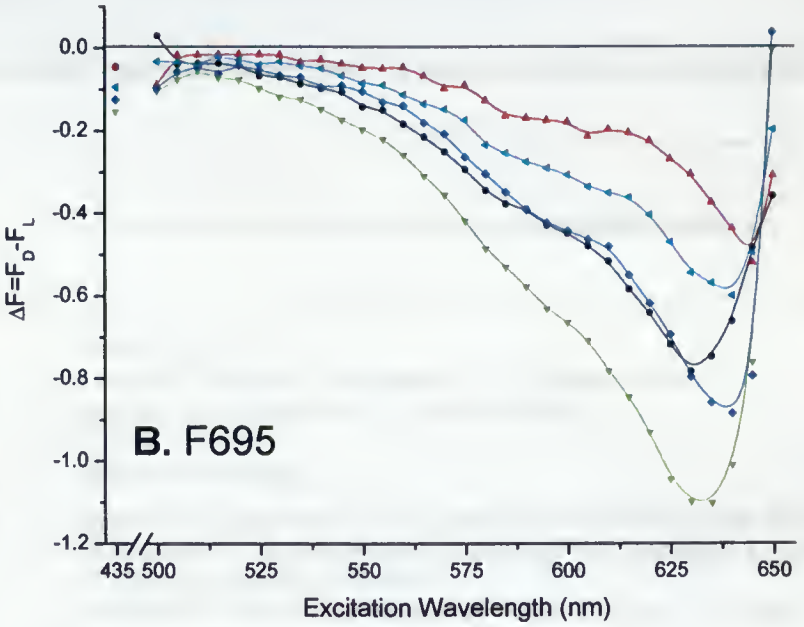


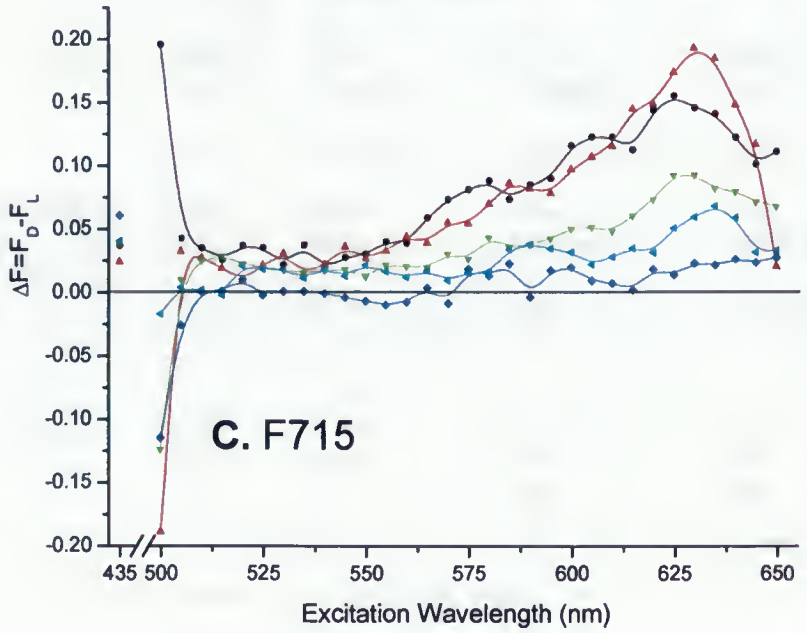


**Figure 20.** State transition dependent changes in 77K excitation spectra emission peak intensities. Shown is the difference in fluorescence intensity between state 2 and state 1 among L/D samples ($\Delta F = F_D - F_L$) at the emission peaks of **A**, F685; **B**, F695; and **C**, F715. L, D, as previously described. Spectra were neither normalized prior to or after subtraction.

**Table 4.** Variation in excitation energy transfer between light states. Table summarizes conclusions drawn from 77K steady state emission spectra (particularly Figure 20). Statements compare state 2 to state 1.

| Strain | Observed changes in emission peak fluorescence intensities | | | | Corresponding alterations in excitation energy transfer pathways |
|---|---|---|---|---|---|
| | Excited pigment | Contribution to emission peak F685 | F695 | F715 | |
| WT | Chl*a* | Loss | Loss | Gain | Increased PSII→PSI |
| | APC | Loss | Loss | Gain | Increased PBS(core)→PSI at expense of PBS(core)→PSII |
| | PC | Loss | Loss | Gain | Increased PC→PSI at expense of PC→TE→PSII |
| CpcTV$^-$ | Chl*a* | Loss | Loss | Gain | Increased PSII→PSI |
| | APC | Gain | Loss | Small$^{\bullet +}$ gain | Increase in (i) population of non-quenched uncoupled PBS cores and (ii) PBS(core)→PSI$^+$ at expense of (i) PBS(core)→PSII and/or (ii) a "reserve" of quenched uncoupled PBS cores |
| | PC | Loss | Loss | Large$^\bullet$ gain | Increased PC→PSI at expense of (i) PC→TE→PSII and (ii) a "reserve" of previously quenched uncoupled PBS (see above) |
| CpcSU$^-$ | Chl*a* | Loss | Loss | Gain | Increased PSII→PSI |
| | APC | Large$^\bullet$ gain | No change | Gain | Increased PBS(core)→PSI at expense of quenched uncoupled PBS cores; this PBS(core)→PSI coupling is poor, so still see increased TE emission |
| | PC | Large$^\bullet$ loss | Large$^\bullet$ loss | Gain | Increased PC→PSI at expense of PC→TE→PSII |
| CpcSUT$^-$ | Chl*a* | Loss | Loss | Gain | Increased PSII→PSI |
| | APC | Gain | No change | Small$^\bullet$ gain | Increased PBS(core)→PSI at expense of quenched uncoupled PBS cores; this PBS(core)→PSI coupling is poor, so still see increased TE emission |
| | PC | Loss | Loss | Small$^\bullet$ gain | Increased PC→PSI at expense of PC→TE→PSII (The small increase in F715 relative to the decrease in F685 and F695 is due to perturbed E transfer in the rods) |
| CpcC$^-$ | Chl*a* | Loss | Loss | Gain | Increased PSII→PSI |
| | APC | Loss | Loss | Gain | Increased PBS(core)→PSI at expense of PBS(core)→PSII |
| | PC | Loss | Loss | Gain | Increased PC→PSI at expense of PC→TE→PSII |

$^\bullet$, relative descriptor; $^+$, may not be significant

Chl*a*- and phycobilin- absorbed excitation energy (Figures 10-15, Figure 21). If the redistributions of Chl*a* and PBS E are controlled by separate mechanisms as prescribed under the commonly accepted "combination models" involving PBS mobility (Mullineaux *et al.*, 1997; Aspinwall *et al.*, 2004; Joshua & Mullineaux, 2004), then high M buffer treatment should only affect that constituent which involves rearrangement of complexes associated extrinsically with the thylakoid membrane (i.e. PBS). The observed results suggest that both the Chl*a*- and phycobilin- dependent mechanisms involve the rearrangement of PBS. Interestingly, low levels of both Chl*a* and phycobilin E redistribution still occurred among the treated cells although it was in the "opposite direction" (i.e. state 2 conditions produced larger F695:F715 than state 1 conditions, Figures 10 & 21). This "reverse spillover" is likely attributed to changes in the excitation energy transfer rate constants (*K*) between PSII and PSI (i.e. a loss of spillover). Appendices XVI-XVIII further explore these subtle changes among phosphate "fixed" samples.

A state transition mechanism model more consistent with that in McConnell *et al.* (2002) fits this study's observations better than the models proposed under Mullineaux and coworkers (Mullineaux *et al.*, 1997; Aspinwall *et al.*, 2004; Joshua & Mullineaux, 2004). McConnell *et al.* (2002) proposed Chl*a* and phycobilin E transfer pathways to be controlled by more restrained changes in the orientations between PBS-PSII complexes and PSI, and not by large scale movement of PBS across the thylakoid surface. The model of McConnell *et al.* demands strong PBS-PSII association and a weak, transient PBS-PSII to PSI connection. For the present work, phosphate concentrations of 1 M were needed to lock all cell strains in state 2, yet 0.7-0.8 M could effectively lock cells in

state 1 (data not shown) suggesting that the PBS-PSII association is more stable than the PBS-PSI association. Other studies required phosphate solutions of only 0.5 M phosphate to prevent PBS mobility (Joshua & Mullineaux, 2004). Such strong ionic conditions were likely needed because the *Synechococcus* sp. PCC 7002 cells used in the present investigation have shorter rods than many other cyanobacteria. This is especially true for the CpcTV$^-$/SUT$^-$/C$^-$ strains, since their rods are predicted to be only one disc in length. The loss in rod surface area provided less "glue" surface between the PBS and the thylakoid membrane during the osmotic treatment.

For high M phosphate treatment to prevent the redistribution of Chl*a*-absorbed excitation energy, PBS movement must be somehow involved in the spillover process. The PBS is a very large complex closely associated with the thylakoid face. Because PBS form a relatively stable association with PSII (Clement-Metral *et al.*, 1985), believed to be mediated by insertion of the hydrophobic loop domain of ApcE into a cleft within the PSII dimer (Barber *et al.*, 2003), locking an associated PBS tightly to the thylakoid surface could prevent any restrained changes in the physical positioning of PSII which may occur during spillover (PSII would be "pinched down" by the PBS core). The thylakoid-proximal rods provide a large surface area to strengthen the "bond" between PBS and the membrane surface during exposure to high osmotic buffer.

**State transitions involve alterations in PBS-PSI energy coupling**

The state transition was dominated by the redistribution of PC-absorbed excitation energy within all the strains: state 2 was characterized by a decrease in TE and PSII emission originating from PC excitation and an increase in PSI emission originating from

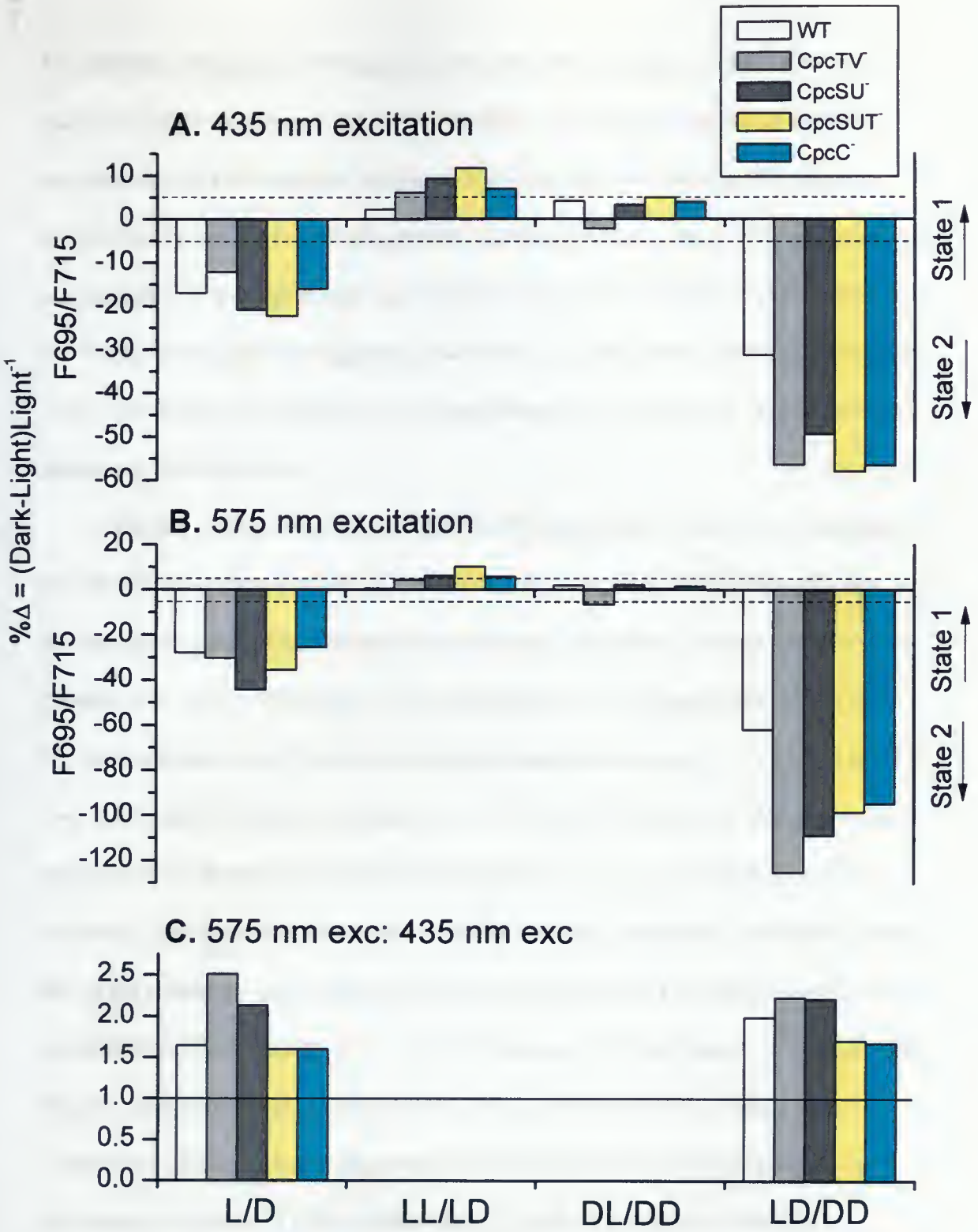


**Figure 21.** Light state dependent changes in F695/F715. State 1 is characterized by higher F695/F715; State 2 is characterized by lower F695/F715. Shown are the percentage changes in F695/F715 between state 1 (blue light illumination) and state 2 (dark adaptation). $\%\Delta = 100\ (F695/F715_{Dark} - F695/F715_{Light})\ (F695/F715_{Light})^{-1}$. L, D, LL, LD, DL, DD, as previously described. LD/DD, used to contrast cells locked in state 1 to cells locked in state 2. **A**, percentage change observed with 435 nm excitation. **B**, percentage change observed with 575 nm excitation. **C**, the ratio of B:A as an indication of whether the major contributor to the state transition is from the redistribution of Chl*a*- or phycobilin- absorbed excitation energy. Dashed lines represent 5% significance levels.

PC excitation (Figure 20). We are not just seeing the consequence of PC forming the majority of PBS absorbance, for APC-absorbed E contributed more to TE and PSII emission than did PC-absorbed E (Figure 16). The state 2 increase in PSI emission predominately arises from PC-absorbed E, but the contribution from APC-absorbed E is also important and roughly correlates with the loss in APC-absorbed E contribution to PSII emission (Figure 20), suggesting that there is an enhancement in PBS-PSI coupling. State 2 in several of the strains is also characterized by an increase in the population of uncoupled PBS (Table 4).

Further evidence for changes in PBS-PSI association between state 1 and state 2 can be elucidated from examining F755. F755/60 arises from the farthest-red long-wavelength absorbing Chl*a* located on the monomer-monomer interface of PSI trimers (Shubin *et al.*, 1991; Shubin *et al.*, 1992; Kruip *et al.*, 1999; Karapetyan, 2004). With 575 nm excitation, state 1 cells consistently showed an increase in F755 relative to F715 over state 2 cells (Figure 8-2, Appendices VI-P & VIII-O). However, this effect was absent when preferentially exciting Chl*a* (Figure 8-1); thus it is dependent on PBS excitation. I propose that the decrease in F755 observed under state 2 conditions results from PBS excitation energy entering PSI at a more E transfer favorable location, one in which PBS excitation energy is less likely to be trapped by the longest-wavelength Chl*a*. High M phosphate treatment inhibited the state 2 decrease in F755 (Figure 10-2, Appendices VI-P & VIII-O) suggesting that this effect is due to shifts in the physical alignment/positioning of PBS to PSI trimer. Li *et al.* (2006) has attributed such differences in F760 to spillover of Chl*a* E in *Spirulina platensis*; however, in the present study no changes in F760 where observed when preferentially exciting Chl*a*.

**Direct PC to PSI excitation energy transfer**

PC-absorbed excitation energy was the major contributor to PSI emission, whereas most of PSII emission was derived from APC-absorbed excitation energy (Figure 16). This is evidence for the direct PC-to-PSI E transfer pathway in which E transfer through the PBS core/TE is circumvented. State 2-minus-state 1 difference excitation spectra (Figure 20) also show that PC-absorbed excitation energy preferentially excites PSI in state 2. Direct PC-to-PSI E transfer would likely originate from PC chromophores that are excitationally isolated from their acceptor chromophore, as with the chromophores that show long E transfer lifetimes and the energy sink "fluorescing" chromophores (Figure 3). When looking at Figure 20, the difference peaks for F715 may be blue shifted over those for F695 possibly indicating that higher energy PC chromophores preferentially transfer their E to PSI in state 2. The excitation difference peaks at ~625 and ~605 nm (particularly noticeable in WT) may arise from non-linker associated β83 and β153 chromophores, respectively (though assigning the difference peaks to individual chromophores is risky due to the "noisy" nature of the difference spectra). The β153 chromophores are likely candidates for direct E transfer to PSI for they are peripheral on the rod and would be in closest proximity to PSI Chl*a*, and furthermore, are the sensitizing chromophores for the longest lifetime intra-hexamer E transfer pathway (Figure 3).

In cyanobacteria, FNR is attached to the distal PC discs closest to the thylakoid membrane (Schluchter & Bryant, 1992; Gómez-Lojero *et al.*, 2003). To optimize PSI-FNR interaction, PBS rods would need to associate with PSI. Such a configuration would also optimize the direct PC-to-PSI E transfer pathway.

# SUMMARY AND CONCLUSIONS

**The CpcB lyase null mutations alter but do not prevent PC chromophorylation: Evidence for alternate lyases?**

The Cpc$^-$ mutations did specifically target PC: there was a cellular reduction in PC content, PC absorbance and fluorescence bands were shifted, and excitation energy transfer involving PC was perturbed. The β PC lyase null mutations did not, however, prevent chromophorylation at the targeted phycobilin binding sites. Instead it appears that the chromophore is placed within the binding domain in a new orientation, one which is unfavorable to E transfer. In evidence, the mutation associated shifts in CpcB 10K absorbance bands are minor (no more than a 2 nm blue shift) whereas the disruption in PC energy transfer is significant. The most plausible explanation for this "residual" CpcB chromophorylation is that other, less specific lyases are able to act on the bilin binding sites (albeit in a less proficient manor). The β153 binding site is less accessible to alternate lyase activity than the β83 site, for the CpcTV$^-$/SUT$^-$ strains showed greater reduction in PC content, larger shifts in PC absorbance and fluorescence bands, and greater perturbation of PC E transfer. Binding site stereochemistry is likely the discriminating factor in determining alternate lyase accessibility. The β83 site has *R* stereochemistry, as does the CpcA-84 site (and all of the APC binding sites), whereas the *S* configuration of the β153 site is unique among the phycobilin binding sites within *Synechococcus* sp. PCC 7002 (Duerring *et al.*, 1991; Ritter *et al.*; 1999; Shen *et al.*, 2006). The most likely substitute lyase for CpcSU (the β83 lyase) would be CpcE/F (the

α84 lyase), for the α84 and β83 lyases have been shown to be somewhat interchangeable in *Synechococcus* sp. PCC 7002 and other cyanobacteria (Swanson *et al.*, 1992; Shen *et al.*, 2004; Bhalerao *et al.*, 1994).

Both the β153 and β83 chromophores were affected in all the CpcB lyase$^-$ mutations, with the α84-β83 interaction being the most susceptible, so it seems that PC functionality is dependent on all of its chromophores. The degree of PC impairment was correlated more to the accessibility of the targeted bilin binding site to substitute lyase activity than to the function of the specific chromophore. Because chromophorylation is a prerequisite to subunit folding, altering the positioning of a chromophore can potentially change the surrounding protein's secondary and tertiary structures (Anderson & Toole, 1998; Toole *et al.*, 1998). In support, the CpcC$^-$ mutant, which is missing a structural PC linker polypeptide, showed similar spectroscopic properties and disruption in E transfer as the CpcTV$^-$/SUT$^-$ strains.

**Insights into the Light State Transition**

All of the strains were state transition competent and showed redistributions of both Chl*a*- and phycobilin- absorbed excitation energy. High M phosphate treatment effectively prevented large scale redistributions of both Chl*a*- and phycobilin- absorbed excitation energy suggesting that the two processes are not entirely independent. The state transition was dominated by the redistribution of PC-absorbed excitation energy, with state 2 characterized by a loss in PC contribution to PSII emission and an increase in

PC contribution to PSI emission. The state 1-to-state 2 transition may also involve the enhancement of PBS-PSI energetic coupling brought about through the physical movement and/or reorientation of PBS, for phycobilin excitation dependent, light state induced changes in emission from Chl*a* of the PSI trimer monomer-monomer interface were inhibited with high M phosphate treatment. Since high M phosphate treatment did not prevent minor levels of "reverse spillover" of Chl*a*- (and phycobilin-) absorbed excitation energy, spillover may be regulated on a smaller scale by the E transfer rates between neighboring PSII and PSI. The Cpc$^-$ mutant strains showed a larger (in magnitude) state transition than WT, perhaps to compensate for the reduced viability of their PBS in harvesting and transferring photon energy to the photosystems.

**Concluding Remarks**

The CpcB lyase$^-$ strains were able to cope with their potentially very costly mutations. The contribution of PC chromophores to the PBS absorbance cross section increases the potential photosynthetic yield within cells, especially when grown under less than optimal light conditions; therefore, functioning PC is beneficial to the cells. Under light limiting conditions regulatory pathways activate the synthesis of PC (de Lorimier *et al.*, 1992), so within the CpcB lyase$^-$ strains less than optimal methods of chromophorylating PC would be possible and even favored over the complete loss of PC. The CpcB lyase$^-$ mutants were able to produce chromophorylated PC, albeit the resultant PC was a poor light harvesting partner within the PBS. The spectroscopic evidence implies that the chromophores were attached within the correct β PC binding domains yet

were in E transfer unfavorable orientations - alternate, less specific lyases must have been acting on the binding sites. The differential loss in PBS antenna function among the mutant strains can be attributed to the binding site specificities of the substitute lyases; the β83 site was evidently more accessible than the β153 site. The $Cpc^-$ strains were still capable of redistributing PC-absorbed excitation energy via the light state transition mechanism and, in fact, were able to reallocate more E than WT. All in all, this study exemplifies the highly adaptive and responsive biological forces found within cyanobacteria.

# CITED LITERATURE


Adir N (2005) Elucidation of the molecular structures of components of the phycobilisome: reconstructing a giant. Photosyn. Res. 85: 15-32.

Ajlani G, Vernotte C (1998) Construction and characterization of a phycobiliprotein-less mutant of *Synechocystis* sp. PCC 6803. Plant. Molec. Biol. 37(3): 577-580.

Allen JF (1992) Protein phosphorylation in regulation of photosynthesis. Biochim. Biophys. Acta 1098: 275-335.

Allen JF, Forsberg J (2001) Molecular recognition in thylakoid structure and function. Trends in Plant Science, 6 pp. 317–326.

Allen JF, Holmes NG (1986) A general model for regulation of photosynthetic unit function by protein phosphorylation. FEBS Lett. 202: 175-181.

Anderson LK, Toole CM (1998) A model for early events in the assembly pathway of cyanobacterial phycobilisomes. Mol. Microbiol. 30(3): 467–474.

Andrizhiyevskayaa EG, Schwabe TME, Germano M, D'Haene S, Kruip J, van Grondelle R, Dekker JP (2002) Spectroscopic properties of PSI–IsiA supercomplexes from the cyanobacterium *Synechococcus* PCC 7942. Biochim. Biophys. Acta 1556: 265– 272.

Apt KE, Collier JL, Grossman AR (1995) Evolution of the phycobiliproteins. J. Mol. Biol. 248: 79-96.

Arciero DM, Bryant DA, Glazer AN (1988) In vitro attachment of bilins to apophycocyanin. J. Biol. Chem. 263: 18350–18357.

Aro E-M, Virgin I, Andersson B (1993) Photoinhibition of photosystem II: inactivation, protein damage and turnover. Biochim. Biophys. Acta. 1143: 113–134.

Ashby MK, Mullineaux CW (1999) The role of ApcD and ApcF in energy transfer from phycobilisomes to PSI and PSII in a cyanobacterium. Photosyn. Res. 61: 169-179.

Aspinwall CL, Sarcina M, Mullineaux CW (2004) Phycobilisome mobility in the cyanobacterium *Synechococcus* sp. PCC 7942 is influenced by the trimerisation of photosystem I. Photosyn. Res. 79: 179-187.

Bald D, Kruip J, Rögner M (1996) Supramolecular architecture of cyanobacterial thylakoid membranes: How is the phycobilisome connected with the photosystems? Photosyn. Res. 49: 118.

Barber J, Morris EP, da Fonseco PCA (2003) Interaction of the allophycocyanin core complex with photosystem II. Photochem. Photobiol. Sci. 2: 536-541.

Bhalerao RP, Gustafsson P (1994) Factors influencing the phycobilisome rod composition of the cyanobacterium *Synechococcus* sp. PCC 7942: Effects of reduced phycocyanin content, lack of rod-linkers, and over-expression of the rod-terminating linker. Physiologia Plantarum 90(1): 187.

Bhalerao RP, Lind LK, Gustafsson P (1994) Cloning of the *cpcE* and *cpcF* genes from *Synechococcus* sp. PCC 6301 and their inactivation in *Synechococcus* sp. PCC 7942. Plant Mol. Biol. 26(1): 313-326.

Bhalerao RP, Collier JL, Gustafsson P, Grossman AR (1995) The structure of phycobilisomes in mutants of *Synechococcus* sp. strain PCC-7942 devoid of specific linker polypeptides. Photochem. Photobiol. 61: 298-302.

Biggins J, Bruce D (1989) Regulation of excitation energy transfer in organisms containing phycobilins. Photosynth. Res. 20: 1-34.

Binder A, Hauser R, Krogmann D (1984) Respiration in energy-transducing membranes of the thermophilic cyanobacterium *Mastigocladus laminosus*. I: Relation of the respiratory and photosynthetic electron transport. Biochim. Biophys. Acta 765: 241–246.

Bittersmann E, Vermass WFJ (1991) Fluorescence lifetime studies of cyanobacterial photosystem II mutants. Biochim. Biophys. Acta 1098:105-116.

Brimble S, Bruce D (1989) Pigment orientation and excitation energy transfer in *Porphyridium cruentum* and *Synechococcus* sp. PCC 6301 cross-linked in light state 1 and light state 2 with glutaraldehyde. Biochim. Biophys. Acta 973: 315-323.

Bruce D, Biggins J (1985) Mechanism of the light-state transition in photosynthesis. V: 77 K linear dichroism of *Anacystis nidulans* in State 1 and State 2. Biochim. Biophys. Acta 810: 295-301.

Bruce D, Brimble S, Bryant DA (1989) State transitions in a phycobilisome-less mutant of the cyanobacterium *Synechococcus* sp. 7002. Biochim. Biophys. Acta 974: 66-73.

Bryant DA (ed.) (1994) The molecular biology of cyanobacteria. Kluwer Academic Publishers, Dordrecht, The Netherlands.

Campbell D, Hurry V, Clarke A, Gustafsson P, Öquist G (1998) Chlorophyll fluorescence analysis of cyanobacterial photosynthesis and acclimation. Microbiol. Molec. Biol. Rev. 62:667-683.

Clement-Metral JD, Gantt E, Redlinger T (1985) A photosystem II-phycobilisome preparation from the red alga, *Porphyridium cruentum*: oxygen evolution, ultrastructure, and polypeptide resolution. Arch. Biochem. Biophys. 238(1): 10-7.

Cobley JC, Clark AC, Weerasurya S, Queseda FA, Xiao JY, Bandrapali N, D'Silva I, Thounaojam M, Oda JF, Sumiyoshi T, Chu M-H (2002) CpeR is an activator required for expression of the phycoerythrin operon (*cpeBA*) in the cyanobacterium *Fremyella diplosiphon* and is encoded in the phycoerythrin linker-polypeptide operon (*cpeCDESTR*). Mol. Microbiol. 44(6): 1517–1531.

Contreras-Martel C, Martinez-Oyanedel J, Poo-Caama G, Bruna C, Bunster M (2007) The structure at 2 Å resolution of phycocyanin from *Gracilaria chilensis* and the energy transfer network in a PC-PC complex. Annu. Rev. Biophys. Biophys. Chem. 125: 388.

Debreczeny MP, Sauer K, Zhou J, Bryant DA (1993) Monomeric C-phycocyanin at room temperature and 77°K: resolution of the absorption and fluorescence spectra of the individual chromophores and the energy transfer rate constants. J. Phys. Chem. 97: 9852–9862.

Debreczeny MP, Sauer K, Zhou J, Bryant DA (1995) Comparison of calculated and experimentally resolved rate constants for excitation energy transfer in C-Phycocyanin. 2. Trimers. J. Phys. Chem. 99: 8420-8431.

de Lorimier RM, Bryant DA, Stevens SE Jr (1990) Genetic analysis of a 9 kDa phycocyanin-associated linker polypeptide. Biochim. Biophys. Acta. 1019(1): 29-41.

de Lorimier RM, Smith RL, Stevens SE Jr (1992) Regulation of phycobilisome structure and gene expression by light intensity. Plant Phys. 98: 1003-1010.

Demidov AA, Mimuro M (1995) Deconvolution of C-phycocyanin β-84 and β-155 chromophore absorption and fluorescence spectra of cyanobacterium *Mastigocladus laminosus*. Biophysical J. 68: 1500-1506.

Duerring M, Schmidt GB, Huber R (1991) Isolation, crystallization, crystal structure analysis and refinement of constitutive C-phycocyanin from the chromatically adapting cyanobacterium *Fremyella diplosiphon* at 1.66 Å resolution. J. Mol. Biol. 217(3): 577–592.

Emlyn-Jones D, Ashby MK, Mullineaux CW (1999) A gene required for the regulation of photosynthetic light-harvesting in the cyanobacterium *Synechocystis* 6803. Molec. Microbiol. 33: 1050–1058.

Fairchild CD, Zhao J, Zhou J, Colson SE, Bryant DA, Glazer AN (1992) Phycocyanin α-subunit phycocyanobilin lyase. Proc. Natl. Acad. Sci. USA 89: 7017–7021.

Fairchild CD, Glazer A (1994) Oligomeric structure, enzyme kinetics, and substrate specificity of the phycocyanin α subunit phycocyanobilin lyase. J Biol Chem 269: 8686–8694.

Federman S, Malkin R, Scherz A (2000) Excitation energy transfer in aggregates of photosystem I and photosystem II of the cyanobacterium *Synechocystis* sp PCC 6803: Can assembly of the pigment-protein complexes control the extent of spillover? Photosynth. Res. 64: 199-207.

Finazzi G, Barbagallo RP, Bergo E, Barbato R, Forti G (2001) Photoinhibition of *Chlamydomonas reinhardtii* in State 1 and State 2. Damages to the photosynthetic apparatus under linear and cyclic electron flow. J. Biol. Chem. 276: 22251–22257.

Fork DC, Satoh K (1983) State 1-state 2 transitions in the thermophylic blue-green alga (cyanobacterium) *Synechococcus lividus*. Photochem. Photobiol. 37: 421-427.

Förster T (1948) Zwishenmolekulare energiewanderung und fluoreszenz. Ann. Phys. 2: 55.

Förster T (1959) Transfer mechanisms of electronic excitation. Discuss. Faraday Soc. 27: 7.

Förster T (1965) Delocalized excitation and excitation transfer. In: Sinanoglu O (Ed.) Modern Quantum Chemistry Part III. Academic Press, New York, pg. 93.

Friedrich J, Scheer H, Zickendraht-Wendelstadt B, Haarer D (1981) High-resolution optical studies on C-phycocyanin via photochemical hole burning. J. Am. Chem. Soc. 103: 1030.

Fujimori T, Hihara Y, Sonoike K (2005) PsaK2 subunit in photosystem I is involved in state transition under high light condition in the cyanobacterium *Synechocystis* sp. PCC 6803. J. Biol. Chem. 280(23): 22191-22197.

Gantt E, Grabowski B, Cunningham FX Jr. (2003) 10. Antenna systems of red algae: phycobilisomes with photosystem II and chlorophyll complexes with photosystem 1. In: Green BR & Parson WW (Eds.) Advances in Photosynthesis and respiration. Vol 13, 307. Kluwer Academic Publishers, Dordrecht, The Netherlands.

Gindt YM, Zhou J, Bryant DA, Sauer K (1994) Spectroscopic studies of phycobilisome subcore preparations lacking key core chromophores: assignment of excited state energies to the $L_{cm}$, $\beta^{18}$ and $\alpha^{AP\text{-}B}$ chromophores. Biochim. Biophys. Acta 1186: 153-162.

Glazer AN (1982) Phycobilisomes: structure and dynamics. Ann. Rev. Microbiol. 36: 173-198.

Glazer AN (1984) Phycobilisomes: a macromolecular complex optimized for light energy transfer. Biochim. Biophys. Act 768: 29-51.

Glazer AN, Chan C, Williams RC, Yeh SW, Clark JH (1985) Kinetics of energy flow in the phycobilisome core. Science 29 230(4729): 1051 – 1053.

Glazer AN, Melis A (1987) Photochemical reaction centers: Structure, organization, and function. Ann. Rev. Plant Physiol. 38: 11-45.

Glazer AN (1989) Light guides. JBC 264: 1-4.

Gómez-Lojero C, Pérez-Gómez B, Shen G, Schlucter WM, Bryant DA (2003) Interaction of ferredoxin:$NADP^+$ oxidoreductase with phycobilisomes and phycobilisome substructures of the cyanobacterium *Synechococcus* sp. strain PCC 7002. Biochem. 42: 13800-11.

Gray BH, Gantt E (1975) Spectral properties of phycobilisomes and phycobiliproteins from the blue-green alga – *Nostoc* sp. Photochem. Photobiol. 21: 121.

Groot M-L, Peterman EJG, van Stokkum IHM, Dekker JP, van Grondelle R (1995) Triplet and fluorescing states of the CP47 antenna complex of photosystem II studied as a function of temperature. Biophys. J. 68: 281-90.

Groot M-L, Frese RN, de Weerd FL, Bromek K, Pettersson Å, Peterman EJG, van Stokkum IHM, van Grondelle R, Dekker JP (1999) Spectroscopic properties of the CP43 core antenna protein of photosystem II. Biophys. J. 77: 3328-40.

Grossman AR, Schaefer MR, Chiang GG, Collier JL (1993) The Phycobilisome, a light-harvesting complex responsive to environmental conditions. Microbiol. Reviews 57: 725-749.

Grossman AR, Bhaya D, He Q (2001) Tracking the light environment by cyanobacteria and the dynamic nature of light harvesting. JBC 276: 11449-11452.

Homer-Dixon J, Gantt E, Bruce D (1994) Pigment orientation changes accompanying the light state transition in *Synechococcus* sp. PCC 6301. Photosynth. Res. 40: 35-44.

Huang C, Yuan X, Zhao J, Bryant DA (2003) Kinetic analyses of state transitions of the cyanobacterium *Synechococcus* sp. PCC 7002 and its mutant strains impaired in electron transport. Biochim. Biophys. Acta 1607: 121-130.

Jones LW, Myers J (1963) A common link between photosynthesis and respiration in a blue-green alga. Nature 199:670-672.

Joshua S, Mullineaux CW (2004) Phycobilisome diffusion is required for light-state transitions in cyanobacteria. Plant Physiol. 135: 2112-2119.

Joshua S, Bailey S, Mann NH, Mullineaux CW (2005) Involvement of phycobilisome diffusion in energy quenching in cyanobacteria. Plant Physiol. 138(3): 1577–1585.

Karapetyan NV (2004) Interaction of pigment-protein complexes within aggregates stimulates dissipation of excess energy. Biochem. 69(11): 1299-1304.

Ke B (2001) Advances in Photosynthesis Vol. 10. Photosynthesis: Photobiochemistry and Photobiophysics. Kluwer Academic Publishers, Dordrecht, The Netherlands.

Klotz AV, Glazer AN (1985) Characterization of the bilin attachment sites in R-phycoerythrin. J. Biol. Chem. 260: 4856-4863.

Kruip J, Karapetyan NV, Terekhova IV, Rögner M (1999) In vitro oligomerization of a membrane protein complex: Liposome-based reconstitution of trimeric photosystem I from isolated monomers. J. Biol. Chem. 274: 18181-18188.

LeClerc JC, Hoarau J, Remy R (1979) Analysis of absorption spectra changes induced by temperature lowering on phycobilisomes, thylakoids, and chlorophyll-protein complexes. Biochim. Biophys. Acta 547: 398-409.

Lecomte JTJ, Kao Y, Cocco MJ (1996) The native state of apomyoglobin described by proton NMR spectroscopy: the A-B-G-H interface of wild-type sperm whale apomyoglobin. Proteins 25: 267–285.

Li D, Xie J, Zhao J, Xia A, Li D, Gong Y (2004) Light-induced excitation energy redistribution in *Spirulina platensis* cells: "spillover" or "mobile PBSs"? Biochim. Biophys. Acta 1608: 114-121.

Li H, Li D, Yang S, Xie J, Zhao J (2006) The state transition mechanism – simply depending on light-on and -off in *Spirulina platensis*. Biochim. Biophys. Acta. 1757(11): 1512-9.

Li Y, Zhang JP, Xie J, Zhao JQ, Jiang LJ (2001) Temperature-induced decoupling of phycobilisomes from reaction center. Biochim. Biophys. Acta 1504: 229-234.

Lichtlé C, Thomas JC (1976) Étude ultrastructurale des thylacoides des algues a phycobiliproteins, comparison des résultants obtenus par fixation classique et cryodécapage. Phycologia 15: 393.

MacColl R, Guard-Friar D (1987) Phycobiliproteins. CRC Press, Inc. Boca Raton, Florida.

MacColl R (1998) Cyanobacterial phycobilisomes. J. Structur. Biol. 124: 311-334.

MacColl R (2004) Allophycocyanin and energy transfer. Biochim. Biophys. Acta 1657: 73-81.

McConnell MD, Koop R, Vasil'ev S, Bruce D (2002) Regulation of the distribution of chlorophyll and phycobilin-absorbed excitation energy in cyanobacteria. A structure-based model for the light state transition. Plant Physiol. 130: 1201-1212.

Mimuro M, Füglistaller P, Rümbeli R, Zuber H (1986 a) Functional assignment of chromophores and energy transfer in C-phycocyanin isolated from the thermophilic cyanobacterium *Mastigocladus laminosus*. Biochim. Biophys. Acta 848: 155-66.

Mimuro M, Lipschultz CA, Gantt E (1986 b) Energy flow in the phycobilisome core of *Nostoc* sp. (MAC); two independent terminal pigments. Biochim. Biophys. Acta 933: 78-486.

Mimuro M (1989) Studies on excitation energy flow in the photosynthetic pigment system; structure and energy transfer mechanisms. Bot. Mag. Tokyo 103:244.

Mimuro M, Yamazaki I, Tamai N, Katoh T (1989) Excitation energy transfer in phycobilisomes at -196°C isolated from the cyanobacterium *Anabaena variabilis* (M-3); evidence for the plural transfer pathways to the terminal emitters. Biochim. Biophys. Acta 973: 153-162.

Mimuro M, Kikuchi H, Murakami A (1999) 5. Structure and function of phycobilisomes. In: Singhal GS, Renger G, Sopory SK, Irrgang K-D, Govindjee (Eds.) Concepts in photobiology: Photosynthesis and photomorphogenesis. Narosa Publishing House, New Delhi, India. pp.104.

Mimuro M, Kikuchi H (2003) 9. Antenna systems and energy transfer in cyanophyta and rhodophyta. In: Green BR & Parson WW (Eds.) Advances in Photosynthesis and respiration. Vol 13, 282. Kluwer Academic Publishers, Dordrecht, The Netherlands.

Mörschel E, Rhiel E (1987) Phycobilisomes and thylakoids. In: Harris JR, Horne RW (Eds.) Electron Microscopy of Proteins. Academic Press, London, vol 6 pp. 209–254.

Mullineaux CW, Allen JF (1986) The state 2 transition in the cyanobacterium *Synechococcus* 6301 can be driven by respiratory electron flow into the plastoquinone pool. FEBS letters 205(1): 155-160.

Mullineaux CW, Allen JF (1990) State 1-State 2 transitions in the cyanobacterium *Synechocystis* 6301 are controlled by the redox state of electron carriers between photosystems I and II. Phosynth. Res. 22: 157-166.

Mullineaux CW, Bittersmann E, Allen JF, Holzwarth AR (1990) Picosecond time-resolved energy transfer from the phycobilisome to photosystem II in light-state 2 in the cyanobacterium *Synechococcus* 6301. Biochim. Biophys. Acta 1015: 231-242.

Mullineaux CW, Holzwarth AR (1991) Kinetics of excitation energy transfer in the cyanobacterial phycobilisome-photosystem II complex. Biochim. Biophys. Acta 1098: 68-79.

Mullineaux CW (1992) Excitation energy transfer from phycobilisomes to photosystem I in a cyanobacterium. Biochim. Biophys. Acta. 1100: 285-292.

Mullineaux CW (1994) Excitation energy transfer from PBS to PSI in a cyanobacterial mutant lacking PSII. Biochim. Biophys. Acta. 1184: 71-77.

Mullineaux CW, Tobin MJ, Jones GR (1997) Mobility of photosynthetic complexes in thylakoid membranes. Nature 390: 421-424.

Mullineaux CW (1999) The thylakoid membranes of cyanobacteria: structure, dynamics and function. Aust. J. Plant Physiol. 26: 671-677.

Mullineaux CW (2004) FRAP analysis of photosynthetic membranes. J. Exper. Botany 55: 1207-1211.

Mullineaux CW, Emlyn-Jones D (2005) State transitions: an example of acclimation to low light stress. J. Exp. Bot. 56: 389-393.

Myers J, Graham J-R, Wang RT (1980) Light harvesting in *Anacystis nidulans* studied in pigment mutants. Plant Physiol. 66: 1144-1149.

Nield J, Rizkallah PJ, Barber J, Chayen NE (2003) The 1.45 Å three-dimensional structure of C-phycocyanin from the thermophilic cyanobacterium *Synechococcus elongatus*. J. Struct. Biol. 141: 149-155.

Olive J, M'Bina J, Vernotte C, Astier C, Wollman FA (1986) Randomization of the EF particles in thylakoid membranes of *Synechocystis* 6714 upon transition from state 1 to state 2. FEBS 208: 308-312.

Olive J, Ajlani G, Astier C, Recouvreur M, Vernotte C (1997) Ultrastructure and light adaptation of phycobilisome mutants of *Synechocystis* PCC 6803. Biochim. Biophys. Acta 1319: 275-282.

Padyana AK, Ramakumar S (2006) Lateral energy transfer model for adjacent light-harvesting antennae rods of C-phycocyanins. Biochim. Biophys. Acta 1757(3): 161-165.

Pizarro SA, Sauer K (2001) Spectroscopic study of the light-harvesting protein C-phycocyanin associated with colorless linker peptides. Photochem. Photobiol. 73(5): 556-63.

Plank T, Toole C, Anderson LK (1995) Subunit interactions and protein stability in the cyanobacterial light-harvesting proteins. J. Bacteriol. 177: 6798–6803.

Ritter S, Hiller RG, Wrench PM, Welte W, Diederichs K (1999) Crystal structure of a phycourobilin-containing phycoerythrin at 1.90-Å resolution. J. Struct. Biol. 126(2): 86–97.

Rögner M, Nixon PJ, Diner BA (1990) Purification and characterization of photosystem I and photosystem II core complexes from wild-type and phycocyanin-deficient strains of the cyanobacterium *Synechocystis* PCC 6803. J. Biol. Chem. 265: 6189-6196.

Rouag D, Dominy PJ (1994) State transitions in the cyanobacterium *Synechococcus* 6301 (PCC): dependence on light intensity or spectral composition. Photosyn. Res. 40: 107-117.

Sarcina M, Mullineaux CW (2004) Mobility of the IsiA chlorophyll-binding protein in cyanobacterial thylakoid membranes. J. Biol. Chem. 279: 36514–36518.

Scheer H (2003) 2. The Pigments. In: Green BR & Parson WW (Eds.) Advances in Photosynthesis and respiration. Vol 13, 55. Kluwer Academic Publishers, Dordrecht, The Netherlands.

Schluchter WM, Bryant DA (1992) Molecular characterization of Ferredoxin-$NADP^+$ Oxidoreductase in cyanobacteria: cloning and sequence of the *petH* gene of *Synechococcus* sp. PCC 7002 and studies on the gene product. Biochem. 131: 3092-3102.

Schluchter WM, Glazer AN (1999) Biosynthesis of phycobiliproteins in Cyanobacteria. In: Peschek G, Löffelhardt W, Schmetterer G, (Eds.) The Phototrophic Prokaryotes. pp. 83–95. Kluwer Academic/Plenum Press, New York.

Shubin VV, Murthy SDS, Karapetyan NV, Mohanty P (1991) Origin of the 77 K variable fluorescence at 758 nm in the cyanobacterium *Spirulina platensis*. Biochim. Biophys. Acta 1060: 28-36.

Shubin VV, Bezsmertnaya IN, Karapetyan NV (1992) Isolation from *Spirulina* membranes of two photosystem I-type complexes, one of which contains chlorophyll responsible for the 77 K fluorescence band at 760 nm. FEBS Lett. 309: 340-342.

Scott M, McCollum C, Vasil'ev S, Crozier C, Espie G, Krol M, Huner N, Bruce D (2006) Mechanism of the down regulation of photosynthesis by blue light in the cyanobacterium *Synechocystis* sp. PCC 6803. Biochem. 45:8952-8958.

Shen G, Boussiba S, Vermaas WFJ (1993) *Synechocystis* sp PCC 6803 strains lacking photosystem I and phycobilisome function. Plant Cell 5: 1853-1863.

Shen G, Bryant DA (1995) Characterization of a *Synechococcus* sp. strain PCC 7002 mutant lacking photosystem I. Protein assembly and energy distribution in the absence of the photosystem I reaction center core complex. Photosyn. Research 44(1-2): 41-53.

Shen G, Saunèe NA, Gallo E, Begovic Z, Schluchter WM, Bryant DA (2004) Identification of a new family of phycobiliprotein lyases in cyanobacteria: characterization of a β-phycocyanin lyase. 8th Cyanobacterial Molecular Biology Workshop. August 2004. Ste. Adele, Quebec.

Shen G, Saunée NA, Williams SR, Gallo EF, Schluchter WM, Bryant DA (2006) Identification and characterization of a new class of bilin lyase. The cpcT gene encodes a bilin lyase responsible for attachment of phycocyanobilin to Cys-153 on the β-subunit of phycocyanin in *Synechococcus* sp. PCC 7002. JBC 281(26): 17768–78.

Schluchter WM, Bryant DA (1992) Molecular characterization of ferredoxin-$NADP^+$ oxidoreductase in cyanobacteria: Cloning and sequence of petH gene of *Synechococcus* sp PCC 7002 and studies in gene product. Biochem. 31: 3092-3102.

Stamatakis K, Papageorgiou GC (2001) The osmolality of the cell suspension regulates phycobilisome-to-photosystem I excitation transfers in cyanobacteria. Biochim. Biophys. Acta 1506: 172-181.

Stec B, Troxler RF, Teeter MM (1999) Crystal structure of C-phycocyanin from *Cyanidium caldarium* provides a new perspective on phycobilisome assembly. Biophys. J. 76: 2912–2921.

Su X, Fraenkel PG, Bogorad L (1992) Excitation energy transfer from phycocyanin to chlorophyll in an $apcA^-$ defective mutant of *Synechocystis* sp. PCC 6803. J. Biol. Chem. 267 (32): 22944-22950.

Swanson RV, Zhou J, Leary JA, Williams T, de Lorimier R, Bryant DA, AN Glazer (1992) Characterization of phycocyanin produced by cpcE and cpcF mutants and identification of an intergenic suppressor of the defect in bilin attachment. J. Biol. Chem. 267 (23): 16146-16154.

Toole CM, Plank TL, Grossman AR, Anderson LK (1998) Bilin deletions and subunit stability in cyanobacterial light-harvesting proteins. Mol. Microbiol. 30: 475–486.

Thomas BA, McMahon LP, Klotz AV (1995) $N^5$-methylasparagine and energy-transfer efficiency in C-phycocyanin. Biochem. 34: 3758–3770.

van Amerongen H, Dekker JP (2003) In: Green BR & Parson WW (Eds.) Advances in Photosynthesis and respiration. Vol 13, 220-251. Kluwer Academic Publishers, Dordrecht, The Netherlands.

van Grondelle R, Dekker J, Gillbro T, Sundstrom V (1994) Energy transfer and trapping in photosynthesis. Biochim. Biophys. Acta 1187:1-65.

van Thor JJ, Mullineaux CW, Mathijs HCP, Hellingwerf KJ (1998) Light harvesting and state transitions in cyanobacteria. Bot. Acta. 111: 430-443.

Wilson A, Ajlani G, Verbavatz J-M, Vass I, Kerfeld CA, Kirilovsky D. (2006) A soluble carotenoid protein involved in phycobilisome-related energy dissipation in cyanobacteria. Plant Cell 18: 992-1007.

Wollman FA (2001) State transitions reveal the dynamics and flexibility of the photosynthetic apparatus. EMBO J. 20: 3623-3630.

Xie J, Zhao J-Q, Peng C (2002) Analysis of the disk-to-disk energy transfer processes in C-Phycocyanin complexes by computer simulation technique. Photosynthetica 40(2): 251-257.

Yu M-H, Glazer AN (1982) Cyanobacterial phycobilisomes: role of the linker polypeptides in the assembly of phycocyanin. J Biol Chem 257: 3429–3433.

Yu L, Zhao J, Bryant DA, Goldbeck JH (1993) PsaE is required for *in vivo* cyclic electron flow around photosystem I in the cyanobacterium *Synechococcus* sp. PCC 7002. Plant Physiol. 103: 171-180.

Zhang J, Zhao J, Jiang L, Zheng X, Zhao F, Wang H (1997) Studies on the energy transfer among the rod-core complexes from phycobilisome of *Anabaena variabilis* by time resolved fluorescence emission and anisotropy spectra. Biochim. Biophys. Acta 1320: 285–296.

Zhao K-H, Su P, Li J, Tu J-M, Zhou M, Bubenzer C, Scheer H (2006 a) Chromophore attachment to phycobiliprotein beta-subunits: Phycocyanobilin:cysteine-beta84 phycobiliprotein lyase activity of CpeS-like protein from *Anabaena* Sp. PCC 7120. J. Biol. Chem. 281(13): 8573 - 8581.

Zhao K-H, Wu D, Zhang L, Zhou M, Böhm S, Bubenzer C, Scheer H (2006 b) Chromophore attachment in phycocyanin. Functional amino acids of phycocyanobilin -α-phycocyanin lyase and evidence for chromophore binding. FEBS Journal 273(6): 1262–1274.

Zhao J, Zhou J, Bryant DA (1992) Energy transfer processes in phycobilisomes as deduced from analyses of mutants of *Synechococcus* sp. PCC 7002. In: Murata N (ed.) Research in Photosynthesis. Vol 1, 25-32. Kluwer Academic Publishers, Dordrecht, The Netherlands.

Zhao J, Gaozhong S, Bryant DA (2001) Photosystem stoichiometry and state transitions in a mutant of the cyanobacterium *Synechococcus* sp. PCC 7002 lacking phycocyanin. Biochim. Biophys. Acta 1505: 248-257.

Zhou J, Gasparich GE, Stirewalt VA, deLorimier R, Bryant DA (1992) The *cpcE* and *cpcF* genes of *Synechococcus* sp. PCC 7002: construction and phenotypic characterization of interposon mutants. J Biol Chem 267: 16138–16145.

Zilinskas BA, Greenwald LS (1986) Phycobilisome structure and function. Photosynth. Res. 10: 7–35.

Appendix I

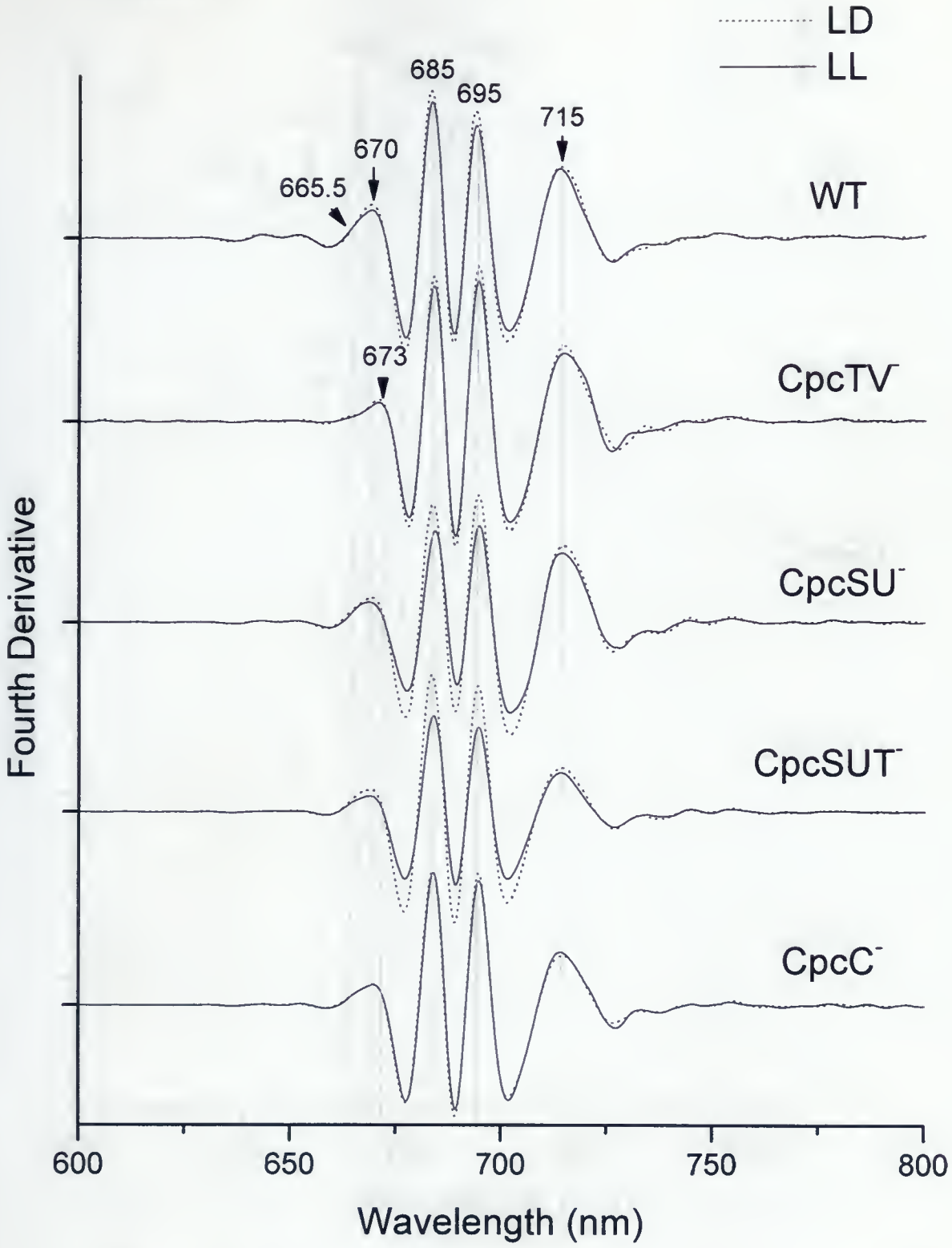


Fourth derivative analysis of 77K emission spectra from LL/LD treated cells with 435 nm excitation. Notation same as in Figure 10-1. Differentiation interval of 7.5 nm.

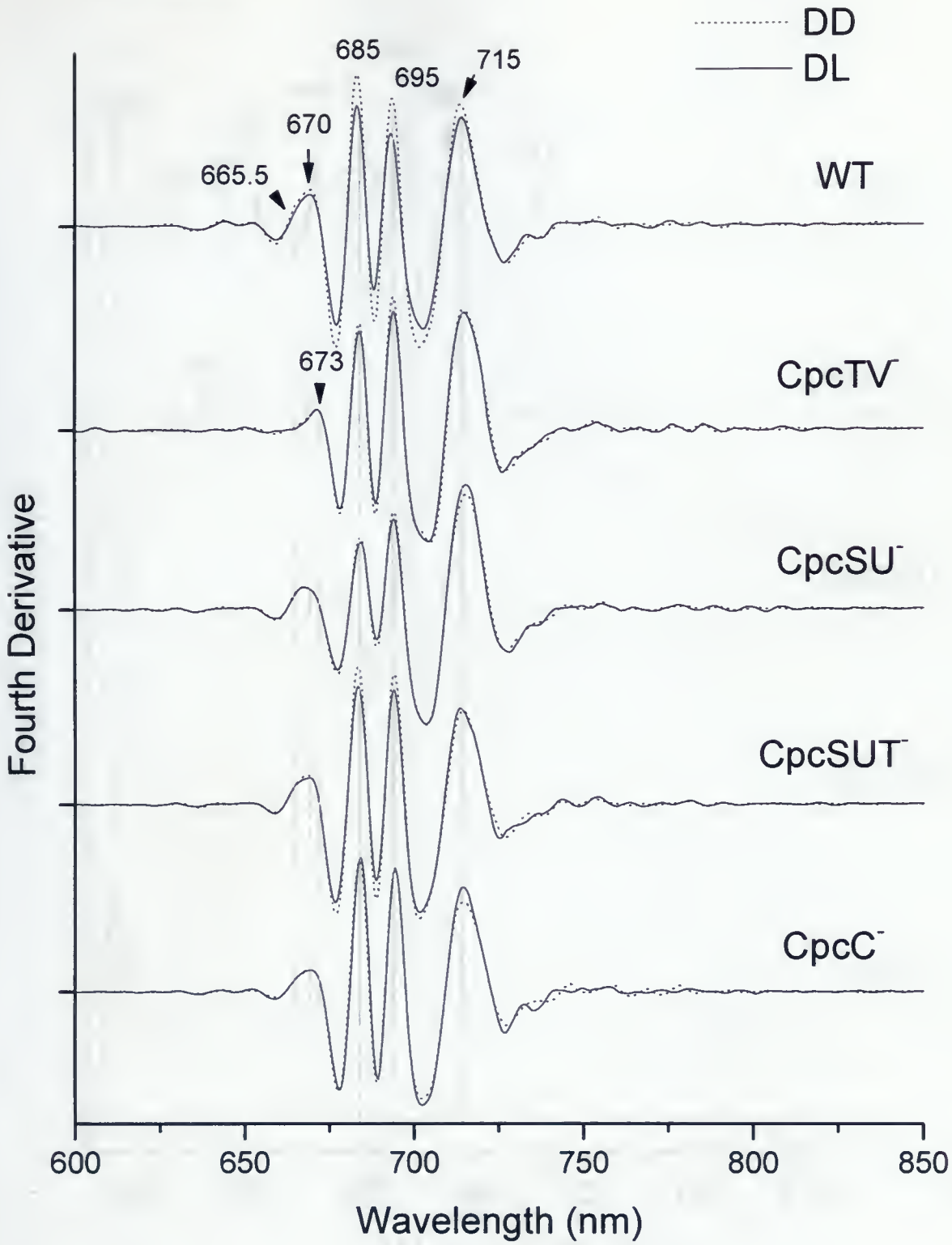


Fourth derivative analysis of 77K emission spectra from DD/DL treated cells with 435 nm excitation. Notation same as in Figure 10-1. Differentiation interval of 7.5 nm.

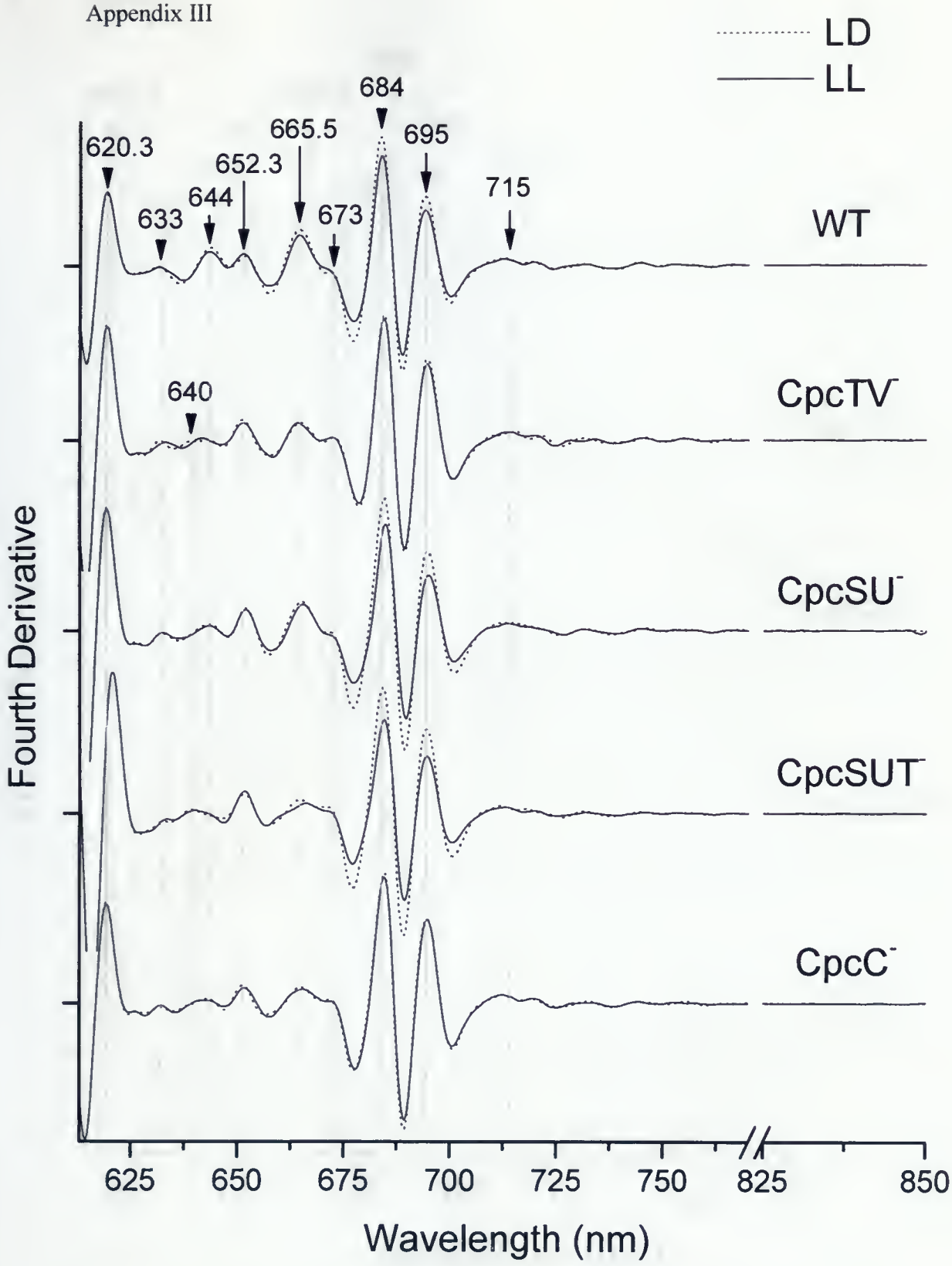


Fourth derivative analysis of 77K emission spectra from LL/LD treated cells with 575 nm excitation. Notation same as in Figure 10-2. Differentiation interval of 7.5 nm.

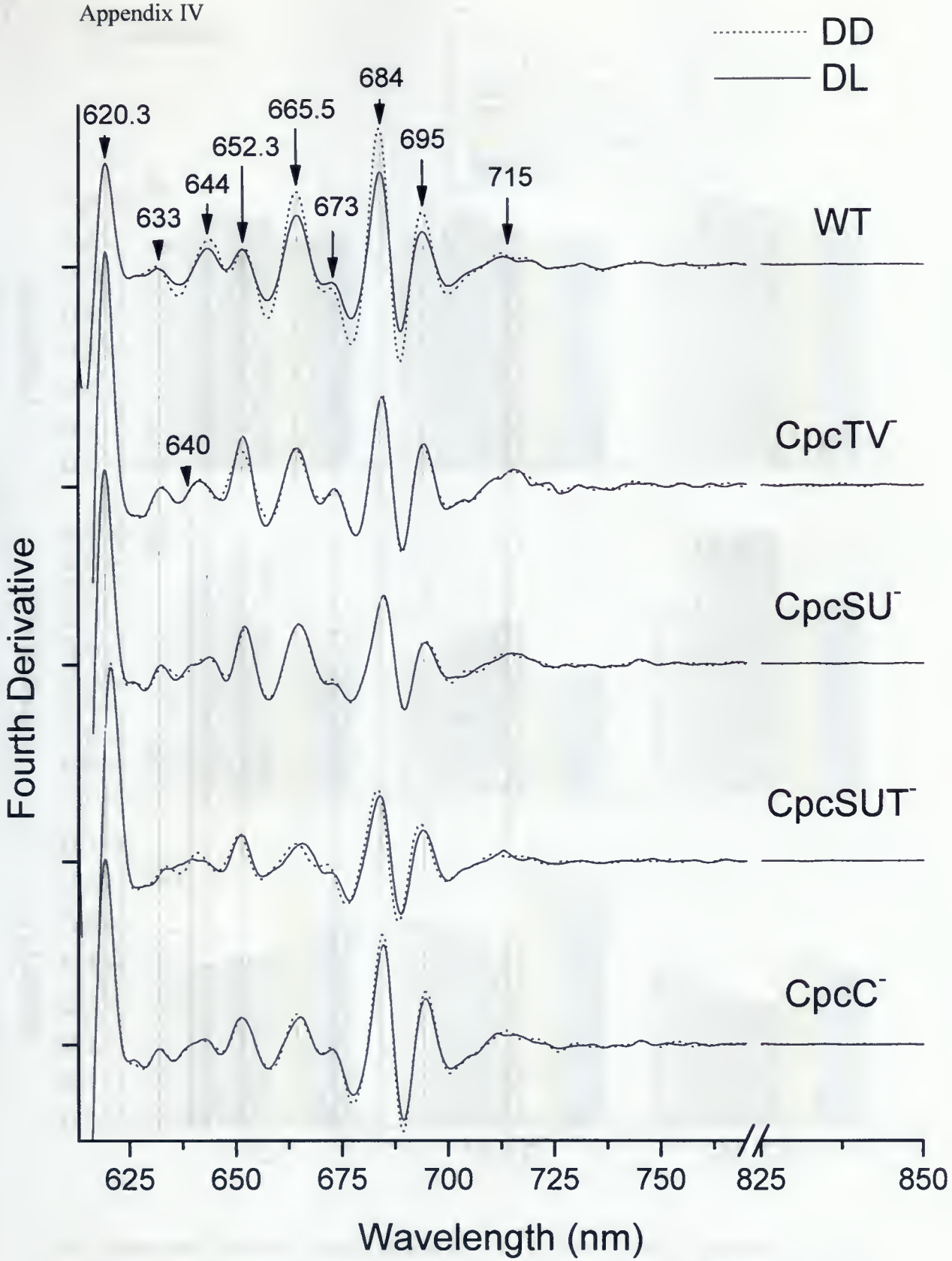


Fourth derivative analysis of 77K emission spectra from DD/DL treated cells with 575 nm excitation. Notation same as in Figure 10-2. Differentiation interval of 7.5 nm.

Appendix V

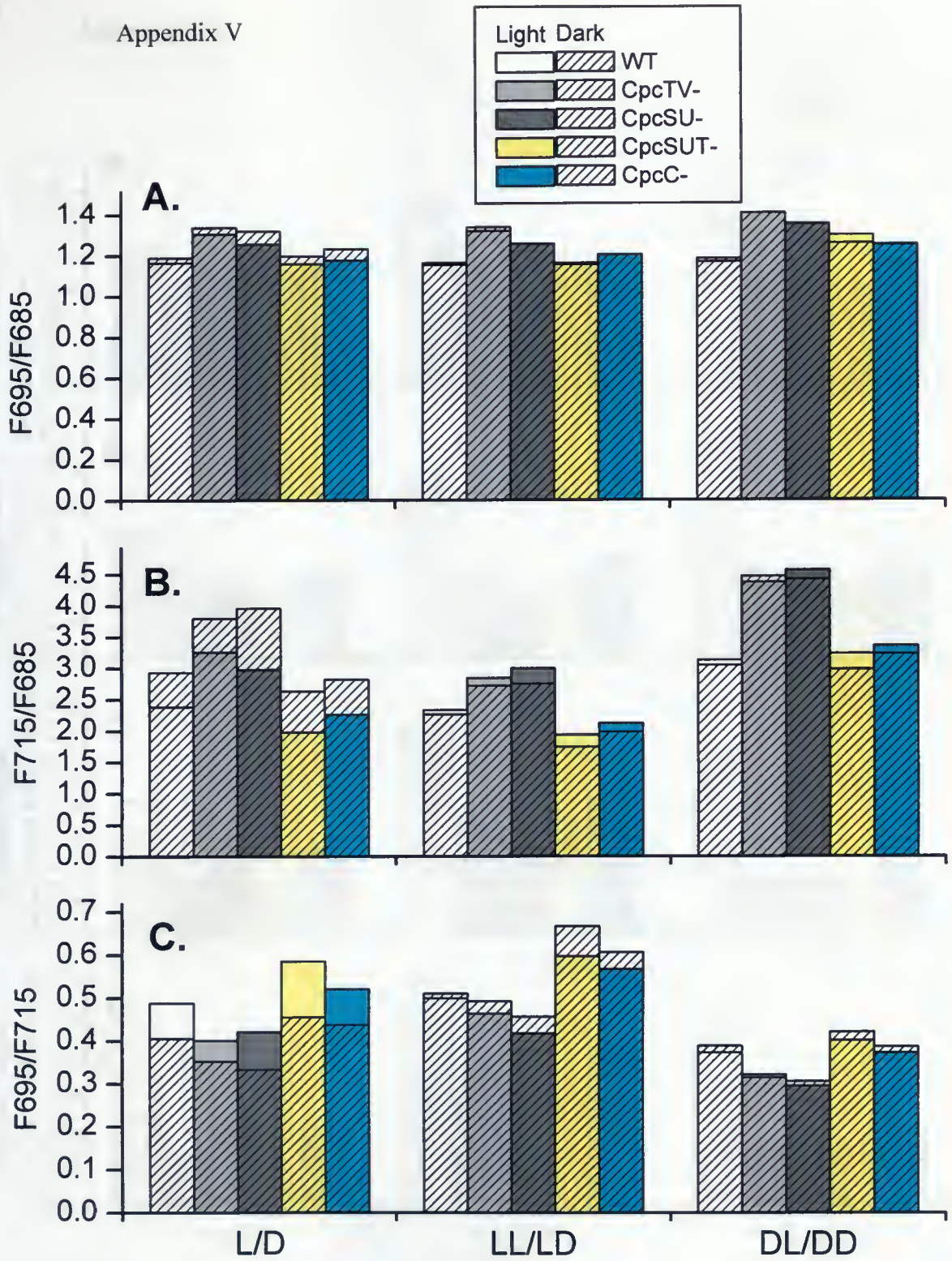


77K emission peak ratios from 435 nm excitation. L, D, LL, LD, DD, DL, as previously described. Major emission peaks are denoted by $F_n$, in which n stands for peak location in nm. Light, denotes last treatment that the sample received was illumination with blue light. Dark, denotes last treatment that the sample received was dark adaptation. **A**, **B**, **C**, F695/F685, F715/F685, F695/F715, respectively.

Appendix VI

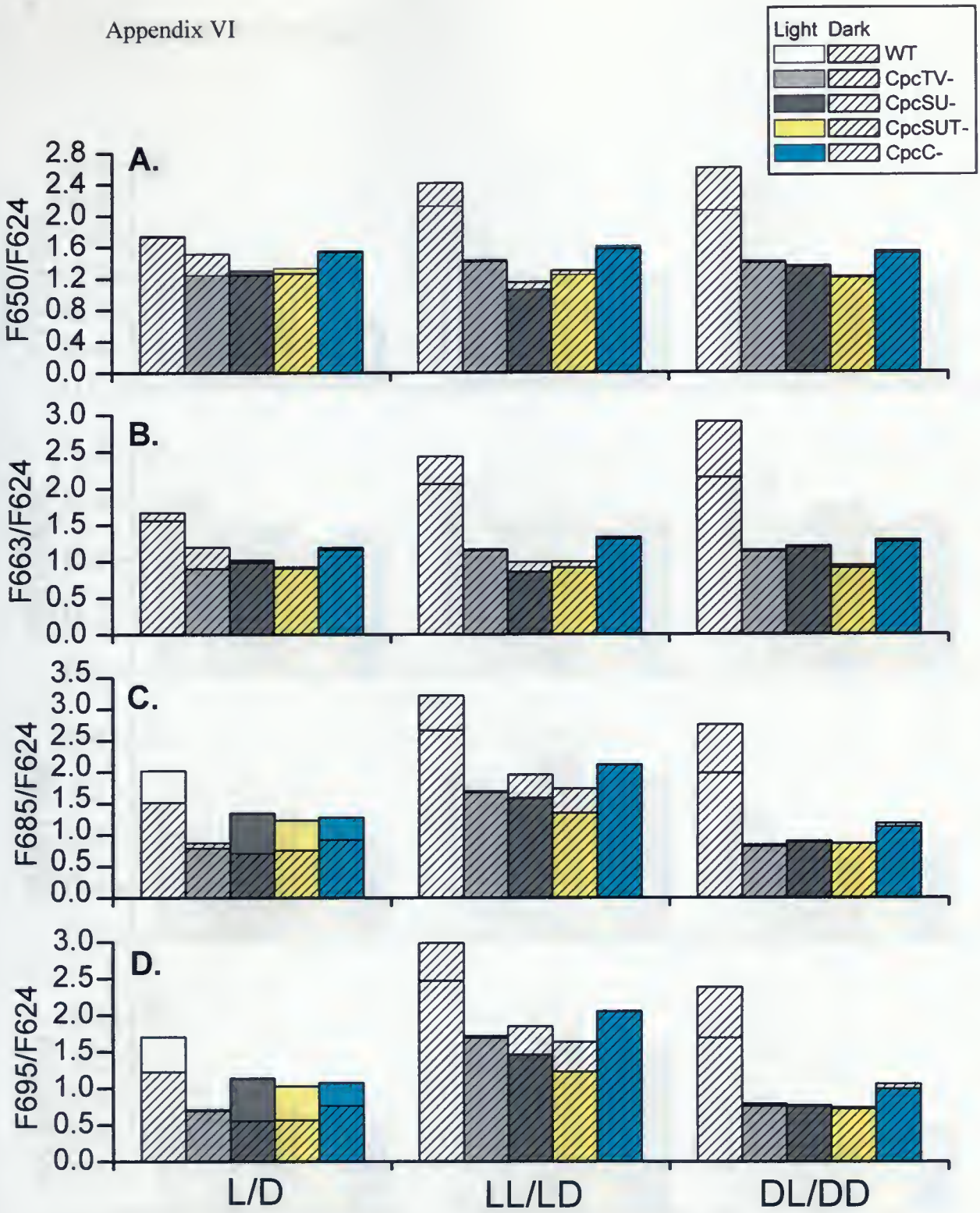


77K emission peak ratios from 575 nm excitation. L, D, LL, LD, DD, DL, as previously described. Major emission peaks are denoted by $F_n$, in which n stands for peak location in nm. Light, denotes last treatment that the sample received was illumination with blue light. Dark, denotes last treatment that the sample received was dark adaptation. **A-P**, F650/F624, F663/F624, F685/F624, F695/F624, F715/F624, F663/F650, F685/F650, F695/F650, F715/F650, F685/F663, F695/F663, F715/F663, F695/F685, F715/F685, F695/F715, F715/F755, respectively.

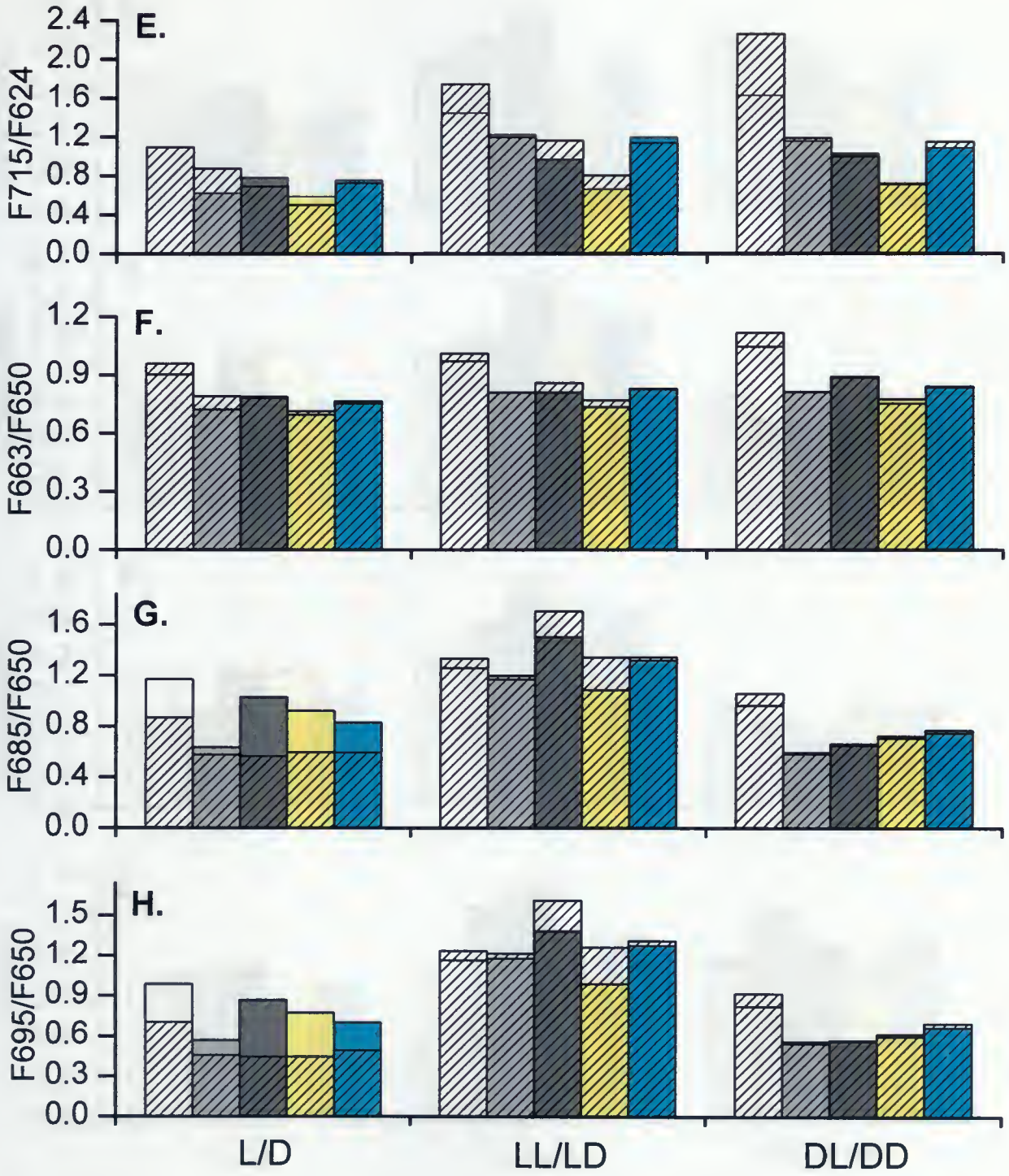
E.
F715/F624
2.4
2.0
1.6
1.2
0.8
0.4
0.0
F.
F663/F650
1.2
0.9
0.6
0.3
0.0
G.
F685/F650
1.6
1.2
0.8
0.4
0.0
H.
F695/F650
1.5
1.2
0.9
0.6
0.3
0.0
L/D
LL/LD
DL/DD

Appendix VI (continued)

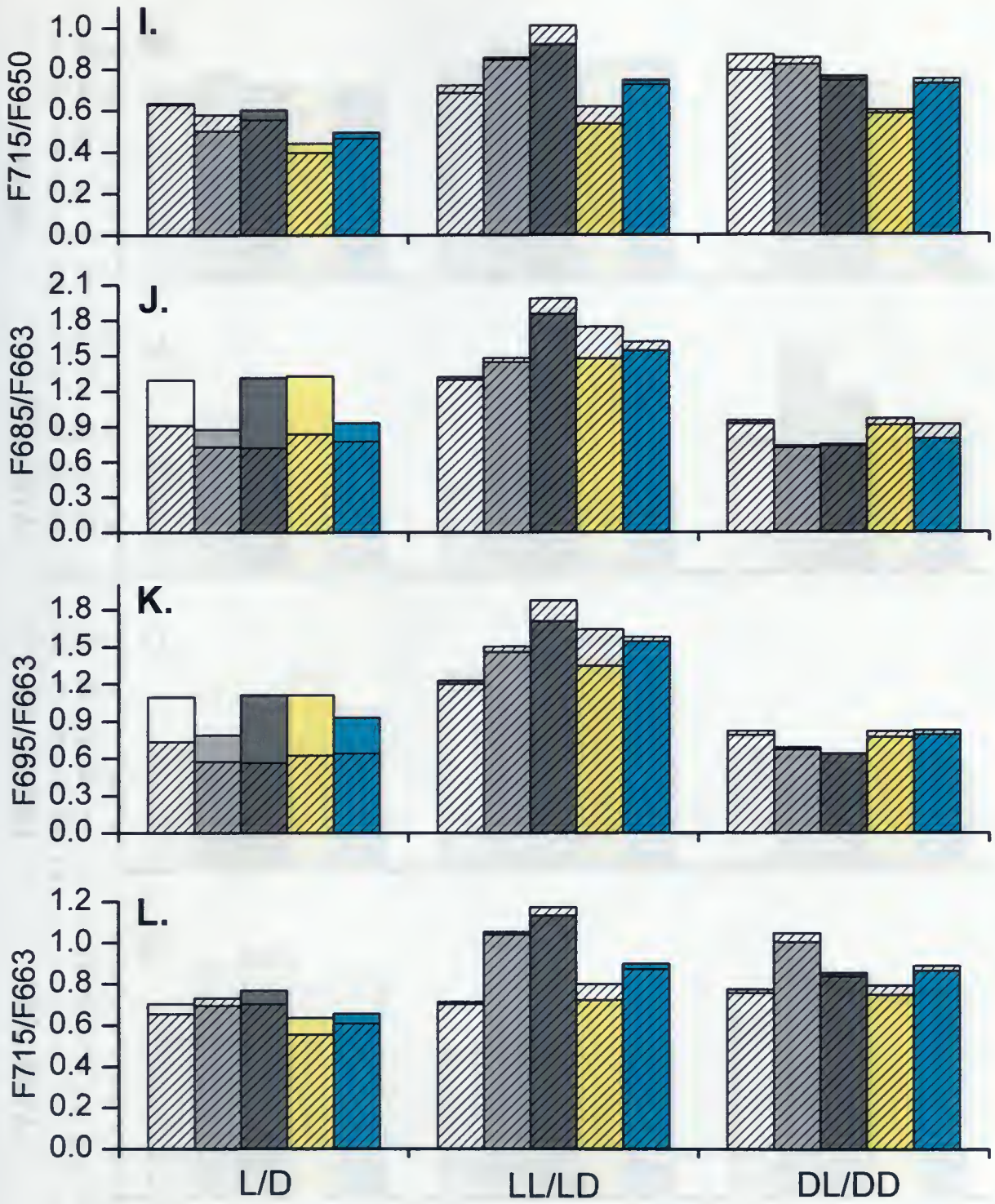

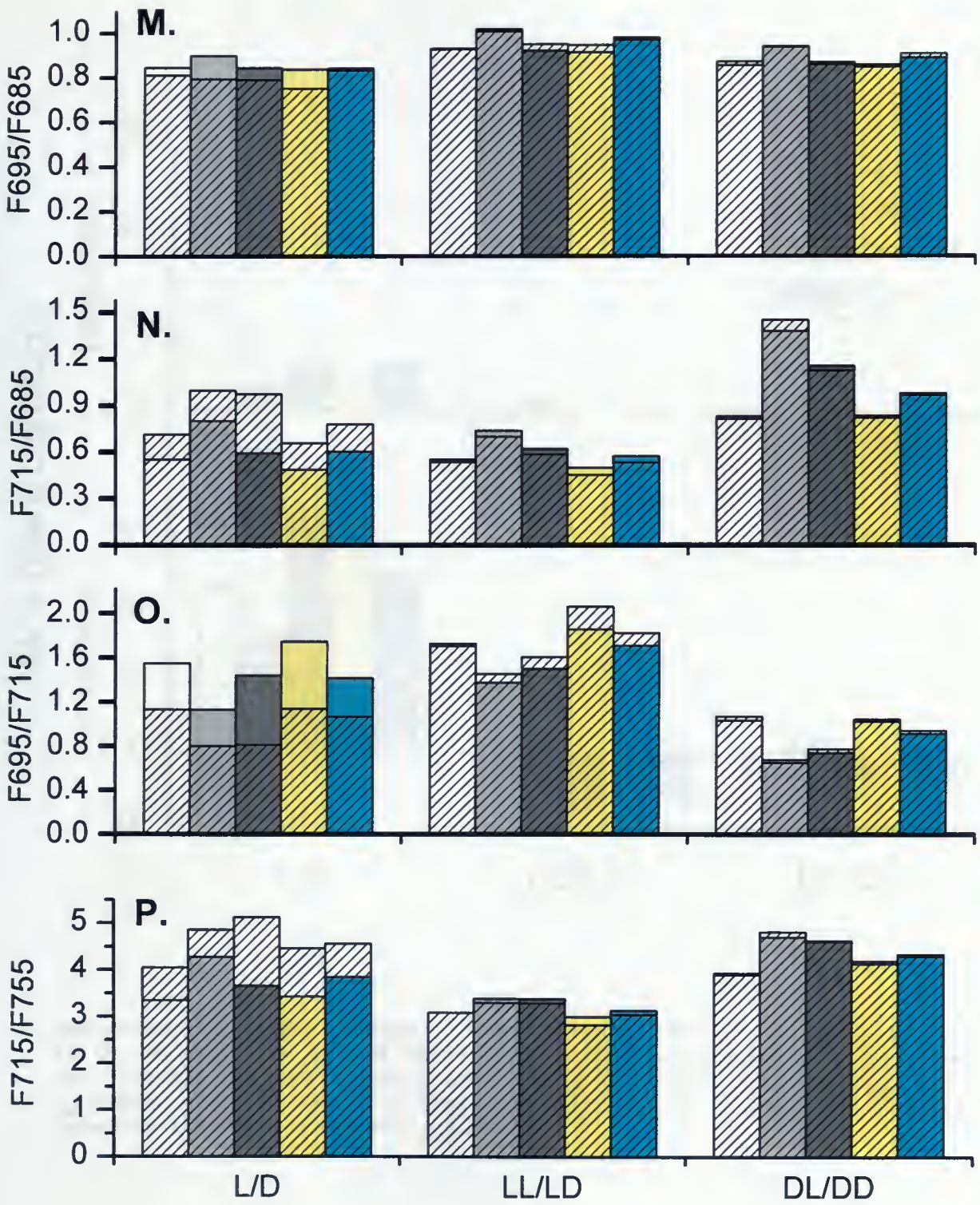
M.
F695/F685
1.0
0.8
0.6
0.4
0.2
0.0
N.
F715/F685
1.5
1.2
0.9
0.6
0.3
0.0
O.
F695/F715
2.0
1.6
1.2
0.8
0.4
0.0
P.
F715/F755
5
4
3
2
1
0
L/D
LL/LD
DL/DD

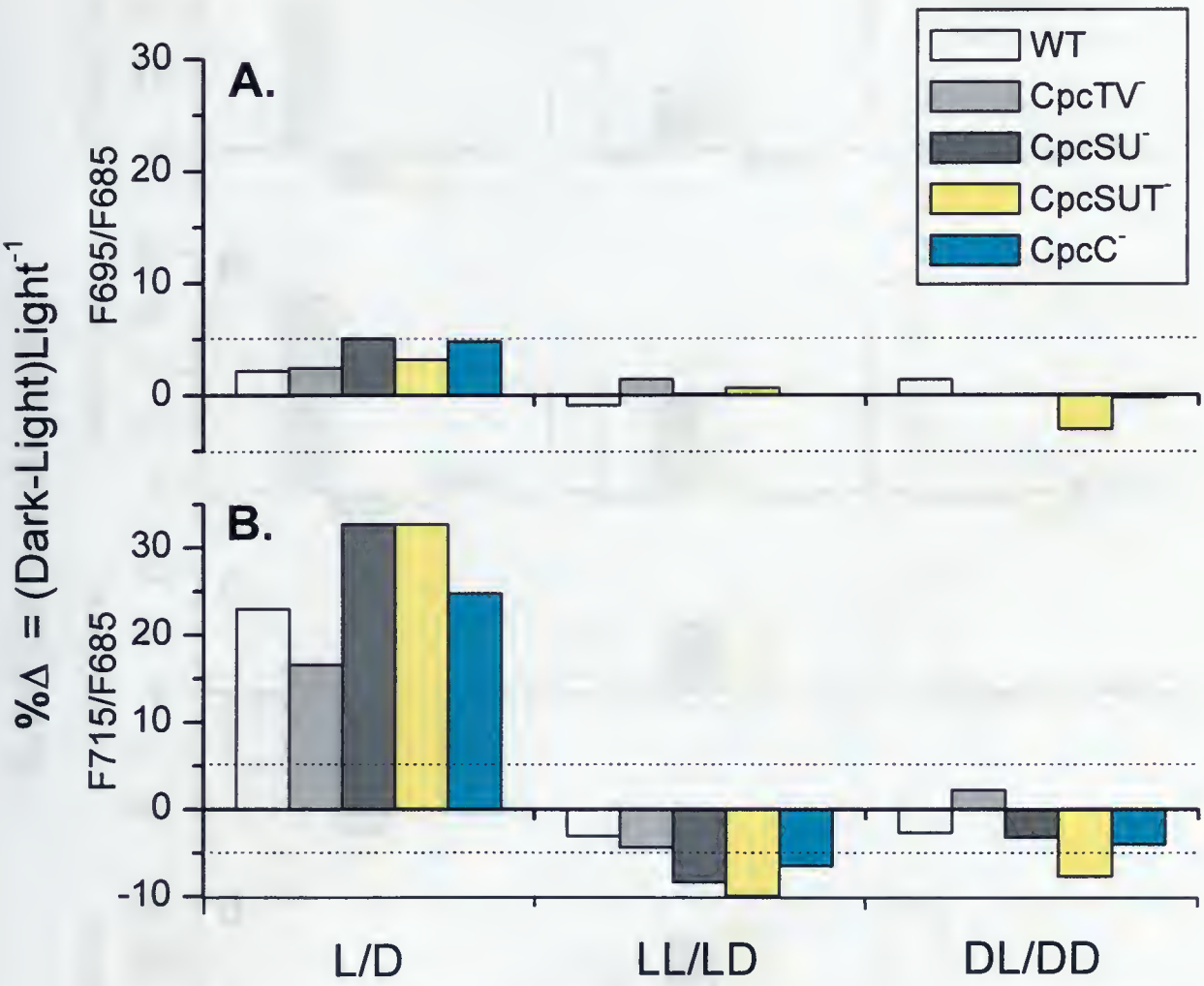


State transition dependent percent changes in 77K emission peak ratios from 435 nm excitation. L, D, LL, LD, DD, DL, as previously described. Shown are the percentage changes in peak ratio values between state 1 (blue light illumination) and state 2 (dark adaptation). $\%\Delta = 100\ (Fn/Fx_{Dark} - Fn/Fx_{Light})\ (Fn/Fx_{Light})^{-1}$ where Fn and Fx are emission peak values at n and x nm, respectively. **A**, **B**, F695/F685, F715/F685, respectively. Dashed lines represent 5% significance levels.

Appendix VIII

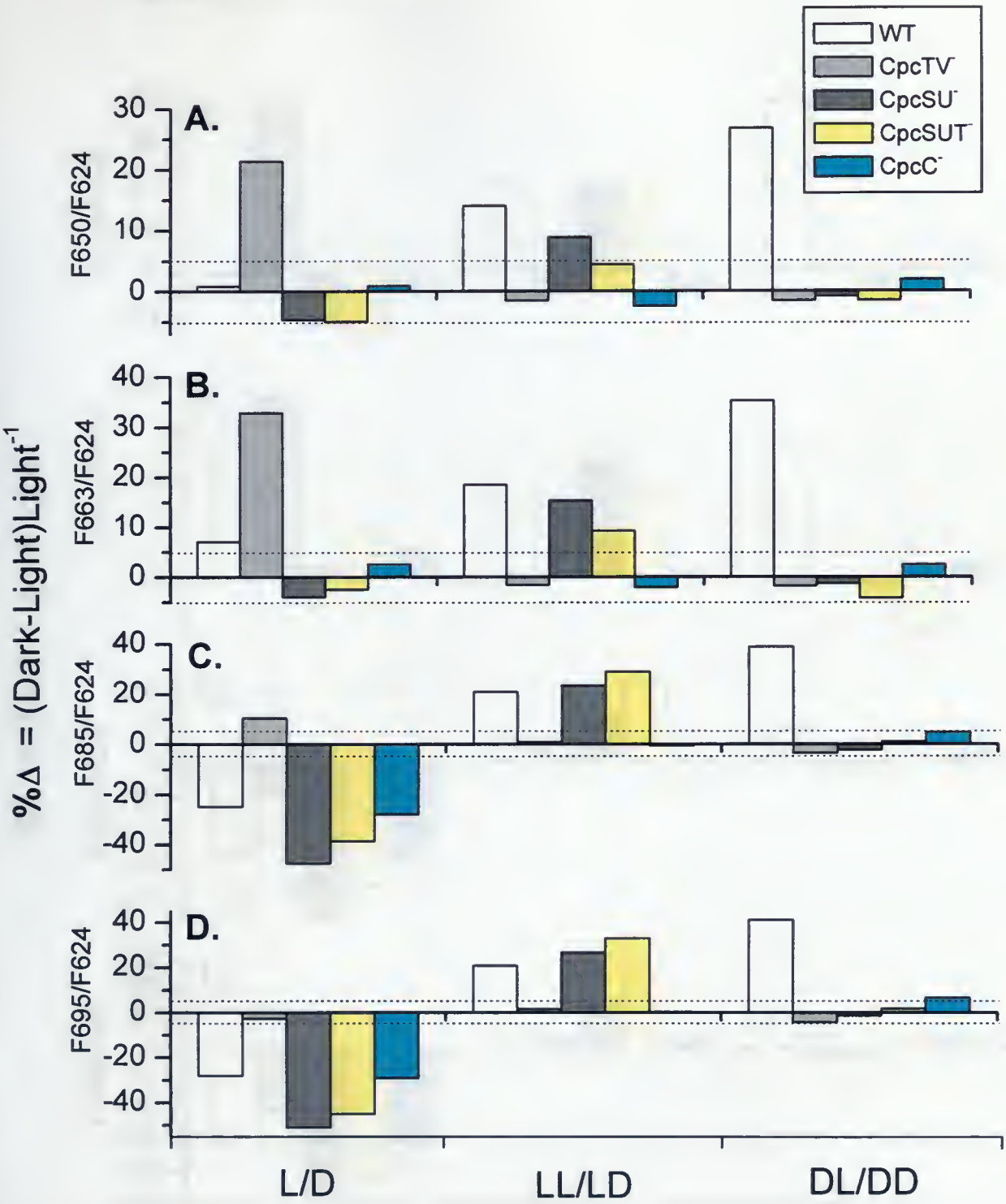


State transition dependent percent changes in 77K emission peak ratios from 575 nm excitation. L, D, LL, LD, DD, DL, as previously described. Shown are the percentage changes in peak ratio values between state 1 (blue light illumination) and state 2 (dark adaptation). $\%\Delta = 100\ (Fn/Fx_{Dark} - Fn/Fx_{Light})\ (Fn/Fx_{Light})^{-1}$ where Fn and Fx are emission peak values at n and x nm, respectively. **A-O**, F650/F624, F663/F624, F685/F624, F695/F624, F715/F624, F663/F650, F685/F650, F695/F650, F715/F650, F685/F663, F695/F663, F715/F663, F695/F685, F715/F685, F715/F755, respectively. Dashed lines represent 5% significance levels.

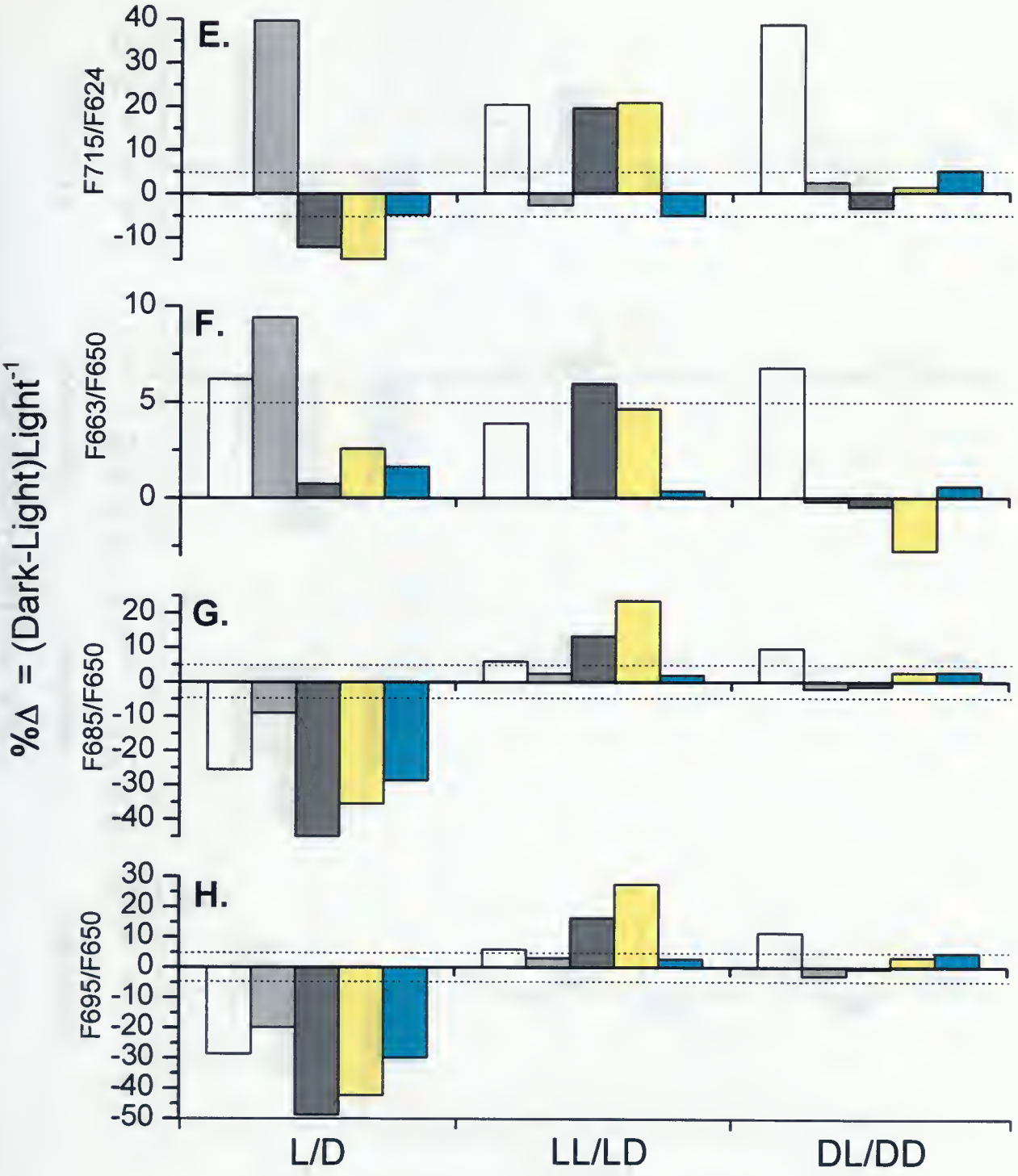
%Δ = (Dark-Light)Light-1
E.
F715/F624
40
30
20
10
0
-10
F.
F663/F650
10
5
0
G.
F685/F650
20
10
0
-10
-20
-30
-40
H.
F695/F650
30
20
10
0
-10
-20
-30
-40
-50
L/D
LL/LD
DL/DD

Appendix VIII (continued)

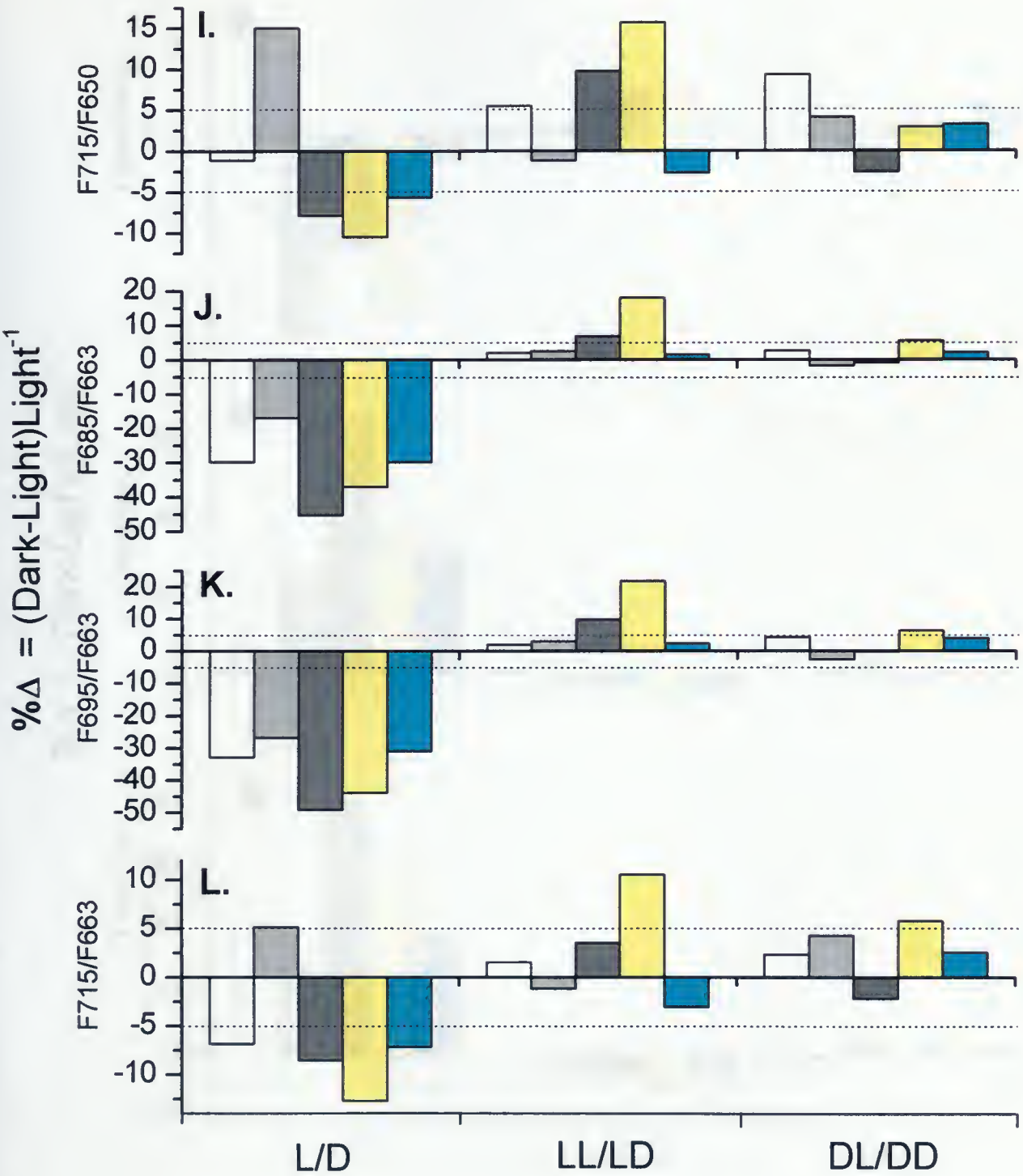

Appendix VIII (continued)

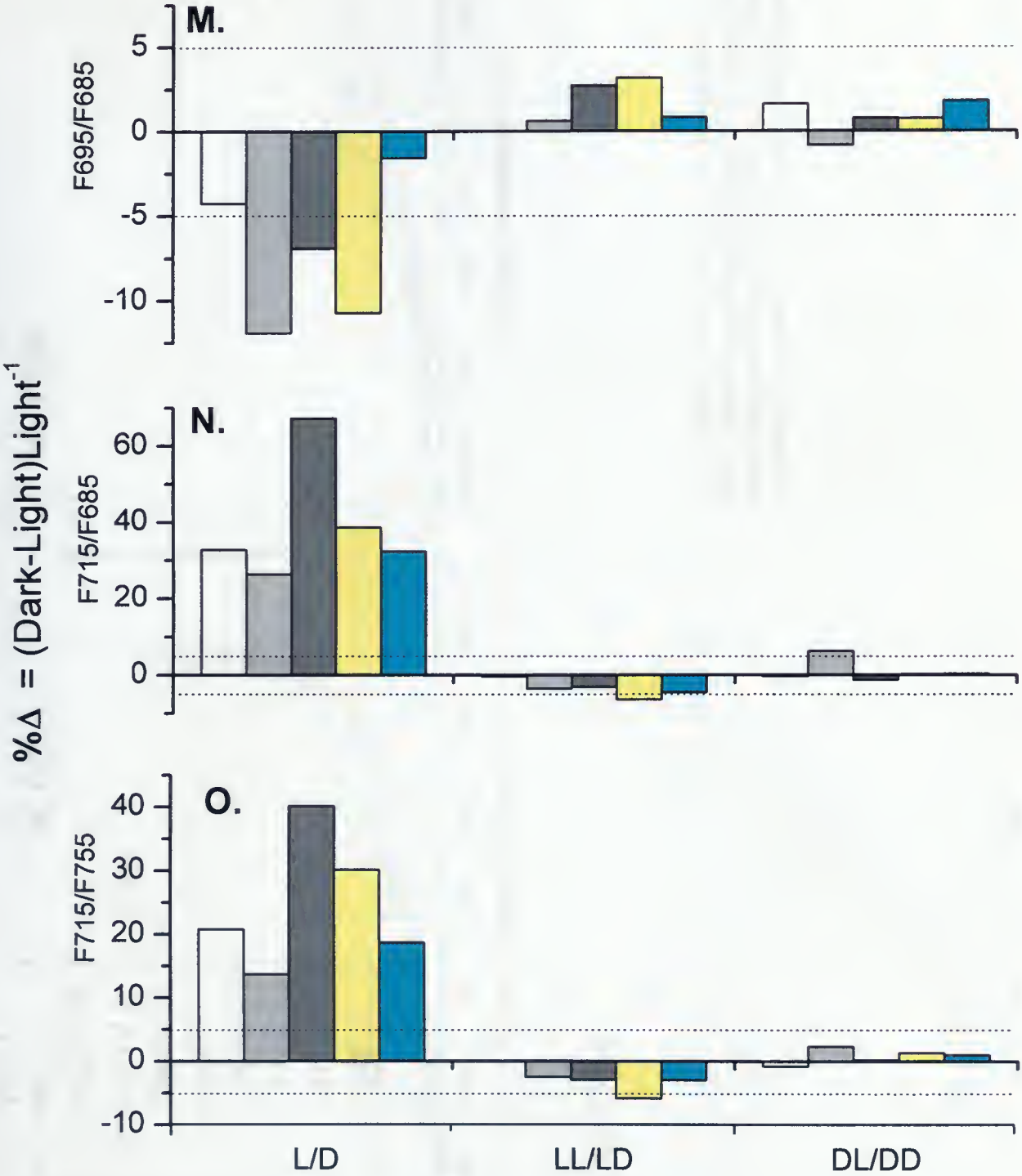

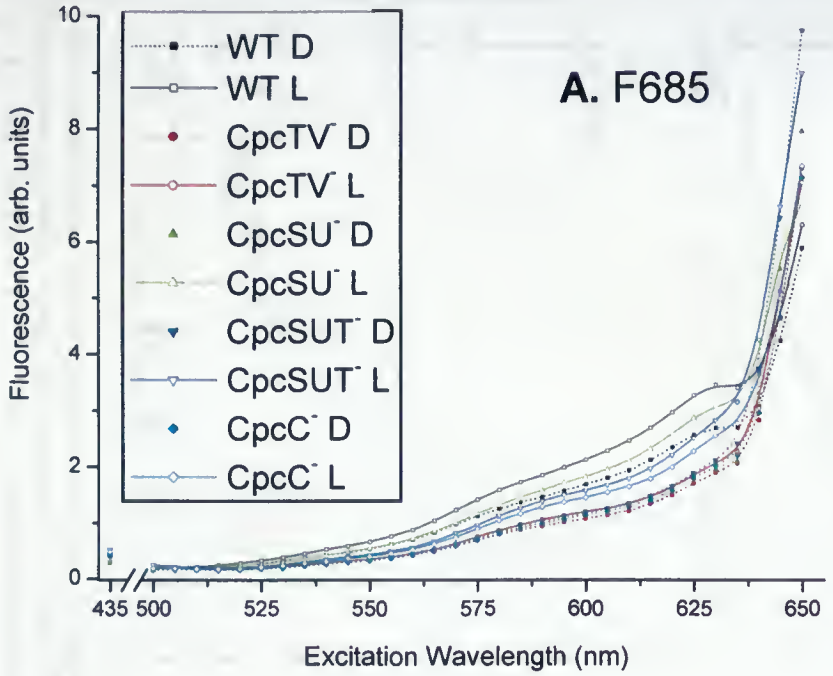


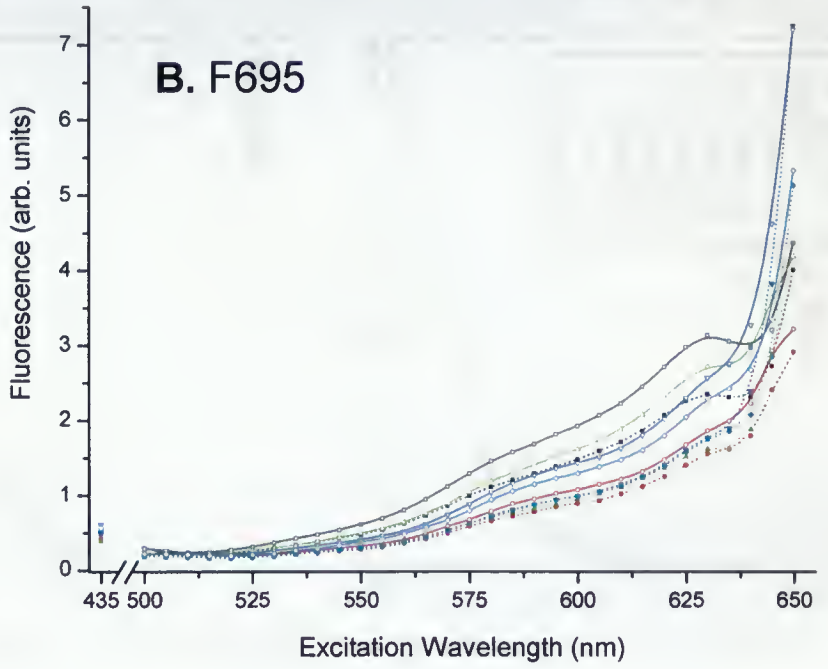


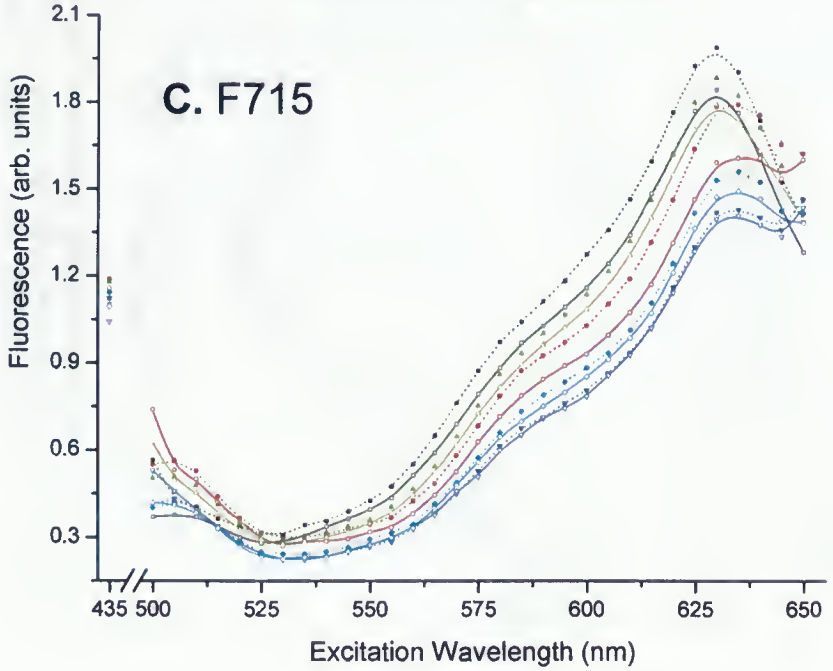


77K excitation spectra emission peak intensities from L/D treated cells. Plotted are excitation wavelength vs. fluorescence amplitude at the emission peaks of **A**, F685; **B**, F695; **C**, F715. Emission spectra collected as in Figures 11 - 15. L, D, as previously described.

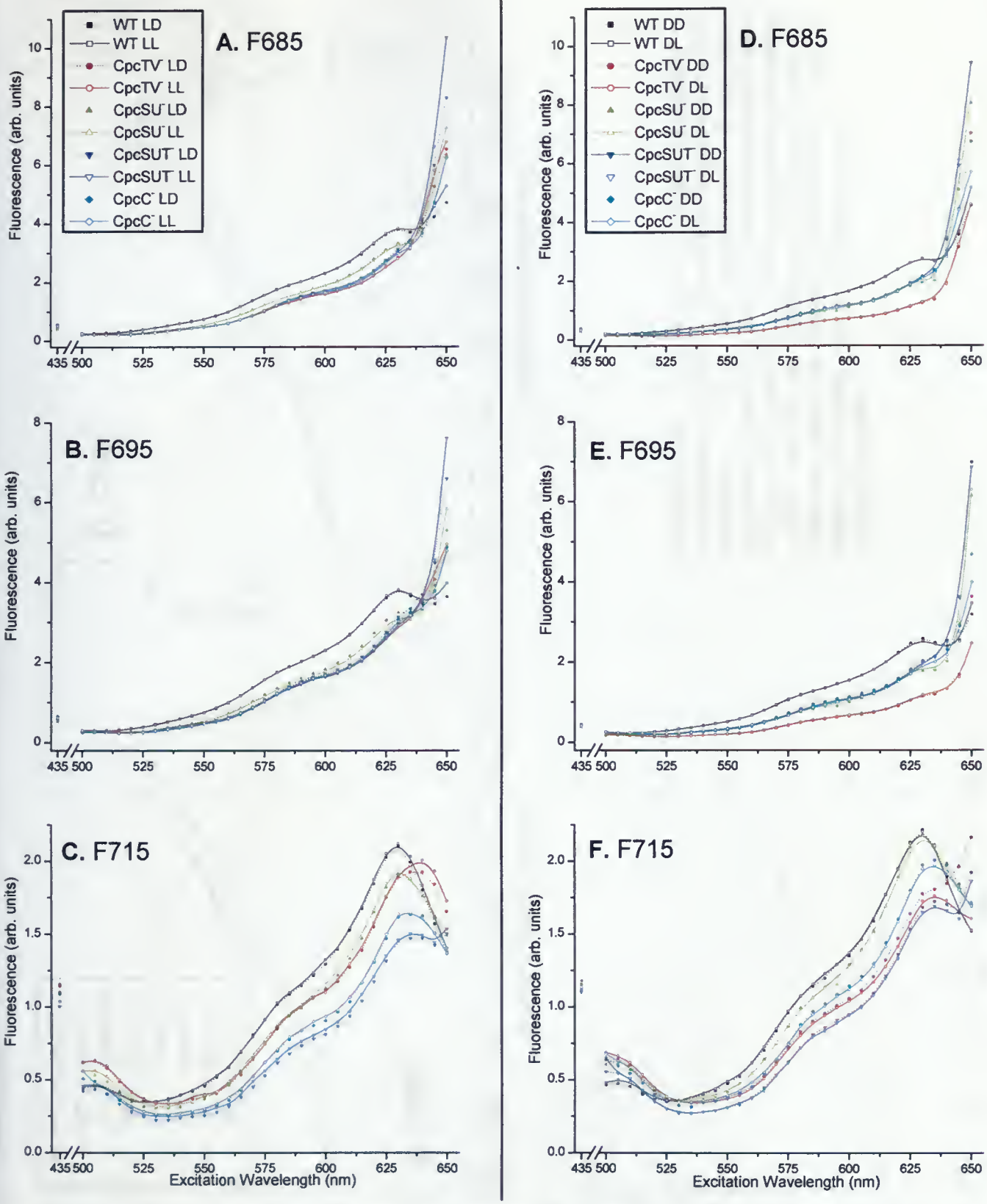


77K excitation spectra emission peak intensities from 1 M phosphate treated cells. Plotted are excitation wavelength vs. fluorescence amplitude for LL/LD samples (**A**, **B**, **C**) and DD/DL samples (**D**, **E**, **F**) at the emission peaks of F685 (**A**, **D**), F695 (**D**, **E**), F715 (**C**, **F**). Emission spectra collected as in Figures 11 - 15. LL, LD, DD, DL, as previously described.

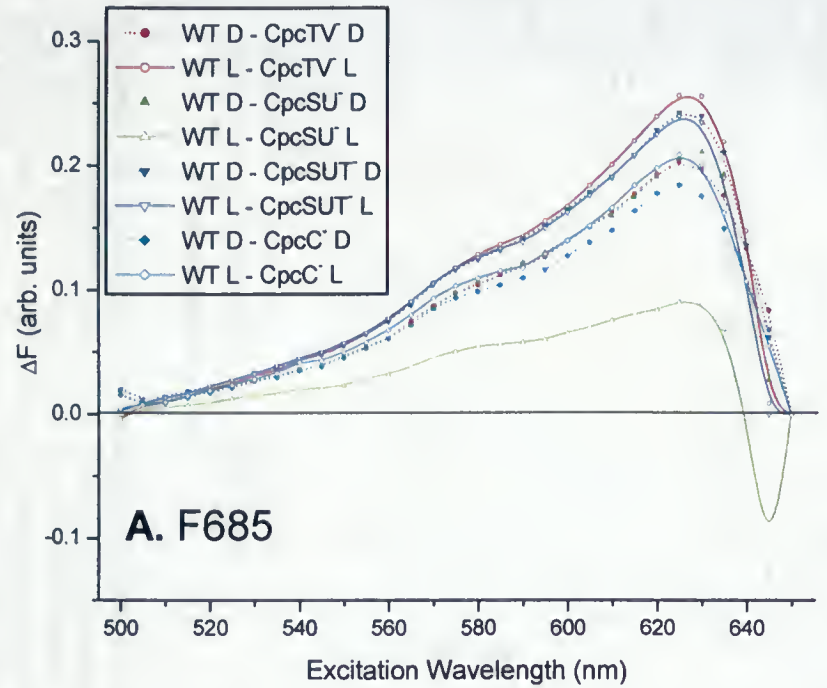


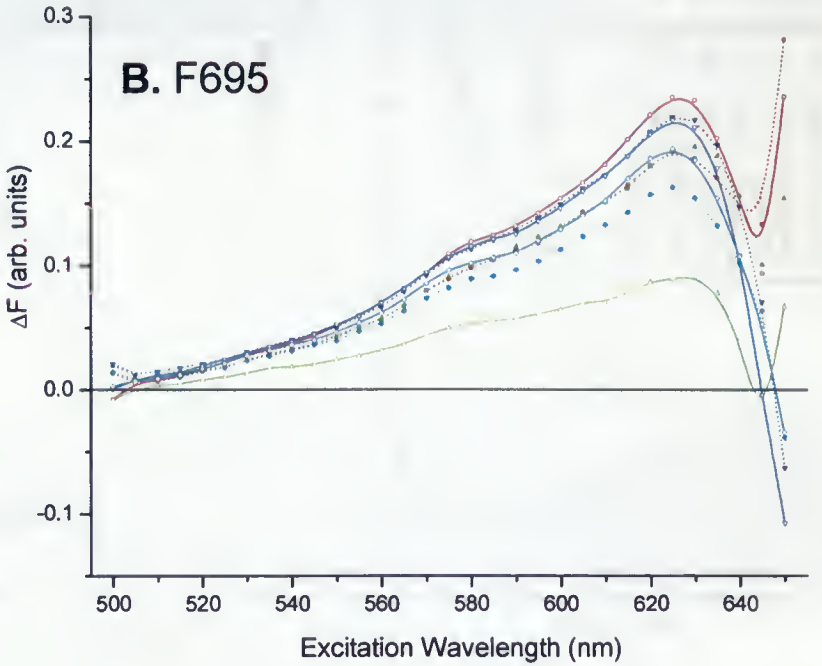


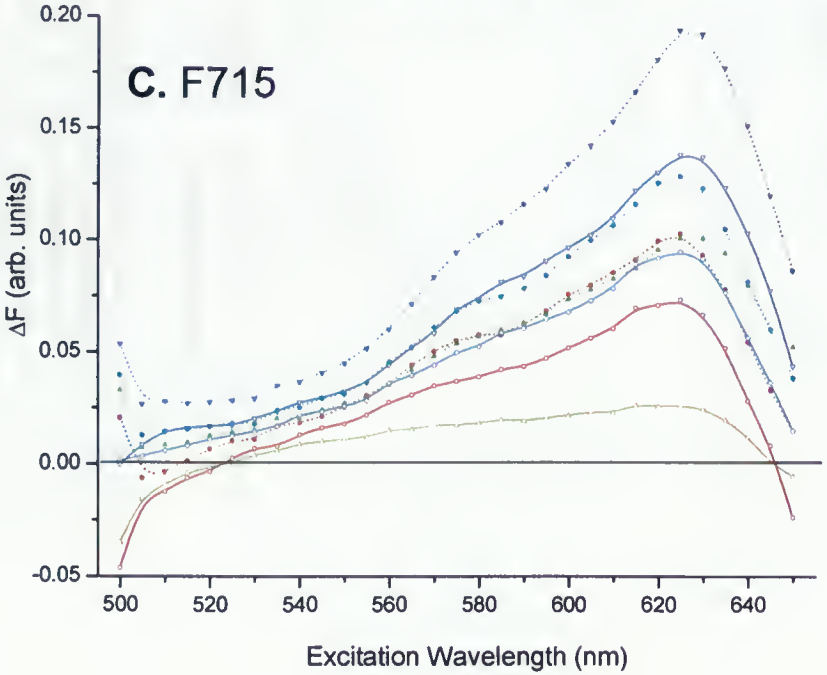


Differential loss in phycobiliprotein excitation contribution to terminal acceptor emission at 77K among the mutant strains for L/D treated cells. **A**, **B**, **C**, the subtractions (ΔF) of Cpc⁻ strain fluorescence intensity from that of WT at the emission peaks F685, F695, and F715, respectively. Excitation spectra were normalized to F685 with 650 nm excitation (as in Figure 16) prior to subtraction; spectra can therefore be considered as corrected to number of fluorescing PBS core terminal emitters. L, D, as previously described.

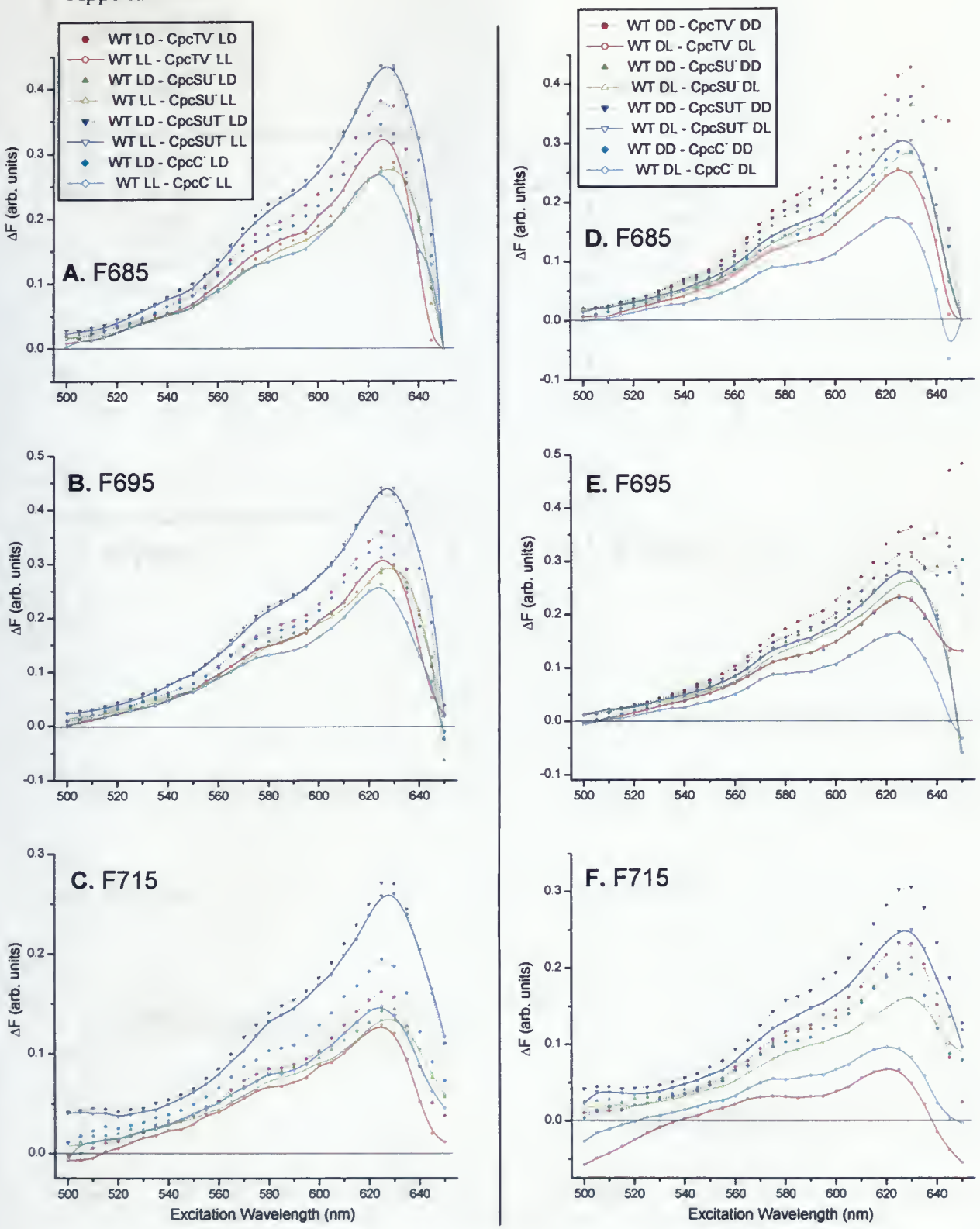


Differential loss in phycobiliprotein excitation contribution to terminal acceptor emission at 77K among the mutant strains for 1 M phosphate treated cells. Plotted are the subtractions (ΔF) of Cpc⁻ strain fluorescence intensity from that of WT for LL/LD samples (**A**, **B**, **C**) and DD/DL samples (**D**, **E**, **F**) at the emission peaks of F685 (**A**, **D**), F695 (**D**, **E**), and F715 (**C**, **F**). Excitation spectra were normalized to F685 with 650 nm excitation (as in Figure 16) prior to subtraction; spectra can therefore be considered as corrected to number of fluorescing PBS core terminal emitters. LL, LD, DD, DL, as previously described.

Appendix XIII

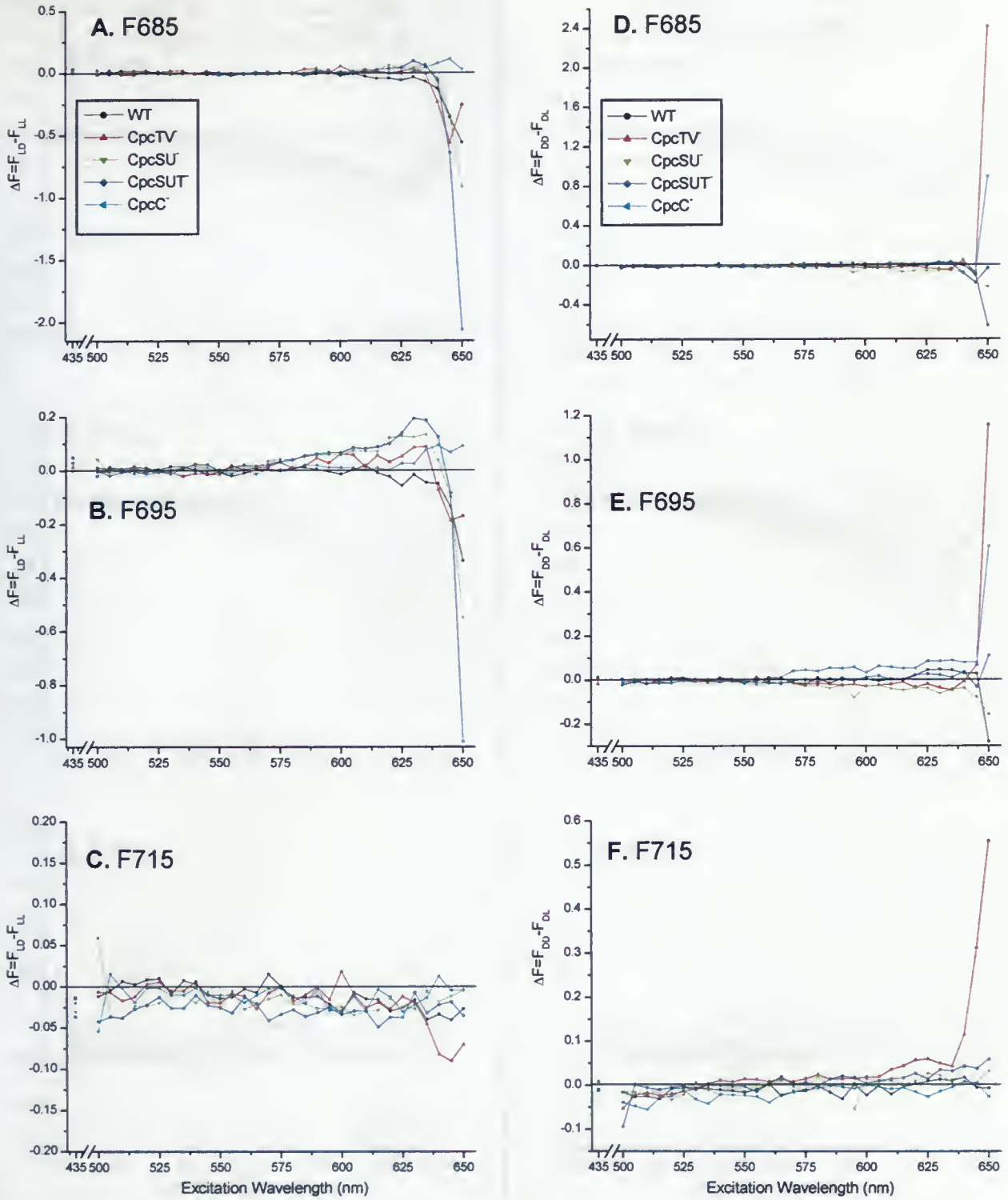


State transition dependent changes in 77K excitation spectra emission peak intensities among cells locked into their pre-adapted light state via 1 M phosphate. Shown is the difference in fluorescence intensity from cells in LL and LD conditions ($\Delta F = F_{LD}-F_{LL}$) at the emission peaks of **A**, F685; **B**, F695; **C**, F715; and the difference in fluorescence intensity from cells in DD and DL conditions ($\Delta F = F_{DD}-F_{DL}$) at the emission peaks of **D**, F685; **E**, F695; **F**, F715. Spectra were not normalized prior to or after subtraction. DD, DL, LD, LL, as previously described.

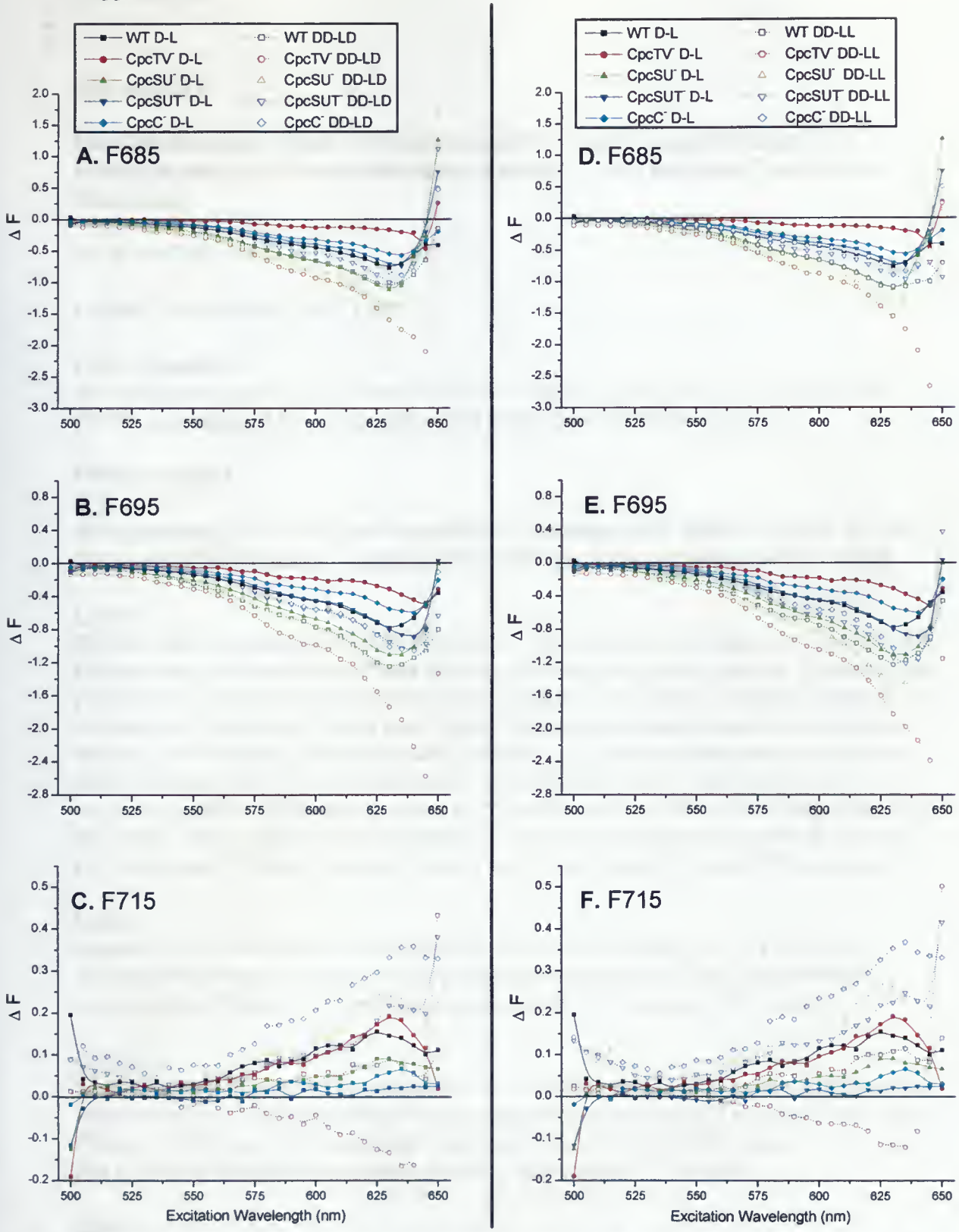


State transition dependent changes in 77K excitation spectra emission peak intensities between cells locked in state 2 and state 1 via 1 M phosphate. **A**, **B**, **C**, the difference in fluorescence intensity between cells in DD and LD conditions (DD-LD = [$\Delta F = F_{DD}-F_{LD}$]) at the emission peaks of F685, F695, F715, respectively. **D**, **E**, **F**, the difference in fluorescence intensity between cells in DD and LL conditions (DD-LL = [$\Delta F = F_{DD}-F_{LL}$]) at the emission peaks of F685, F695, F715, respectively. $\Delta F$ was calculated to contrast cells locked in state 2 (DD) to cells locked in state 1 (LD or LL). Non-treated state 2 minus state 1 emission peak intensities (D-L = [$\Delta F = F_D-F_L$]) were plotted for baseline comparison. Spectra were not normalized prior to or after subtraction. L, D, DD, LD, LL, as previously described.

Appendix XV

**Detailed summary of the redistributions of Chl*a*- and phycobilin- absorbed excitation energy for each strain under standard state 1 and state 2 conditions (L/D treatments)**

(Also see Table 4)

D (state 2) as compared to L (state 1):

**Chl*a* dependent**
All strains show typical spillover of Chl*a* E as seen by a decrease in PSII fluorescence (F695) accompanied by an increase in PSI fluorescence (F715) in state 2.

**PBS dependent**
WT
State transition predominantly characterized by increase in PC→PSI E transfer, but also PBS core→PSI E transfer. Increased PBS→PSI E transfer at expense of PBS→PSII.

CpcTV$^-$
Mostly observe enhanced PC→PSI E transfer. PSI is likely receiving most of its E from PC that could not transfer its E thru the rods and core to the photosystems. Shows a large population of PBS cores associated with PSI in state 1 and state 2. In state 2, there is an increase in TE emission (F685) (see Figure 20); excitation spectra also show increased levels of F673 in both state 1 and state 2 (Figure 12). This may indicate uncoupled or poorly coupled PBS cores (unquenched). This increase in F673 may be indicative of a large population of PBS cores coupled to PSI with poor E coupling permitting large F673 emission. Large scale movement of PBS to PSI would be required for PBS to transfer E to PSI because PC-PSI E transfer is poor (would need more PBS core-PSI interaction).

CpcSU$^-$
Largest effect due to enhanced PC→PSI E transfer at expense of PC→TE→PSII. "Reserve" PBS cores (i.e. quenched non-photosystem coupled PBS) couple to PSI; however this PBS core-PSI coupling is weak resulting in increased TE emission.

CpcSUT$^-$
State transition dominated by decrease in PC→PSII E transfer in congruence with only a minor increase in PC→PSI (which can be explained by perturbed E transfer in the rods). "Reserve" PBS cores (i.e. quenched non-photosystem coupled PBS) couple to PSI; yet this PBS core-PSI coupling is weak resulting in increased TE emission.

CpcC$^-$
State transition characterized by increase in PC→PSI and PBS core→PSI E transfer. Increased PBS→PSI E transfer at expense of PBS→PSII.

Appendix XVI

**High M phosphate treatment does not exclusively prohibit the redistribution of Chl*a*- and phycobilin- absorbed excitation energy**

I. "Reverse spillover"

For Chl*a* excitation, the LL/LD spectra in Figure 10-1 are general described as those from state 1 in Figure 8-1; thus cells are locked in state 1. In fact F695/F715 may be increased (Appendix V, panel C). Conversely, the DD/DL spectra in Figure 10-1 are ascribed to being in state 2 and F695/F715 may also be diminished in several of the strains (Appendix V, panel C). The high M phosphate treatment pairs (i.e. LL/LD and DD/DL) show a "reverse spillover" of Chl*a* E (perhaps not in WT) (Figure 21); here PSII fluorescence is increased at the expense of PSI fluorescence in the samples exposed lastly to state 2 conditions. The effect is more conspicuous in the LD/LL samples than in DD/DL.

As for 575 nm excitation, both LL and LD cells (Figure 10-2) can be generally described as locked in state 1 conditions with little change in F695:F715 (Figure 21), yet reverse spillover of PC E may be seen in the mutant strains (however not in WT), as shown by an increase in F695 at the expense of F715 in LD (Figure 21). Reverse spillover seems to preferentially involve PC excitation and not APC excitation (seen as increase in PC excitation contribution to F695 in Appendix XIII). The DD/DL samples do not show reverse spillover of PBS E (Figure 8-2).

Reverse spillover (of both Chl*a* and PBS E) is likely a loss of PSII→PSI E transfer under state 2 conditions induced by the high M phosphate treatment. Loss of PC→PSII→PSI E transfer is seen as an increase in PC excitation contribution to PSII fluorescence at loss of PC excitation contribution to PSI (Appendix XIII).

II. Phycobilin fluorescence quenching

The losses in PBS fluorescence yield between the LL and LD samples in Figure 10-2 are suggestive of phycobilin fluorescence quenching. Particularly for CpcSU$^-$ and CpcSUT$^-$, there are substantial decreases in both PC and APC emission from the LD samples as compared to the LL samples. Why would PBS fluorescence be quenched under the LD treatment? These cells were pre-adapted to state 1 before the addition of the phosphate buffer. In state 1, PSII receives more phycobilin-absorbed excitation energy than does PSI. Upon exposure to dark conditions (LD) the cells would still attempt a transition to state 2; however, PBS mobility is no longer an available means by which to preferentially excite PSI. Reducing PSII excitation, as by PBS quenching, could instead be a way to preferentially excite PSI in the LD samples.

III. PSII fluorescence quenching among cells locked in state 1

LD and LL high M phosphate treated cells may have experienced low levels of photoprotective PSII fluorescence quenching as compared to cells in standard L conditions. These phosphate treated cells were exposed continuously to blue light for either 10 min (LD) or 15 min (LL). Though the blue light used was not of high intensity, the length of exposure may have been enough to initiate quenching of PSII fluorescence.

Appendix XVII

**Detailed summary of the redistributions of Chl*a*- and phycobilin- absorbed excitation energy for each strain when cells are locked in state 1 with high M phosphate treatment (LL/LD treatments)**

LD as compared to LL:
(For reasoning behind "reverse spillover" and phycobilin quenching see Appendix XVI)

WT
Little perceivable reverse spillover of Chl*a* E. Some PC quenching in LD.

CpcTV$^-$
Reverse spillover of both Chl*a* and PBS E. No apparent PBS quenching.

CpcSU$^-$
Reverse spillover of both Chl*a* and PBS E. Significant quenching of PBS in LD.

CpcSUT$^-$
Reverse spillover of both Chl*a* and PBS E. Significant quenching of PBS in LD.

CpcC$^-$
Reverse spillover of both Chl*a* and PBS E. No apparent PBS quenching.

Appendix XVIII

**Detailed summary of the redistributions of Chl*a*- and phycobilin- absorbed excitation energy for each strain when cells are locked in state 2 with high M phosphate treatment (DD/DL treatments)**

DD as compared to DL:
(For reasoning behind "reverse spillover" and phycobilin quenching see Appendix XVI)

WT
Possible reverse spillover of Chl*a* E. PC fluorescence quenching in DD very similar to that observed in LD.

CpcTV$^-$

Possible spillover of Chl*a* (Figure 10-1) and PBS E (shown as increase in F715 at expense of F695 with no change in F624, F650, and F663 in Figure 10-2).

PBS core fluorescence quenching in DL perceived as an increase in APC excitation contribution to TE, PSII, and PSI emission in DD (Appendix XIII). There was no visible increase in PC excitation contribution to TE or PSII fluorescence because CpcTV$^-$ has poor PC→TE→PSII E transfer; conversely, an increase in PC excitation contribution to PSI was seen because PC→PSI E transfer is still competent. Cells may need to quench PBS in DL to prevent over excitation of PSI because of the large PBS antennae for PSI in this strain. This strain shows the largest contribution of APC-absorbed E to PSI emission (Appendix IX).

There is a large loss in amplitude of PC excitation contribution to TE and PSII (and to a lesser extent, PSI) fluorescence in the DD/DL samples as compared to the LD/LL samples (see Figure 10-2, Figure 17, Appendix X); however, APC E is still reaching PSI. This loss in PC→TE, PC→TE→PSII, and PC→PSI likely arises from greatly enhanced PBS core-PSI coupling. CpcTV$^-$ showed the most PBS core coupling to PSI of all the strains (Table 4), furthermore in the DD/DL treatment PBS core-PSI coupling would be enhanced due to the high M phosphate buffer. If PBS core-PSI coupling was greatly enhanced in the DD/DL samples then the above observations could be explained by: (i) the apparent loss in PC and APC excitation contribution to TE fluorescence would be due to reduced TE emission (TE fluorescence yield decreased because more E is transferred to PSI), (ii) the loss in PC and APC excitation contribution to PSII fluorescence would be due to decreased PBS-PSII coupling, (iii) APC excitation contribution to PSI emission would be increased in the DD/DL samples as compared to LD/LL.

CpcSU$^-$
Possible reverse spillover of Chl*a* E. Inconsequential adjustments in PBS E distribution.

CpcSUT$^-$
Noticeable reverse spillover of Chl*a* E. Inconsequential adjustments in PBS E distribution.

CpcC$^-$

Reverse spillover of Chl*a* E. Quenching of PBS cores in DL as seen by increase in APC excitation contribution to TE and PSII emission (Appendix XIII). PSII coupled PBS are targeted for quenching whereas PBS associated with PSI are not, for there is no change in PBS excitation contribution to PSI emission (Appendix XIII).